To the Graduate Council:

We are submitting herewith a dissertation written by Randall Robert Gore entitled "Dye Laser Excited Fluorescence Spectroscopy of Matrix Isolated Polycyclic Aromatic Hydrocarbons." We recommend that it be accepted in partial fulfillment of the requirements for the degree of Doctor of Philosophy, with a major in Chemistry.

E. L. Wehry, Co-Chairman

Gleb Mamantov, Co-Chairman

We have read this dissertation
and recommend its acceptance:

Accepted for the Council:

Vice Chancellor
Graduate Studies and Research

DYE LASER EXCITED FLUORESCENCE SPECTROSCOPY OF MATRIX ISOLATED POLYCYCLIC AROMATIC HYDROCARBONS

A Dissertation

Presented for the

Doctor of Philosophy

Degree

The University of Tennessee, Knoxville

Randall Robert Gore

March 1981

3043546

DEDICATION

To all too many men, being a good father and a good husband is equated with being a good provider. This can be true, but only if taken in view of a very broad perspective. Those with a more narrow view believe that providing food, clothing, a roof, and the bare part of an education, constitutes being a good provider. A father must also provide love, honor, companionship, and much, much more. This requires time spent with loved ones. Graduate school absorbs tremendous quantities of time and so my wife and children have been left with the short end of the stick too many times. They have been understanding and exceptionally patient. Without this, graduate school would have been impossible. Because of their love and understanding, this dissertation is dedicated to my sons, Robert and J. B., and to my wife, Colean, whom I love with all my heart and soul. I pray that those forces which bind our family together will ever increase, and that this work will contribute at least a small part of a better and brighter future for us and all humanity.

ACKNOWLEDGEMENTS

This achievement in my life has proven to be the most difficult goal I have ever attained to this point and I was ready to acknowledge defeat on many occasions. The encouragement, guidance, and spiritual support I received from many people enabled me to continue towards this goal. These people include my parents, my wife's parents, Dr. Earl Wehry, Dr. Gleb Mamantov, Arlene Garrison, Dick Dickinson, Central Baptist Church of Bearden, and many others to whom I apologize for omitting. Without the presence of this important circle of friends and family, I would not be at this juncture of life.

Financial assistance from the University of Tennessee, the National Science Foundation, my parents, my wife's parents, and from the Central Baptist Church of Bearden is gratefully acknowledged.

All shop personnel in the Chemistry Department at the University of Tennessee contributed a part of their time and talents to this research and their contributions are greatly appreciated.

Finally, if it were not for the advice and encouragement of Dr. Donald Jackman of Pfeiffer College, Misenheimer, N. C., the thought that I was even qualified to go to graduate school would not have even entered my mind.

Thanks to all.

ABSTRACT

Although steady state matrix isolation fluorometry has been shown to be a viable method of analysis for polycyclic aromatic hydrocarbons (PAHs), inadequate resolution of spectral components remains the primary limitation of the technique. In most cases, the broad emission bandwidths (20-200 cm^{-1}) are due to occupation by solute molecules of a large variety of different sites within the matrix (termed "inhomogeneous broadening"). Using the high degree of monochromaticity characteristic of laser light, subsets of this distribution of sites can be selectively excited ("site selection"), resulting in a high degree of spectral resolution.

The importance of inhomogeneous broadening in matrix isolation spectra of PAHs has been confirmed by the achievement of site selection. Emission bandwidths as low as 1.3 cm^{-1} (for perylene in heptane matrices) were obtained. Site selection fluorometry of matrix isolated PAHs has also been shown to exhibit analytical calibration curves which are linear over at least two orders of magnitude. An internal standard was not needed. Expressed in terms of relative standard deviation, the precision of matrix isolation site selection fluorometric analysis was on the order of 8%. Detection limits for benzo(a)pyrene (BaP) and 1,5-dihydroxynaphthalene (1,5-DHN) were approximately 1 ng and 50 ng, respectively. In both cases, the detection limits were limited by peak-to-peak laser intensity variations.

Quantitative calibration curves for BaP and 1,5-DHN using perylene and BaP, respectively, as internal standards were nonlinear.

Linearity was restored when the internal standards were not used. The nonlinearity was shown not to be a function of laser excitation or of site selection, and was attributed to energy transfer, an effect which was previously thought to play an insignificant role in matrix isolation fluorescence spectroscopy.

TABLE OF CONTENTS

CHAPTER		PAGE
I.	INTRODUCTION	1
	A. Background	1
	B. Analytical Background and Methodology	3
	C. Fluorescence Analysis	5
	D. Laser Fluorescence Spectroscopy	11
	E. Site Selection	16
	F. Purpose	26
II.	EXPERIMENTAL DETAILS	27
	A. Materials	27
	B. Equipment	30
	C. Procedures	51
III.	RESULTS AND DISCUSSION	55
	A. Preliminary Studies of Instrumentation	55
	B. Major Instrumental Problems and Solutions	61
	C. Continuum Source Excitation (CSE) in Matrix Isolation Fluorometry (MIF)	70
	D. Time Resolution in MIF	78
	E. Selective Excitation Using Laser Illumination	80
	F. Site Selection of PAHs in Frozen Solutions	83
	G. Site Selection of Matrix Isolated PAHs	87
IV.	CONCLUSIONS	137
LIST OF REFERENCES		139
APPENDIXES		144

CHAPTER PAGE

APPENDIX I. OPERATION OF SAMPLING OSCILLOSCOPE 145

APPENDIX II. OPERATION OF LIQUID HELIUM CRYOSTAT 150

VITA 157

LIST OF TABLES

TABLE		PAGE
I.	LIST OF LASER DYES	28
II.	POLYCYCLIC AROMATIC COMPOUNDS	31
III.	SUMMARY OF PROCEDURE TO ISOLATE CONTAMINATION	56
IV.	COMPARISON OF MATRIX SYSTEMS	71
V.	LIST OF COMPOUNDS IDENTIFIED IN FRACTION-75	77
VI.	SITE SELECTION OF PERYLENE IN ETHANOL FROZEN SOLUTION	85
VII.	COMPOUNDS WHICH EXHIBIT SITE SELECTION	98
VIII.	COMPOUNDS NOT EXHIBITING SITE SELECTION	102
IX.	MOLAR ABSORPTIVITIES FOR SEVERAL PAHS IN ISOOCTANE AT ROOM TEMPERATURE	104
X.	TEMPERATURE DEPENDENCE OF EMISSION BANDWIDTHS	111
XI.	CONSTITUENTS OF SYN F-75	121
XII.	COMPARISON OF PRECISION OF FLUOROMETRIC METHODS	135

LIST OF FIGURES

FIGURE PAGE

1. Comparison of emission spectra of perylene in different matrices 9
2. Fluorescence spectrum of Fraction-75 matrix isolated in nitrogen 12
3. Fluorescence spectrum of Fraction-75 matrix isolated in heptane 13
4. Illustration of homogeneous and heterogeneous broadening . . . 17
5. Illustration of ZPL and PW line shapes 20
6. Illustration of dependence of phonon coupling strength and temperature on line shape 22
7. Mechanistic illustration of dependence of site selection on excitation energy 24
8. Cold end of the Spectrim refrigerator 38
9. Cold end of the Heli-Tran refrigerator 39
10. Knudsen oven assembly used with the Spectrum refrigerator . . 42
11. External cell assembly 43
12. Schematic diagram of vacuum line 45
13. Schematic diagram of the steady state fluorometer 48
14. Schematic diagram of the dye laser spectrometer 50
15. Emission monochromator showing first source of stray light . . 63
16. Emission monochromator showing second source of stray light . 64
17. Cutaway of slit mount 66
18. Effect of polarizing filter on stray dye fluorescence 67

FIGURE PAGE

19. Emission spectra of benzo(a)pyrene in various matrices 73

20. Laser excited fluorescence spectra of Fraction-75 in N_2 . . . 79

21. Illustration of selective excitation by laser excitation . . . 81

22. Site selection of perylene in ethanol at 15 K 84

23. Site selection of perylene in N_2 at 15 K 88

24. Superradiance of perylene in N_2 at 15 K 91

25. Effect of presence or absence of polarizer on benzo(a)pyrene emission spectrum 93

26. Selective excitation of benzo(a)pyrene multiplets in heptane at 15 K 94

27. Demonstration of a distribution of sites within a single multiplet of benzo(a)pyrene in heptane at 15 K 95

28. Fluorescence spectra of benzo(a)pyrene in argon at 15 K using CSE and site selection 96

29. Fluorescence spectra of perylene in argon at 15 K using CSE and site selection 99

30. Fluorescence spectra of benzo(b)fluorene in argon at 15 K using CSE and site selection 100

31. Fluorescence spectra of benzo(k)fluoranthene in argon at 15 K using CSE and site selection 101

32. Energy level diagram illustrating the distribution of vibronic energy levels in the first electronic excited state 106

33. Temperature dependence of site selection of benzo(a)pyrene in heptane 108

FIGURE PAGE

34. Temperature dependence of site selection of perylene in argon 109

35. Temperature dependence of site selection of benzo(k)-fluoranthene in heptane 110

36. CSE fluorescence spectrum of hydroxynaphthalene mixture in argon at 15 K 112

37. Fluorescence spectrum of hydroxynaphthalene mixture at an excitation wavelength of 329 nm 114

38. Fluorescence spectrum of hydroxynaphthalene mixture at an excitation wavelength of 325.5 nm 115

39. Fluorescence spectrum of hydroxynaphthalene mixture at an excitation wavelength of 322 nm 116

40. Fluorescence spectrum of hydroxynaphthalene mixture at an excitation wavelength of 320.5 nm 117

41. Fluorescence spectrum of 1,5-dihydroxynaphthalene in argon . . 118

42. Fluorescence spectrum of two-year-old Fraction-75 in heptane . 119

43. CSE emission spectrum of Syn F-75 in heptane at 15 K 122

44. Site selection of benzo(k)fluoranthene from Syn F-75 in heptane at 15 K 123

45. Site selection of perylene from Syn F-75 in heptane at 15 K . 124

46. Calibration curve for 1,5-dihydroxynaphthalene using site selection 126

47. Graph of ratio of fluorescence intensities for constant, one-to-one ratio of benzo(a)pyrene to perylene 130

FIGURE PAGE

48. Calibration curve for benzo(a)pyrene in heptane at 15 K using site selection 131

49. Calibration curve for benzo(a)pyrene in heptane at 15 K using CSE 132

50. Illustration of delay modes of sampling oscilloscope 147

51. Diagram of Heli-Tran System 151

52. Diagram of top of liquid helium Dewar 152

53. Diagram of top view of Dewar adapter 153

CHAPTER I

INTRODUCTION

A. Background

The United States' known coal and oil shale reserves contain more untapped energy than is contained in the known oil reserves of all the Middle Eastern oil producing countries.[1] It is estimated that these coal and oil shale reserves can supply the increasing energy needs of the United States for several hundred years as well as make the United States a major energy exporter in the future as oil reserves are depleted.[1] Use of these assets, however, presents major technological, economic, and environmental problems.

Industry, especially the transportation industry, depends heavily on the use of liquid and gaseous fuels. These forms are also far easier and cheaper to transport from production sites to final points of use than is coal. Therefore, the coal and oil shales will largely need to be converted to these forms. Such a conversion industry will be vast in order to supply the energy demands of the United States.[2] The conversion would also have to compete with present energy sources in an economic fashion. As the price of oil continues to rise, coal conversion becomes more attractive from this point of view. The environmental problems also demand much attention, and it is to a small portion of this problem that this present work is dedicated.

The nonstoichiometric combustion of hydrocarbon fuels results in a variety of products, many of which pose serious environmental

and health considerations. Polycyclic aromatic hydrocarbons (PAHs) form one class of products which are of particular concern. PAHs are produced not only in the combustion of hydrocarbon fuels, but also in coal conversion[2,3] and various natural processes.[4,5] PAHs have been found not only in coal and oil shale conversion products,[1,2] but also in the interior and exterior environments of conversion facilities.[6-8] The advent of a larger coal and oil shale conversion industry also means the possible advent of extensive pollution of the environment by PAHs and other products if steps are not taken to control the introduction of these products into the environment.

The concern with PAHs lies in the fact that, of the several thousand PAHs, PAH derivatives, and sulfur and nitrogen analogues of PAHs, a significant fraction is either carcinogenic, co-carcinogenic, or a precursor to carcinogenic metabolic products.[2] How PAHs initiate carcinogenesis is not known and has been the subject of much debate and research. The fact that certain PAHs are carcinogenic is well established. In 1775, Pott described a relationship between a high incidence of scrotal cancer in chimney sweeps and the soot which was deposited in the chimneys.[9] Combustion of wood and coal were the primary sources of heat at that time. Malignant tumors were produced on rabbit ears by the application of coal tars in 1915.[9] Benzo(a)-pyrene, a product which was initially isolated from coal tars,[10] has been shown to be a precursor to highly carcinogenic metabolic products.[2] As an example, the concentration of benzo(a)pyrene in urban atmospheres has been linked to the incidence rates of lung cancer in the region of measurement.[3] As a result, much research has been

conducted to learn as much as possible about PAHs, their properties, sources, analysis, and control.

B. Analytical Background and Methodology

The present work is involved with the analytical portion of the problem. Environmental samples containing PAHs present two primary tests of analytical ingenuity. Individual PAHs are commonly present at very low levels. Real samples may also contain hundreds of PAHs, usually including many sets of isomers.[2] Whatever analytical method is used therefore has to be both very sensitive and highly selective.

Most past efforts have been devoted to the development of separation methods to reduce the complexity of the samples. However, the chemical and physical properties of PAHs are quite similar, making separation difficult. Thin layer chromatography (TLC) has been used extensively[11] and continues to be a quick and inexpensive separation method. Although relatively fast, TLC encounters problems with low sensitivity, poor fingerprinting capability, and differences between the spectroscopic properties (diffuse reflectance and fluorescence detection have been commonly used) of the solvated and adsorbed species.[12] Column chromatography with ultraviolet (UV) absorption or fluorescence detection requires large samples, is slow, and exhibits poor fingerprinting capability.[13] Column chromatography does lend itself to specific applications such as removal of interferences.[14,15] Capillary gas chromatography (GC) has advanced quickly in the past few years and can handle very low level, complex samples in a reasonable time.[15,16] While speed and sensitivity are very good, resolution

of isomers is quite poor in most cases and identification is often ambiguous, as retention indices are rather non-specific parameters for identification. Recourse to a confirmatory method such as mass spectrometry (MS) or infrared (IR) analysis is often needed for positive identification. MS, however, is also poor at resolving isomers and IR is generally rather insensitive. GC also experiences problems[17] from decomposition of PAHs during separation, column bleed and deterioration, and limited sample size (about 500 ng per component as an upper limit[18]). Separation efficiencies of high performance liquid chromatography (HPLC) approach those of capillary GC but offer the advantage of higher speed, ambient temperature operation,[19,20] and applicability to larger samples and molecules.[21] Detection has primarily been by UV absorption or fluorescence spectroscopy. Both exhibit relatively poor fingerprinting capabilities and are subject to the usual interferences of overlapping bands and contamination of the solvent. Fluorescence is also subject to self-absorption effects.

Presently the combination of GC and MS shows great promise, but as previously mentioned, has a major disadvantage in its poor resolution of isomers. This is crucial in PAH analysis, because small alterations in the molecular structure of a PAH can drastically alter its carcinogenecity. For example, benzo(a)pyrene and 5-methylchrysene are potent carcinogens while their respective isomers, benzo(e)pyrene and 1-, 2-, 3-, 4-, or 6-methylchrysene, are only mildly carcinogenic or noncarcinogenic.[2] Matrix isolation (MI), which is described in Section C, combined with fluorescence or

Fourier transform infrared (FTIR) spectroscopy, has been shown to be a powerful technique for the resolution of PAH isomers.[22]

C. Fluorescence Analysis

1. General

Although MI-FTIR has the capability of resolving many sets of isomers, the detection limits afforded by infrared techniques are not generally as low as those which can be attained by fluorometric methods. For species with relatively large fluorescence quantum yields, fluorometry is very sensitive and has the ability to detect femtogram quantities of analyte. In ideal cases, the intensity of the fluorescence emission is proportional to the excitation intensity. This is termed the "fluorescence advantage" and enables an increase in signal intensity to be effected by increasing the excitation intensity. This signal increase is generally accompanied by a signal-to-noise ratio increase.

Fluorescence spectroscopy also offers two basic types of spectra, excitation and emission. Techniques using synchronous scanning (simultaneously scanning both emission and excitation monochromators)[24] or three-dimensional contouring (intensity vs. excitation wavelength vs. emission wavelength)[25] offer combinations of both forms of spectra. With this dual nature, identification of components in a mixture can be "double-checked."

Since fluorescence lifetimes are known to vary over a wide range (e. g., 10-500 ns for PAHs), time can be used to add another dimension to fluorescence analysis. Time resolution can aid in

identification of components and/or discrimination against interferences such as short-lived fluorescent sample components and Rayleigh scattering.[26]

2. Room-Temperature Solution Fluorometry

Fluorescence of molecular species in room-temperature solutions exhibits severe analytical disadvantages. Both emission and excitation spectra are broad, leading to overlapping peaks and inner-filter effects. The former limits the number of components in a sample mixture which can be resolved from the other components. Extensive and time-consuming separations to isolate one or two PAHs into each chromatographic fraction are usually used to overcome the problem of overlapping peaks. The inner-filter effect distorts the spectra and decreases the apparent quantum yields which leads to error in identification and quantification. While room-temperature fluorometry offers significant sensitivity advantages, it suffers extensively from resolution disadvantages.

Fluorometry also suffers from "quenching," in which the quantum yield of the solute is reduced in the presence of other solutes. Quenching of molecules in the excited state most commonly occurs by collision with other molecules. Dilution, proper choice of solvent, and/or appropriate attention to purity of materials can reduce quenching. Quenching can also occur by long-range energy-transfer mechanisms. The "critical distance" for Förster energy transfer may be as large as 100 Å.[27] Although dilution aids in reducing or eliminating quenching, dilution also increases the difficulty of analyzing minor components or those with low quantum

yields.

Fluorometric analysis of PAHs in room-temperature solutions is therefore severely limited in its ability to deal with complex, multicomponent samples.

3. Low-Temperature (Frozen) Solution Fluorometry

A number of low-temperature methods have been developed to overcome most of the shortcomings of room-temperature fluorometry, with the major impetus directed toward the increase in resolution. The emission bandwidths of organic fluorophores in a "rigid" matrix at low temperatures (77 K and below) are substantially smaller (as low as 1-100 Å) than the usual spectral bandwidths obtained at room temperature (500-1000 Å is common).[28] This higher degree of resolution allows the reduction of inner-filter effects and the analysis of more complex mixtures. Since diffusion is greatly reduced in solid media at low temperature, quenching is greatly reduced.[28] The quantum yields of fluorophores in this type of matrix may therefore be larger than in fluid media. Lower detection limits usually accompany an increase in the quantum yield of a compound.

Many solvent systems exist which, when frozen, form glass-like matrices. These glassy solids exhibit excellent optical properties if chosen judiciously. Fluorescence emission bandwidths can be as small as 10-20 Å as compared with ten or more times that width in room-temperature solutions.[28]

Some solvents (usually n-paraffins) form crystalline solids, rather than amorphous solids, upon freezing. If the length of the solvent molecule closely matches the length of the PAH molecule

under scrutiny, then the PAH molecule may replace one or more solvent molecules in the crystalline matrix. All of the solute molecules are then in virtually identical "sites," or microenvironments. With a good match in molecular dimensions, the emission bandwidths may be as low as 1 Å.[29] A correlation between the reduction in bandwidths and the presence of nearly identical molecular microenvironments is made in Section E which defines and discusses site selection spectroscopy. It is common for several different sites to form, resulting in multiple narrow-band emissions. The term "Shpol'skii" is given to this effect, the resulting frozen matrix, the resulting spectra, and the required solvent. Figure 1 (p. 9) compares the Shpol'skii emission spectrum with the "glassy" frozen solution and the room-temperature solution emission spectra of perylene. Resolution is significantly increased by utilizing low-temperature methods and even more so if a Shpol'skii solvent system is available.

These low-temperature methods are not without their disadvantages.[30] Solute molecules can form microcrystalline aggregates upon freezing because of the low solubilities of PAHs at low temperatures. Aggregation leads to broadened spectra and possible quenching. The formation of these microcrystals is irreproducible and so both qualitative and quantitative results are affected. A number of experimental parameters, especially the freezing rate, affect the extent of microcrystallite formation. Rapid freezing usually reduces the extent of aggregation but also increases the possibility of cracking the matrix, thus destroying the homogeneity of the sample.

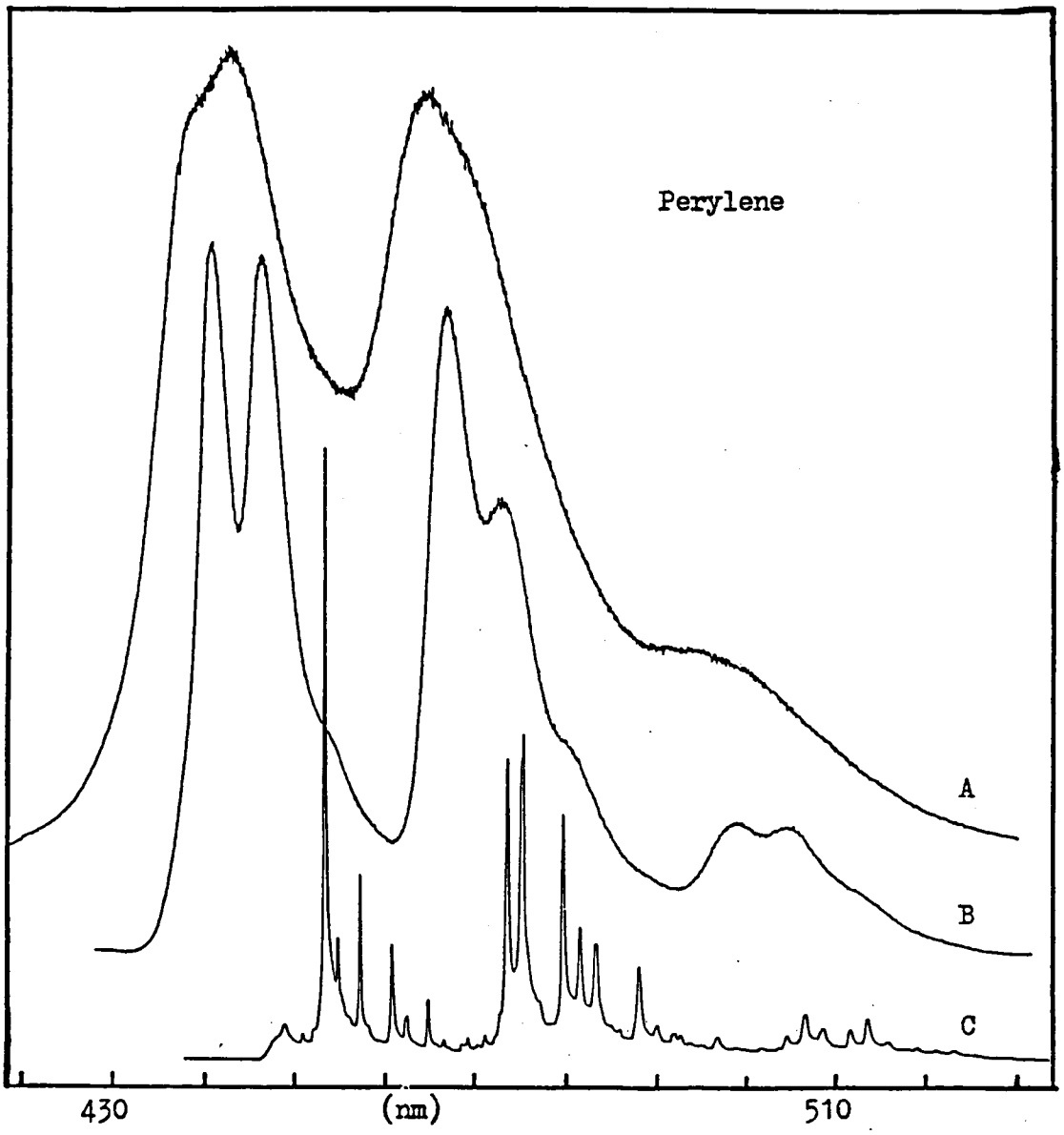

Figure 1. Comparison of emission spectra of perylene in different matrices.

A. Ethanol solution at 296 K. B. Frozen ethanol solution at 15 K.
C. Frozen hexane (Shpol'skii) solution at 15 K.
Excitation wavelength is 313 nm in all cases.

Different PAHs exhibit different molecular dimensions. Since the bandwidths of Shpol'skii spectra are strongly dependent upon a close match between dimensions of solvent and solute, a universal Shpol'skii solvent which would be suitable for all PAHs in a complex mixture is not ayailable. This type of frozen solution fluorometry is therefore rather limited in a general sense.

4. Matrix Isolation Fluorometry

Matrix isolation (MI) fluorometry results in spectra which are qualitatively similar to those obtained from frozen solution fluorometry. The major exception is that the possibility of aggregation is significantly reduced. MI, which was initially developed to trap and study free radicals and transient intermediates,[31] has proven its utility in the fluorescence spectroscopy of PAHs.[22] MI is accomplished by vaporizing the sample, mixing the vapor with a large excess of a diluent ("matrix") gas, and codepositing the mixture onto a cryogenic surface. The matrix-to-sample ratio (M/S) is large enough (10^3-10^6 on a mole basis) that the resulting frozen solid contains the solute molecules isolated from each other by the matrix. The distance between solute molecules is generally large enough that energy transfer is minimized. Diffusion at these temperatures (less than 20 K) is negligible, which eliminates collisional quenching. The resolution achievable in "conventional" matrices, such as nitrogen, is comparable to that observed in glassy frozen solutions when a broadband excitation source is used. A Shpol'skii solvent can be used as the matrix and the resulting spectral bandwidths are similar to those obtained using Shpol'skii frozen solutions.[32] In either

case, aggregate formation is eliminated if the experiment is performed properly.

Detection limits by MI fluorescence spectrometry for individual compounds are as low as 0.4 pg[32] and calibration plots are linear from the detection limit to 1-10 μg, above which negative deviations from linearity start to occur.

Figures 2 (p. 12)[22] and 3 (p. 13)[32] are examples of conventional MI and Shpol'skii MI spectra, respectively. In both figures, the sample is a wastewater effluent from a coking plant which had undergone preliminary fractionation and subsequent characterization by GC. This sample (termed "Fraction-75" and obtained from W. H. Griest of Oak Ridge National Laboratory) was known to contain at least 20 different PAHs. Both figures clearly demonstrate the quality of spectra obtainable by MI fluorescence spectrometry even in samples of substantial complexity as well as the adaptability of MI to a variety of matrices. It should be noted that perylene, benzo(a)pyrene, and benzo(e)pyrene are isomers ($C_{20}H_{12}$), yet are easily separated spectrally.

D. Laser Fluorescence Spectroscopy

The methods for increasing spectral resolution in fluorometry in Section C involve changes in the analytical sample (e. g., its temperature and matrix). With or without modification of the sample under scrutiny, a laser exhibits certain advantages which can be used to enhance resolution. A laser also possesses other desirable characteristics which can be used to advantage in certain cases.

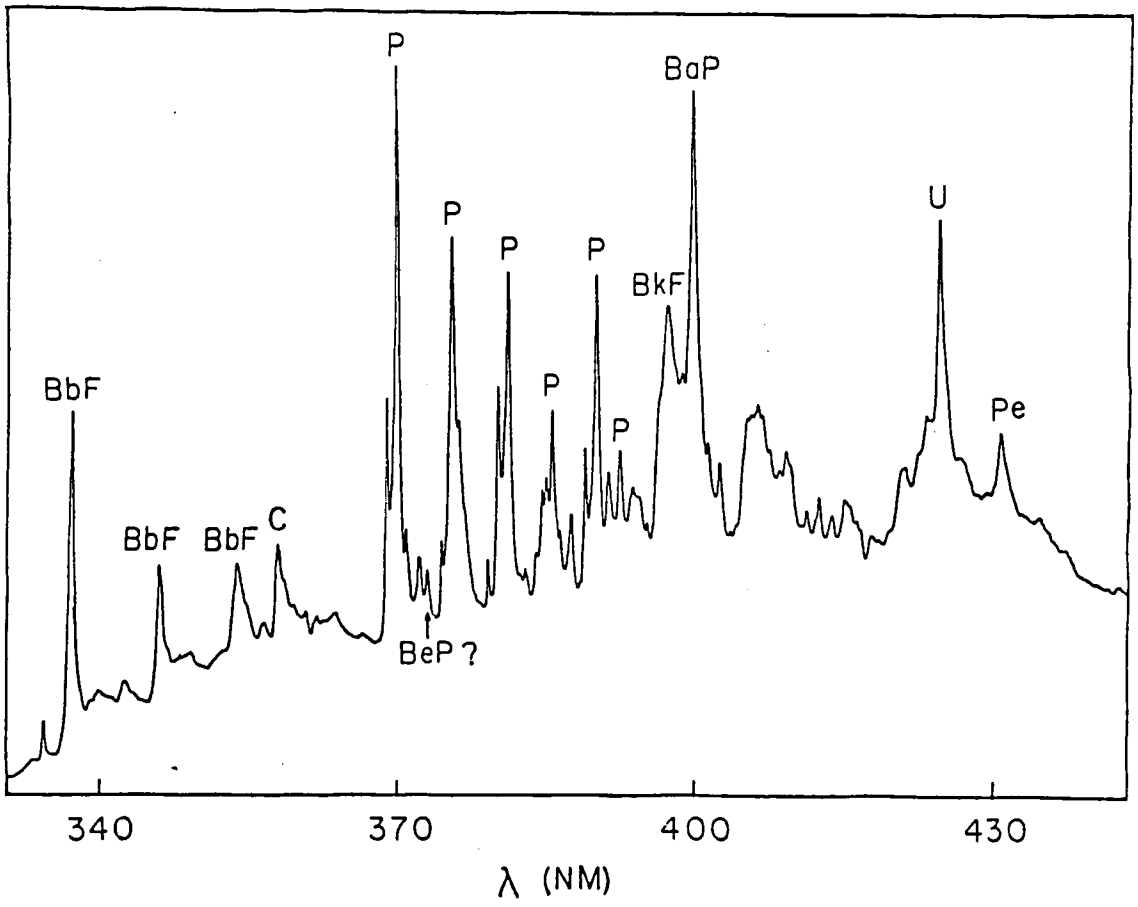

Figure 2. Fluorescence spectrum of Fraction-75 matrix isolated in nitrogen.

BbF: Benzo(b)fluorene; C: Chrysene; P: Pyrene; BeP: Benzo(e) pyrene; BkF: Benzo(k)fluoranthene; BaP: Benzo(a)pyrene; U: Unknown; Pe: Perylene; Excitation wavelength, 313 nm.

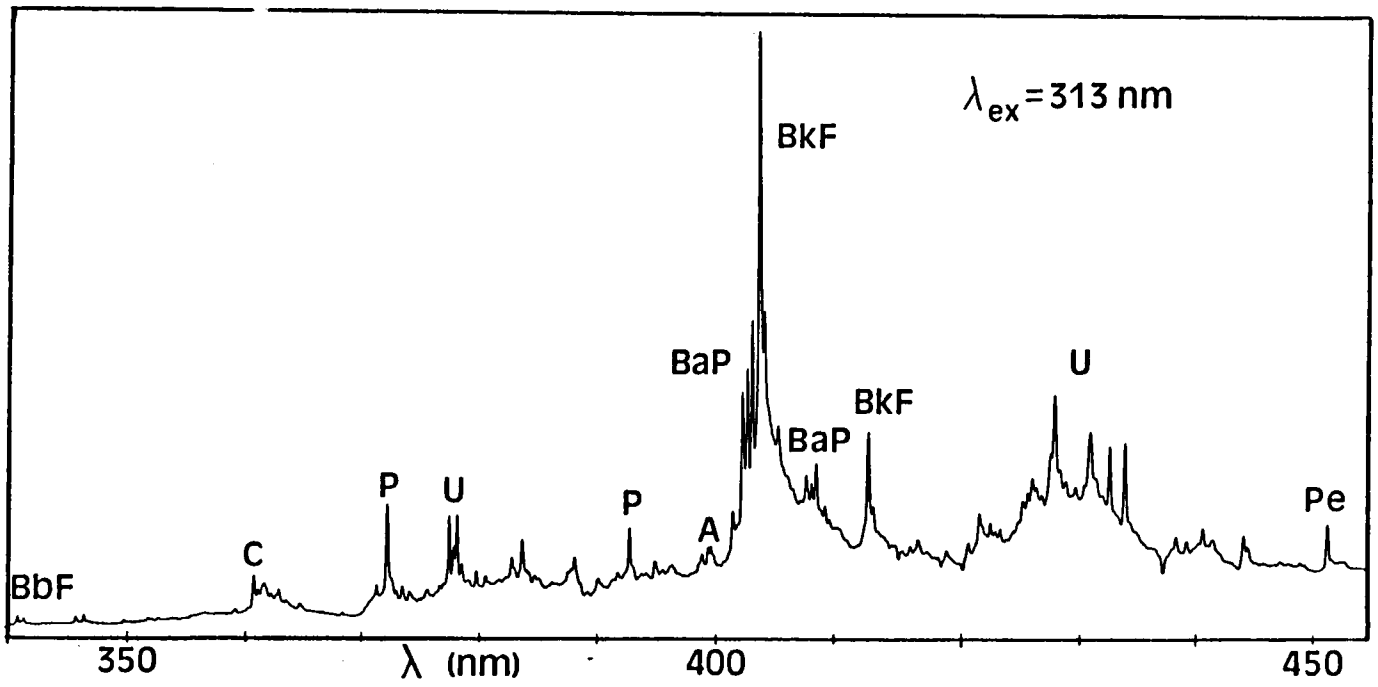

Figure 3. Fluorescence spectrum of Fraction-75 matrix isolated in heptane.

BbF: Benzo(b)fluorene; C: Chrysene; P: Pyrene; U: Unknown; A: Anthracene; BaP: Benzo(a)pyrene; BkF: Benzo(k)fluoranthene; Pe: Perylene.

Excitation systems for fluorescence spectroscopy commonly consist of an arc lamp with filters and/or a monochromator for wavelength selection. These are characterized by broad excitation bandwidths and low intensity per unit wavelength. Pulsed lamps are available but the intensity decreases rapidly as the pulsewidth is decreased. In contrast, laser systems are highly monochromatic and usually exhibit high power per unit wavelength. Pulsed lasers with picosecond pulsewidths are available with very high peak powers.

The highly monochromatic nature of laser light offers a primary advantage in the higher degree of analytical selectively available as compared to a broadband source. Maple[32] demonstrated that, even with complex samples, one component at a time can often be selectively excited by using Shpol'skii MI with a dye laser for excitation. Use of a broadband excitation source would have excited a large number of sample components.

The high power per unit wavelength of laser light may[33,34] or may not[32,35] result in an increased fluorescence advantage when compared to excitation using a broadband source. The fluorescence advantage is greatest when the absorption bandwidth of the sample matches the laser linewidth and the noise is not blank-limited. On the other hand, absorption bandwidths for matrix isolated PAHs in N_2 are much broader than the laser linewidth (50-200 cm^{-1} as compared with less than 1 cm^{-1}) and excitation therefore can be inefficient as compared with broadband excitation.[32] Detection limits in fluorescence are also usually blank limited.[26,35] An increase in absorbed incident power increases the background as well as the analytical

signal. The increased power also increases the heat released by radiationless decay of excited state molecules. This heat may be great enough to warm the matrix locally to the point at which diffusion is sufficiently rapid to destroy the isolation. This problem is greatest for those compounds which have low fluorescence quantum yields, which are the analytes for which the greater incident power offered by a laser should be most important. Finally, the high power of a laser also increases the possibility of photodecomposition of the analyte.

The high peak power and short pulses of pulsed lasers allow the accomplishment of time resolution (TR).[36] TR is accomplished by measuring the fluorescence intensity only during a narrow time "window" which is delayed with respect to the laser pulse. As a result, much of the information is discarded. Since the intensity decreases with an increase in the time window delay time, a tradeoff between sensitivity and the advantages of TR has to be made.

TR has several advantages. If the spectra of two components severely overlap and their fluorescence lifetimes are appreciably different, then the shorter lived component can be discriminated against in favor of the other. For example, benzo(a)pyrene and benzo(k)fluoranthene are isomers, exhibit severe spectral overlap in some matrices, commonly occur together in mixtures, and differ widely in their fluorescence lifetimes (78 ns for the former and 13 ns for the latter in N_2 at 15 K) and their carcinogenicity. Fortunately, benzo(a)pyrene is the carcinogen and is easily detected and quantitated by TR even in the presence of a 500-fold excess of

benzo(k)fluoranthene.[36] TR is not always applicable, as exemplified by the fact that the fluorescence lifetimes of all six isomers of monomethylchrysene are 53 ± 2 ns, a range which is too restricted to accomplish TR.[26] A mixture of these six compounds can be spectrally resolved by conventional broadband source MI fluorometry.[37] If a sample is highly scattering (both Raman and Rayleigh), TR is a valuable method of reducing the background.[26]

E. Site Selection

1. Origin of Finite Bandwidths in Fluorescence Spectroscopy

The Shpol'skii effect, which results in emission bandwidths as low as 1 cm^{-1},[27] is limited to particular matrices as discussed in Section C. Most Shpol'skii systems still exhibit bandwidths which are broadened slightly by matrix effects as discussed below.[37] By using the monochromaticity and high power characteristic of a laser source and the technique of "site selection," fluorescence emission spectra with resolution better than Shpol'skii spectra can often be obtained from a variety of matrix systems (not just Shpol'skii systems). To understand site selection, a knowledge of the origins of the finite spectral bandwidths in fluorometry is needed.

Two extreme possibilities exist to explain the finite width of a fluorescence emission band from a fluorophore in a low-temperature, solid matrix.[39] The band shape may be an accurate representation of the emission band of each molecule contributing to the spectrum as shown in Figure 4a (p. 17); the spectra of all individual molecules of the same compound within the sample presumably

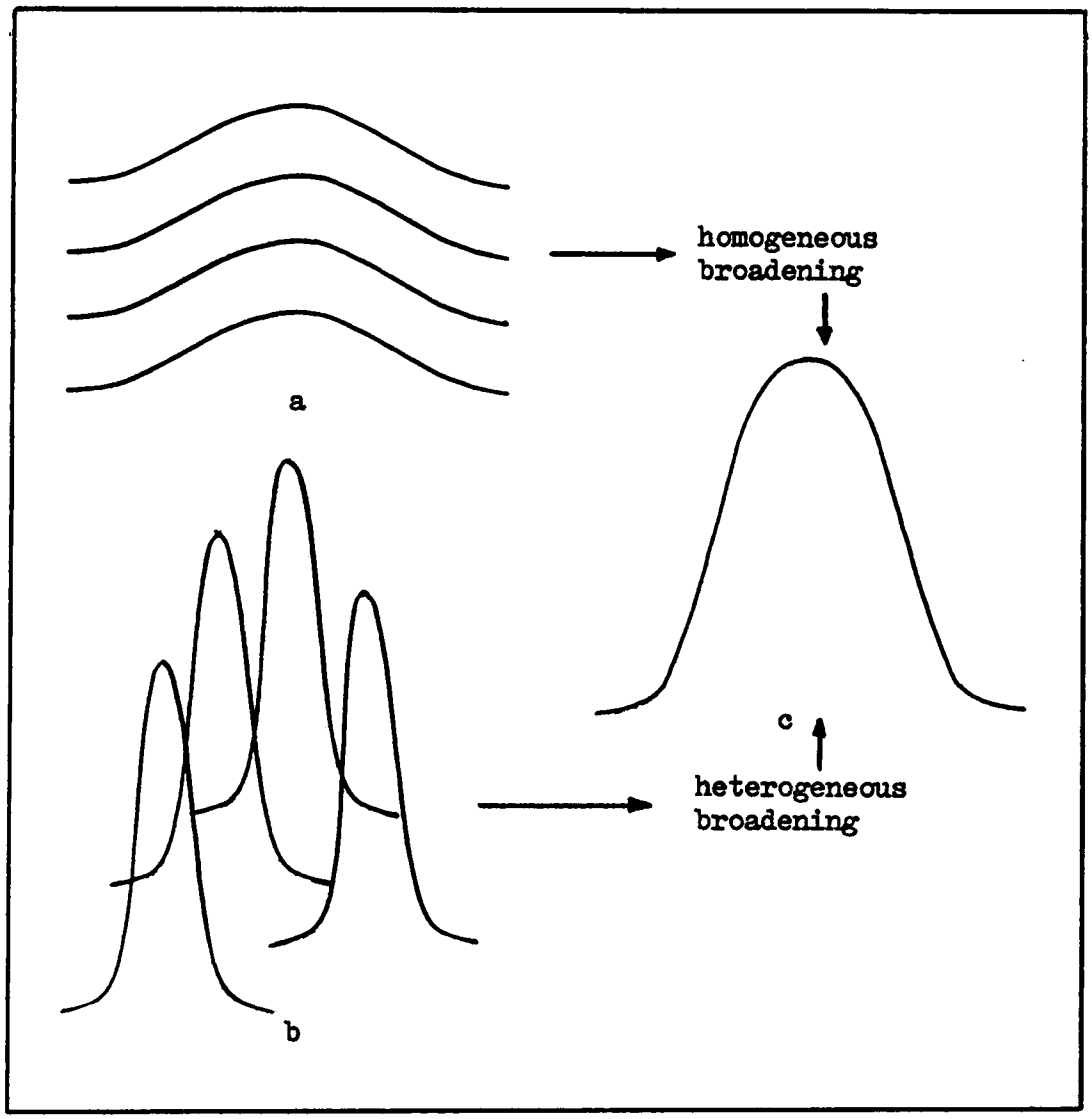

Figure 4. Illustration of homogeneous and heterogeneous broadening.

are identical (within the limits imposed by the Heisenberg Uncertainty Principle). The second possibility is that each molecule has its own sharp emission band which differs slightly in wavelength from that of other molecules of the same compound in the same sample, as shown in Figure 4b (p. 17). The observed emission spectrum then is the convolution of all of the individual molecular spectra, as in Figure 4c (p. 17). The former case is termed "homogeneous broadening" and little can be done in this case to increase spectral resolution. The latter case is termed "heterogeneous broadening." Spectral resolution can be increased either by causing the different molecules in the sample to exhibit more nearly equivalent spectra or by experimentally exciting only those molecules which exhibit virtually identical spectra. The ability to optically select relatively few molecules from a much larger ensemble forms the basis for site selection spectroscopy (SSS).[39]

An understanding of the origin of the spectral differences between different molecules of the same compound is necessary for an understanding of SSS. The differences are a result of solvent (or matrix) effects and are divided into two types of interaction.[40]

The first interaction is the shifting of the excited-state energy levels from the levels exhibited by the same molecules <u>in vacuo</u>. The local solvent field interacts with that of each molecule to shift the molecular orbital energy levels. Two properties result from the equations which describe this interaction.[40] First, the shift is strongly dependent upon the solvent configuration, or "cage" structure. Thus different molecules of the same type, which are

enclosed in different "cages," will exhibit spectra which are shifted in wavelength relative to each other. Each molecule is considered to be in a different "site," or microenvironment. A second important property of the solvent-solute interaction is an almost complete independence of the interaction with changes in the state of vibrational excitation of the solute. That is, when the electronic spectrum of a molecule is shifted by the solvent structure, the vibronic spacings remain essentially the same. Taken together, these properties indicate that all the molecules within the matrix will exhibit the same, individual, narrow-line (1-2 cm^{-1}) emission spectra which are shifted in wavelength by the individual solvent cages surrounding the individual molecules.[40]

The second interaction is that the solvent environment exhibits lattice vibrational modes, or phonon modes, which may couple with the electronic transition of the solute. This coupling occurs because changes in the electronic state of the solute molecule may produce small changes in the equilibrium configuration of the solvent cage. Electronic transitions which occur with no phonon coupling are the narrow lines mentioned above and are termed "zero-phonon lines" (ZPL). Electronic transitions occurring with phonon coupling give rise to a broad band (about 50 cm^{-1} in width) termed a "phonon wing" (PW) about 50 cm^{-1} to the blue of the absorption ZPL and about 50 cm^{-1} to the red of the emission ZPL, as shown in Figure 5 (p. 20).[40]

The ratio of the intensity of the ZPL to the sum of the ZPL and the PW contributions is given by the Debye-Waller factor, which is dependent upon two important parameters.[40] The first is a coupling

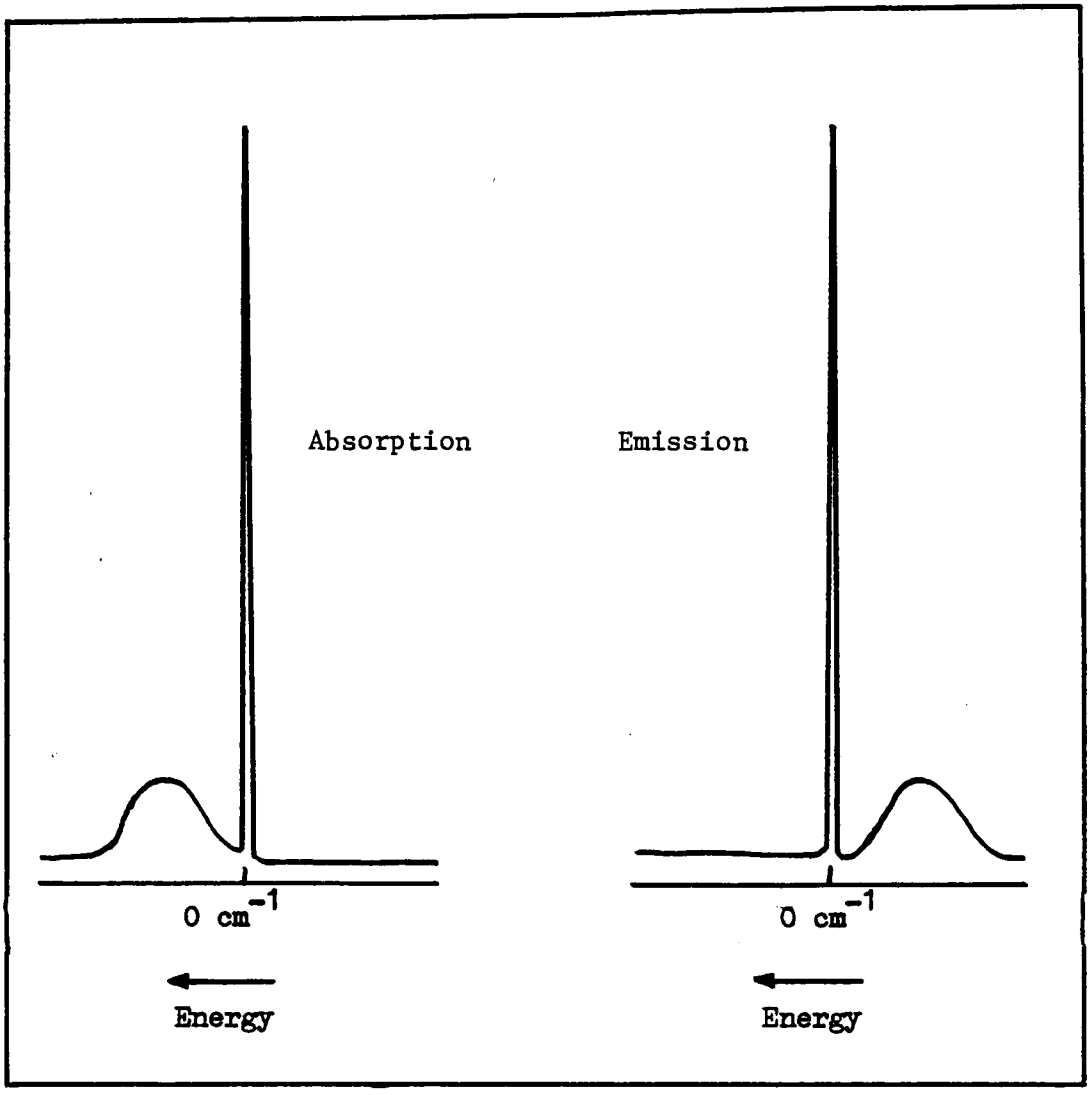

Figure 5. Illustration of ZPL and PW line shapes.

parameter which is related to the displacement energy of the phonon oscillator (i. e., to the magnitude of the changes in the solvent cage structure upon excitation of the absorbing species). The relative intensity of the PW increases as the displacement energy increases. Temperature is the second important parameter. A decrease in temperature reduces the population of the higher phonon modes, which reduces the magnitude of the phonon interaction. As phonon frequencies vary from a few tens of cm^{-1} down to almost zero cm^{-1}, even a temperature near 0 K may populate phonon modes higher than the lowest state. The net result is a strong dependence of the PW contribution on the temperature.[39] Figure 6 (p. 22) illustrates the effects of increased temperature and strong phonon coupling on the ZPL and the PW. An increase in either increases the PW contribution while an increase in temperature also increases the possibility of anti-Stokes phonon interaction which further broadens the spectra.

The finite width of a fluorescence band in the case of heterogeneous broadening is described by the summation of all the contributions of all excited molecules. In a low-temperature solid matrix, the major contribution to the bandwidth in most cases is the shift in wavelength of the electronic spectra of different molecules of the same compound in various microenvironments.[39] The presence of PWs also adds some width to the band. There are two strategies for reducing this width. Experimental conditions can sometimes be chosen such that the solvent shift distribution is quite narrow. This reduces the emission bandwidth and is the approach taken in Shpol'skii experiments.[29] The second approach is to experimentally excite only

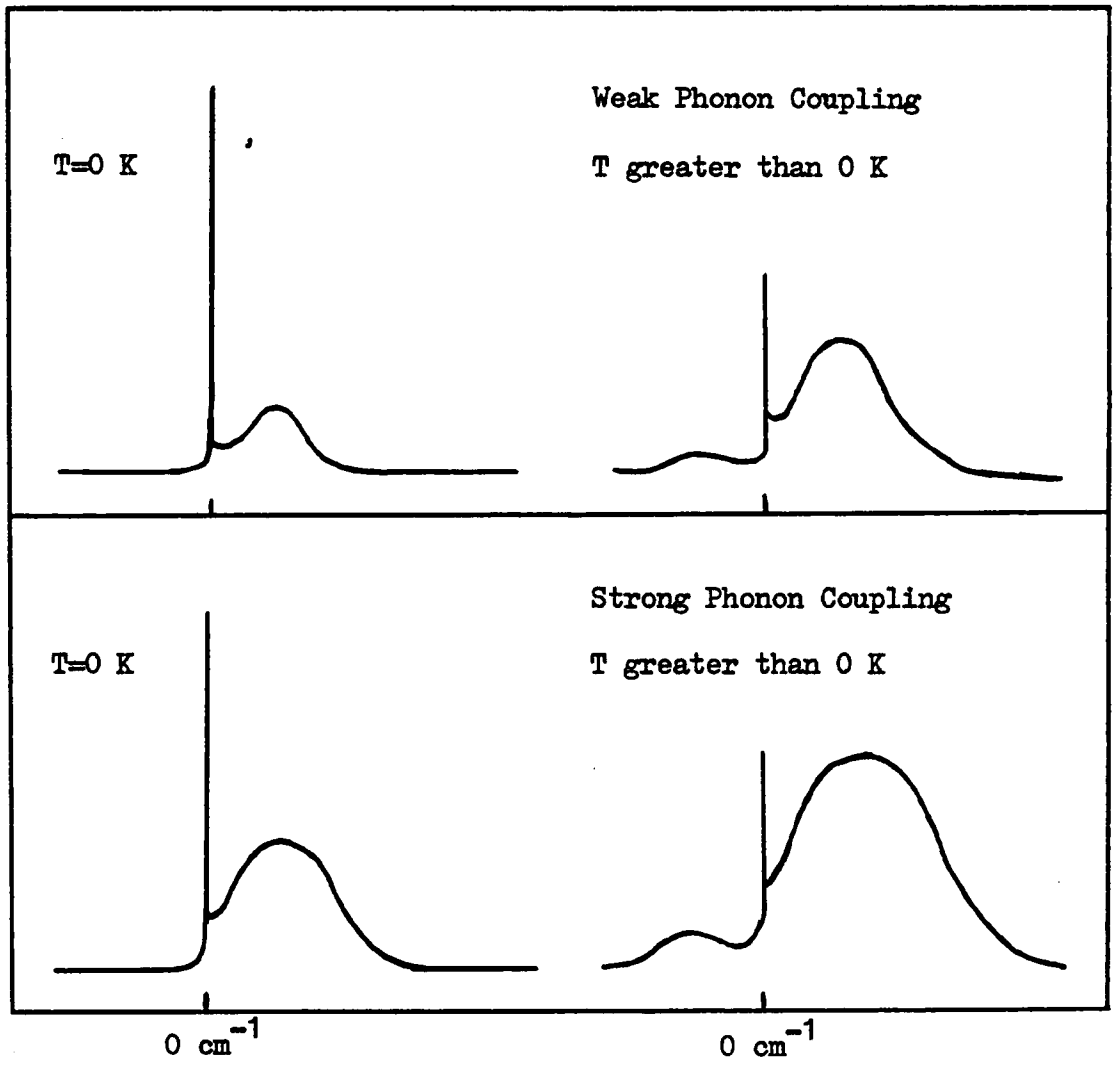

Figure 6. Illustration of dependence of phonon coupling strength and temperature on line shape.

those molecules having virtually the same ZPL transition frequency.[39] The latter strategy is the basis of site selection.

2. Performing Site Selection

Highly monochromatic light is needed to address only molecules exhibiting nearly identical solvent shifts; hence, a laser excitation source is highly desirable.[39] A broadband source would serve only to excite the whole ensemble. Most previous site selection work has been performed by excitation directly into the 0-0 absorption band[38] with excitation into the first vibronic band also possible.[41] The higher vibronic bands of molecules in different sites usually overlap to the extent that excitation into these higher levels tends to populate excited-state levels of molecules in a variety of different environments. The higher energies of excitation therefore lead to broadened spectra.[40] Figure 7 (p. 24) compares the effect of using different excitation energies. Absorption at energy "a" populates only those sites with energy levels equivalent to the site labeled A. At a higher excitation energy, "b," site C is populated by ZPL absorption. There is also a possibility that sites A and B will be excited by absorption into their PWs. This finite probability is dependent upon the degree of phonon coupling and indicates that excitation on the red edge of the 0-0 band is highly desirable. Since the phonon coupling is strongly dependent upon the temperature, as low a temperature as is economically practical is necessary (4.2 K is normally necessary).[39] Excitation at energy "c" illustrates the method of exciting into the first vibronic level. Again, red edge excitation is desirable as illustrated by the absorption labeled "d."

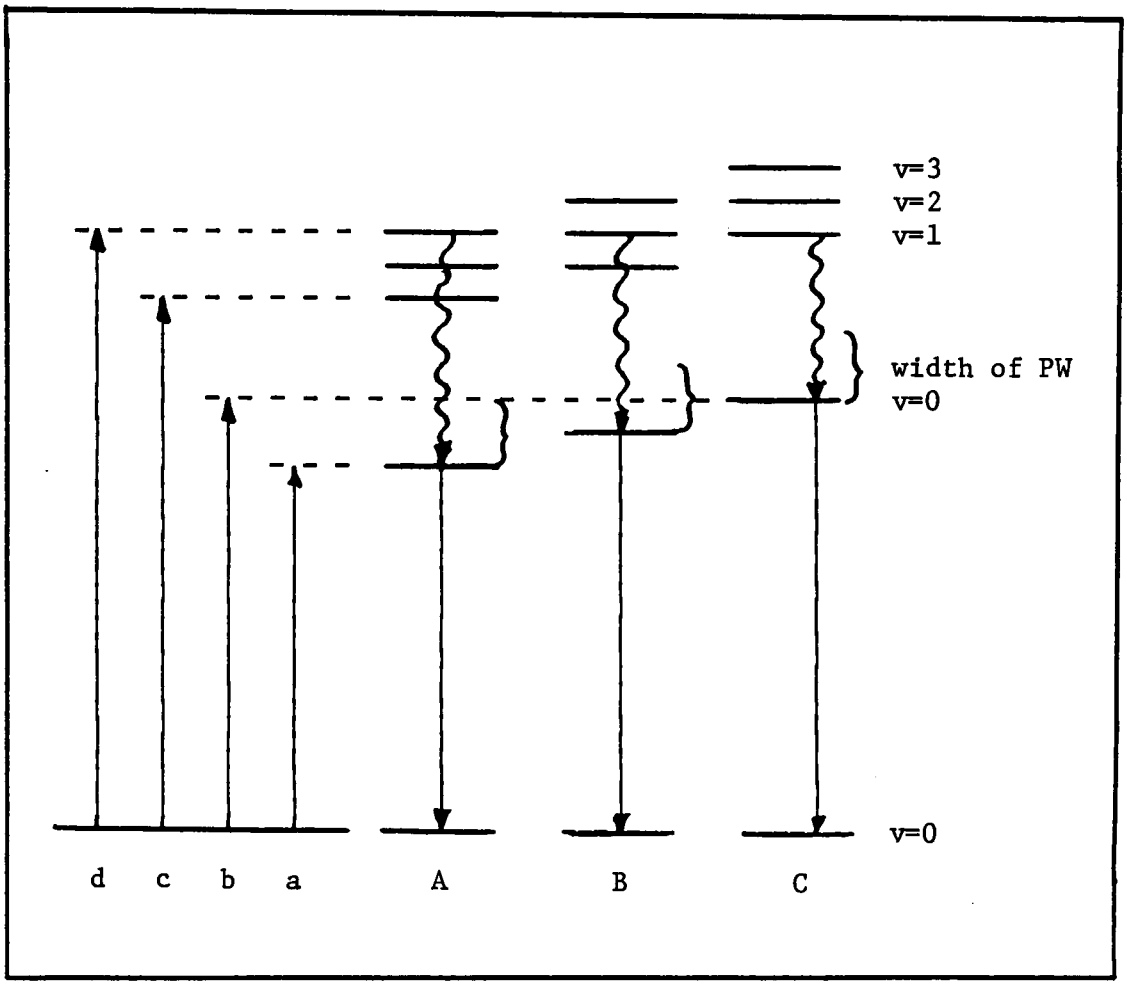

Figure 7. Mechanistic illustration of dependence of site selection on excitation energy.

Excitation at the higher energy excites all sites due to the overlapping vibronic levels. Achievement of site selection under conditions of excitation into the first vibronic band is possible only when the first vibronic level is well above the v=0 level, its corresponding PW, and in the absence of overlap from higher vibronic levels.

3. Conclusion

Site selection spectra can be obtained from molecules embedded in a variety of different matrices. For example, site selection spectra have been obtained from perylene in frozen solutions of n-octane,[37] ethanol,[42] and n-undecane,[39] and by matrix isolation in n-heptane[32] and argon (present work). These spectra of perylene consist of approximately twelve ZPLs with most being less than 1 cm^{-1} wide. It is noteworthy that the ZPLs are generally broadened by instrumental limitations. The ZPLs are superimposed on a broad background composed of the PWs which accompany each ZPL. Similar spectra of other compounds have been obtained. However, instances are known in which no line narrowing is seen even at a temperature of 2 K.[43]

Most of the compounds which have been examined by SSS since Personov's first description[39] have been restricted within a rather narrow range of PAHs.[37,39,41-46] Site selection has also been applied to biological systems[39,47,48] and to photochemistry.[49] Past studies have centered on obtaining physical data on inhomogeneous broadening or on the structure of vibrational states.

Although SSS has obvious analytical potential, it has thus far received little analytical application. Brown, et al.[51], have applied SSS to glassy frozen solutions of PAHs. Linear dynamic ranges of concentration for pyrene and anthracene (individually) extended over three decades in concentration. Detection limits were reported to be sub-part-per-billion and relative precision was about 8%. Standard addition and internal standards were not used. An analysis of a solvent refined coal sample was also reported. Seven PAHs were identified in the sample and the measured concentrations of pyrene and benzo(a)pyrene agreed to within 20% of the values for the same compounds which had been previously obtained from GC-MS. One feature of this work was that no sample preparation (other than dilution) or preseparation was made before the analysis.

F. Purpose

The purpose of the present work is to investigate SSS as applied to the qualitative and quantitative fluorometric analysis of matrix-isolated PAHs. Conventional fluorometry of matrix-isolated PAHs has been demonstrated to be an excellent means of analysis for PAHs, but is still limited in many cases due primarily to insufficient resolution of highly complex mixtures. The qualitative application of SSS to MI fluorometry is obvious. The high resolution capabilities of SSS should enable the analysis of exceedingly complex mixtures of PAHs. Although quantitative SSS may not achieve improved results over conventional MI fluorometry in all cases, it is the purpose of this work to also investigate the quantitative abilities of SSS of matrix-isolated PAHs.

CHAPTER II

EXPERIMENTAL DETAILS

A. Materials

1. Solvents

The solvents acetone, n-heptane, methanol, and 2-propanol were "Distilled in Glass" grade from Burdick and Jackson, Muskegon, Michigan. "Distilled in Glass UV" grade n-hexane from the same supplier was used. Ethanol was pesticide quality from Matheson, Coleman, and Bell of Norwood, Ohio. All solvents were used in various cleaning procedures and all but 2-propanol were used also in the preparation of sample and standard solutions. Ethanol was also used as a solvent for the laser dyes C1 and C120, shown in TABLE I (p. 28). The 2-propanol was used as a solvent for the laser dyes RB, RB+CVP, and R6G+CVP, shown in TABLE I.

2. Laser Dyes

Abbreviations for and pertinent information on the laser dyes used in this work are listed in TABLE I (p. 28). PBD, BBQ, PBBO, DPS, Bis-MSB, C495, and R6G were obtained as stock solutions from Molectron Corporation of Sunnyvale, California. C120, C1, RB, and CVP were obtained as "laser grade" solids from Eastman Organic Chemicals, Rochester, New York.

3. Gases

The following gases and liquified gases from the indicated suppliers were used in the indicated manner.

a. Nitrogen. Nitrogen used for matrix material was research

TABLE I

LIST OF LASER DYES

Abbreviation	Complete Name	Solvent	Concentration (M)	Wavelength Range (nm)
PBD	2-(4-biphenylyl)-5-phenyl-1,3,4-oxadiazole	Toluene/Ethanol	5×10^{-3}	360-386
BBQ	4,4'''-bis-butylactyoxy-quaterphenyl	Toluene/Ethanol 50/50	2.5×10^{-3}	373-399
PBBO	2-(4'-biphenylyl)-6-phenylbenzoxazole	Toluene/Ethanol 70/30	5×10^{-4}	391-411
DPS	4,4'-diphenylstilbene	p-Dioxane	Saturated	396-416
Bis-MSB	1,4-bis-(2-methylstytyl)benzene	p-Dioxane	1.2×10^{-3}	411-430
C120	Coumarin 120	Ethanol	5×10^{-3}	420-457
C1	Coumarin 1	Ethanol	10^{-2}	440-478
C495	Coumarin 495	Ethanol	10^{-2}	515-583
R6G	Rhodamine 6G	Ethanol	5×10^{-3}	568-605
RB	Rhodamine B	Ethanol	5×10^{-3}	594-643
RB+CVP	RB + Cresyl Violet Perchlorate	Ethanol	2.5×10^{-3} in RB 6×10^{-3} in CVP	628-651

TABLE I (CONTINUED)

Abbreviation	Complete Name	Solvent	Concentration (M)	Wavelength Range (nm)
R6G+CVP	R6G + Cresyl Violet Perchlorate	Ethanol	2.5×10^{-3} in R6G 3.3×10^{-3} in CVP	641-687
RB+NBAP	RB + Nile Blue A Perchlorate	Ethanol	3.8×10^{-3} in RB 8×10^{-4} in NBAP	683-710
RB+OXIP	RB + Oxazine 1 Perchlorate	Ethanol	5×10^{-3} in RB 5×10^{-3} in OXIP	705-750

purity (99.9995%) from Matheson Gases of Lyndhurst, New Jersey.

b. Liquefied Nitrogen. Nitrogen for the nitrogen laser was purchased in liquefied form from Oak Ridge National Laboratory, Oak Ridge, Tennessee.

c. Helium. Helium gas, used to pressurize a liquid helium Dewar, was High Purity (99.995%) from Matheson Gases, Lyndhurst, New Jersey.

d. Liquefied Helium. Liquefied helium used for the operation of the Heli-Tran liquid helium refrigerator was obtained from Linde Corporation of Birmingham, Alabama.

e. Argon. Argon used for matrix material was research purity (99.9995%) from Matheson Gases of Lyndhurst, New Jersey.

4. Polycyclic Aromatic Hydrocarbons

All PAHs used in this study are listed in TABLE II (p. 31).

5. Miscellaneous

Flav-O-Rich milk (Louisville, Kentucky) was used as a scattering medium for measuring the laser linewidth and was obtained from Arnold's, University of Tennessee, Knoxville, Tennessee.

B. Equipment

1. Refrigerators

The cryostats used for sample preparation were a closed cycle refrigerator ("Spectrim" Spectrometric Sample Conditioner, CTI Cryogenics, Waltham, MA) and a liquid helium refrigerator (LT-3-110 "Heli-Tran" system, Air Products, Allentown, PA). These refrigerators lowered the temperature of the 0.625" diameter sapphire windows attached to the cold end of each refrigerator to that needed for the

TABLE II

POLYCYCLIC AROMATIC COMPOUNDS

Compound	Structure	Source
1-Naphthol	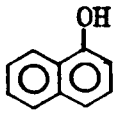	RFR Corp., Hope, RI
2-Naphthol	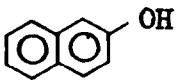	RFR Corp., Hope, RI
1,5-Dihydroxynaphthalene	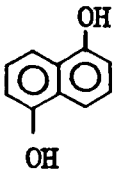	RFR Corp., Hope, RI
1,7-Dihydroxynaphthalene	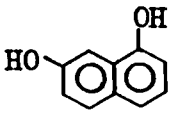	RFR Corp., Hope, RI
2,3-Dihydroxynaphthalene	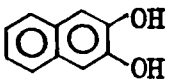	RFR Corp., Hope, RI

TABLE II (CONTINUED)

Compound	Structure	Source
2,7-Dihydroxynaphthalene	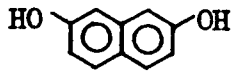	RFR Corp., Hope, RI
Fluoranthene	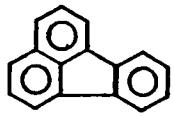	Duke Standards, Palo Alto, CA
Pyrene	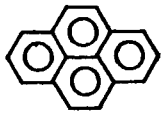	B. Pauric, Philadelphia, PA
Benzo(a)fluorene	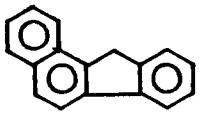	K&K Laboratories, Plainview, NY
Benzo(b)fluorene	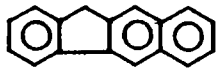	K&K Laboratories, Plainview, NY
Benz(a)anthracene	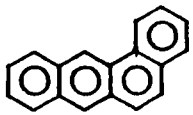	Fluka, AG, Switzerland

TABLE II (CONTINUED)

Compound	Structure	Source
Chrysene	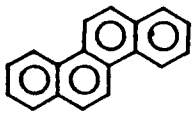	James Hinton, Columbia, SC
Tetracene	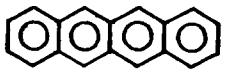	Aldrich, Milwaukee, WI
Benzo(e)pyrene	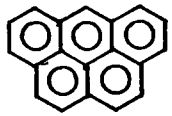	Environment Canada
Benzo(a)pyrene	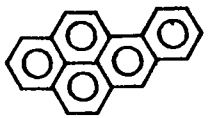	B. Pauric, Philadelphia, PA
Benzo(a)fluoranthene	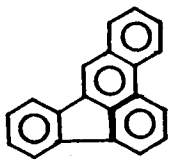	James Hinton, Columbia, SC

TABLE II (CONTINUED)

Compound	Structure	Source
Benzo(b)fluoranthene	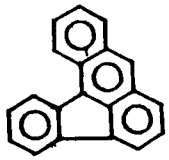	ICN Pharmaceuticals, Plainview, NY
Benzo(k)fluoranthene	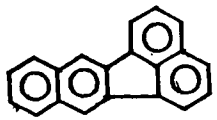	Environment Canada
Perylene	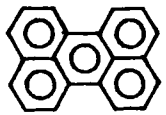	Aldrich, Milwaukee, WI
Benzo(g,h,i)perylene	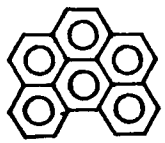	B. Pauric, Philadelphia, PA
Benzo(b)chrysene	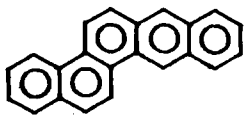	Aldrich, Milwaukee, WI

TABLE II (CONTINUED)

Compound	Structure	Source
1,2,3,4-Dibenzanthracene	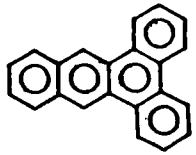	Aldrich, Milwaukee, WI
Pentacene	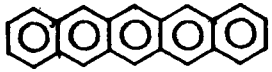	Aldrich, Milwaukee, WI
Coronene	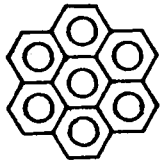	Chem Ser, West Chester, PA
Pyrenopyrene	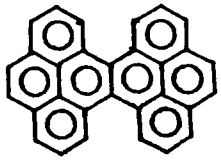	Alfred Bader, Milwaukee, WI

TABLE II (CONTINUED)

Compound	Structure	Source
Rubrene	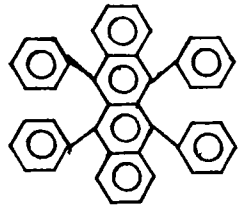	Chem Ser, West Chester, PA

particular experiment. The low temperature limit of the Spectrim was 15 K while that of the Heli-Tran was 4.2 K.

A detailed description of the Spectrim refrigerator is given by Stroupe.[52] Basically, it is a dual expansion stage, closed cycle refrigerator which uses helium as the refrigerant. The system includes a cold end as shown in Figure 8 (p. 38) which contains the expansion stages enclosed in a cold finger, a variable thermal resistor (VTR), a drive motor, the sample window mount, and a vacuum shroud. The cold end is connected to a compressor by helium supply and return lines and a power cord.

Operation was accomplished by evacuating the vacuum shroud to less than 50 microns. This vacuum acted as a heat shield. The Spectrim was then turned on and, in approximately 45 minutes, the cold finger was cooled to about 15 K. The sample window was attached to a cold tip which was in turn connected to the cold finger via the VTR. The VTR controlled the amount of heat conducted from the cold tip and window to the cold finger and could be used as a rough method of temperature control. Futher control of the sample temperature was achieved by controlled heating of the cold tip with an Air Products (Allentown, PA) ADP-E proportional temperature controller. The cold tip temperature was monitored by a chromel vs. gold (0.07 atomic percent Fe) thermocouple connected to the temperature controller.

The Heli-Tran system was used for operation below 15 K. This system consisted of a dual-jacketed helium transfer line connected to a cold end as shown in Figure 9 (p. 39). The cold end housed the

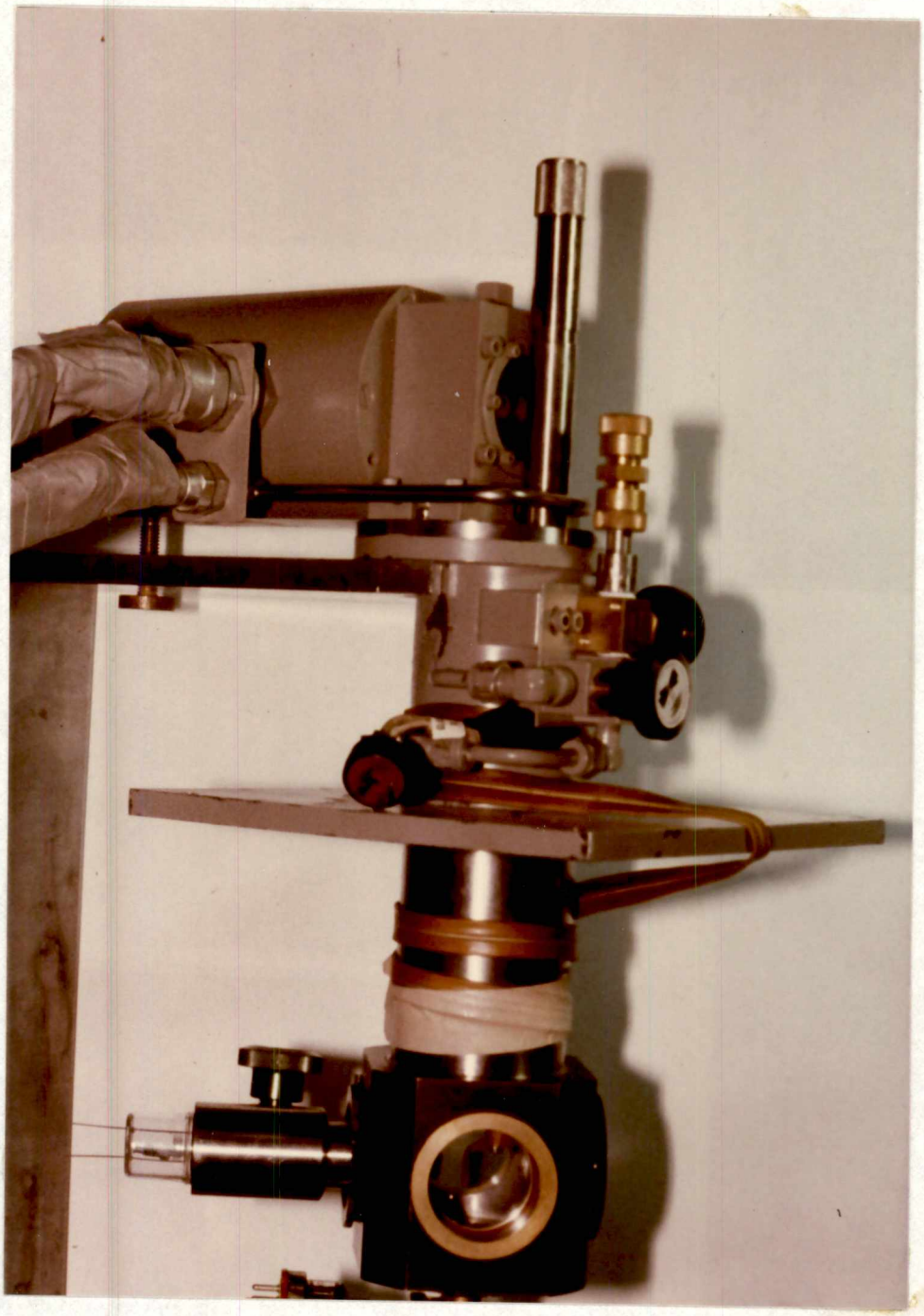

Figure 8. Cold end of the Spectrim refrigerator.

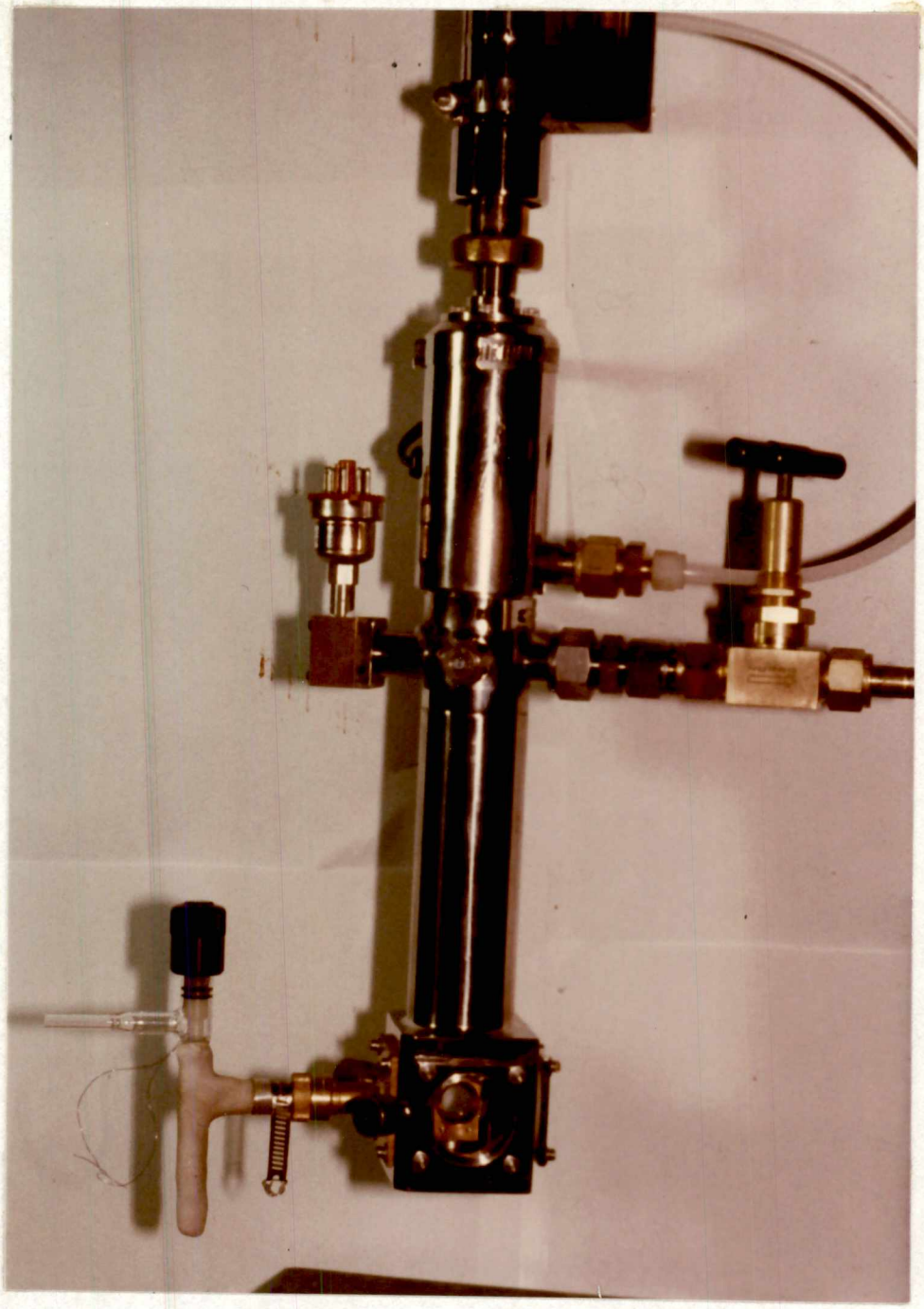

Figure 9. Cold end of the Heli-Tran refrigerator.

cold finger (called a "tip"), sample mount, vacuum shroud, vent gas heater, and a needle valve for rough control of liquid helium delivered to the tip. A tip flow metering valve connected to the tip flow outlet offered fine control of the tip flow and therefore the temperature of the sample. The transfer line contained a jacket through which a portion of the helium flow was diverted to aid in keeping the helium in the liquid state. This shield flow was controlled by a metering valve connected to the shield flow outlet. This valve also offered some degree of rough temperature control. An outer vacuum jacket acted as a heat shield for the shield jacket and inner helium line. This jacket was evacuated to less than 10^{-4} torr for several days prior to each use of the transfer line with a new Dewar of liquid helium.

Initial usage consisted of first purging the transfer line and the shield jacket with helium gas to remove impurities which might condense in the line at liquid helium temperature. Should a plug of this type develop anywhere in the system, the evaporation of the helium within the Dewar could raise the pressure to the point of violently exploding the Dewar. Proper purging of all parts of the system is extremely important for this reason.

Detailed instructions for the insertion of the Heli-Tran into the Dewar and for the operation of the Heli-Tran system are included in the Appendix. Temperature monitoring and control was accomplished with the same temperature controller used with the Spectrim and in the same manner. The vent gas heater is used to prevent the cold escaping helium from damaging the cold end.

2. Sublimation Cells

Two types of vacuun sublimation cells were used. The first was of the Knudsen oven type, shown in Figure 10 (p. 42), and was used for samples which were relatively nonvolatile. Samples which were in solution were injected into the glass cell with either a Hamilton 701N syringe or a 22 gauge nichrome wire. This entire assembly, shown in Figure 10, was then mounted into one port of the cryostat head. This head had five ports, four of which were used for observation and one for the oven assembly. This head assembly formed a vacuum chamber around the sample window. A Nupro bellows seal valve (SS-2H, Crawford Fitting Co., Solon, Ohio) admitted the matrix gas through the side port. The nichrome wire was attached to tungsten wires which fed through the closed end of the male 29/42 ground glass joint. This arrangement enabled electrical heating of the coil and the sample cell.

The second oven design, shown in Figure 11 (p. 43), was used for more volatile samples and for any sample deposited at 4.2 K. At 4.2 K, the Heli-Tran can cryopump the vacuum shroud to the point at which compounds which ordinarily require a considerable amount of heat to sublime will start to deposit during the cooling period rather than only during the deposition period. The external cell had a sample tube which could be cooled by an external cold bath. The cooling medium was usually dry ice/methanol or liquid nitrogen, depending upon the volatility of the sample. The sample tube and the delivery tube were wrapped with 22 gauge nichrome wire which was used to heat the

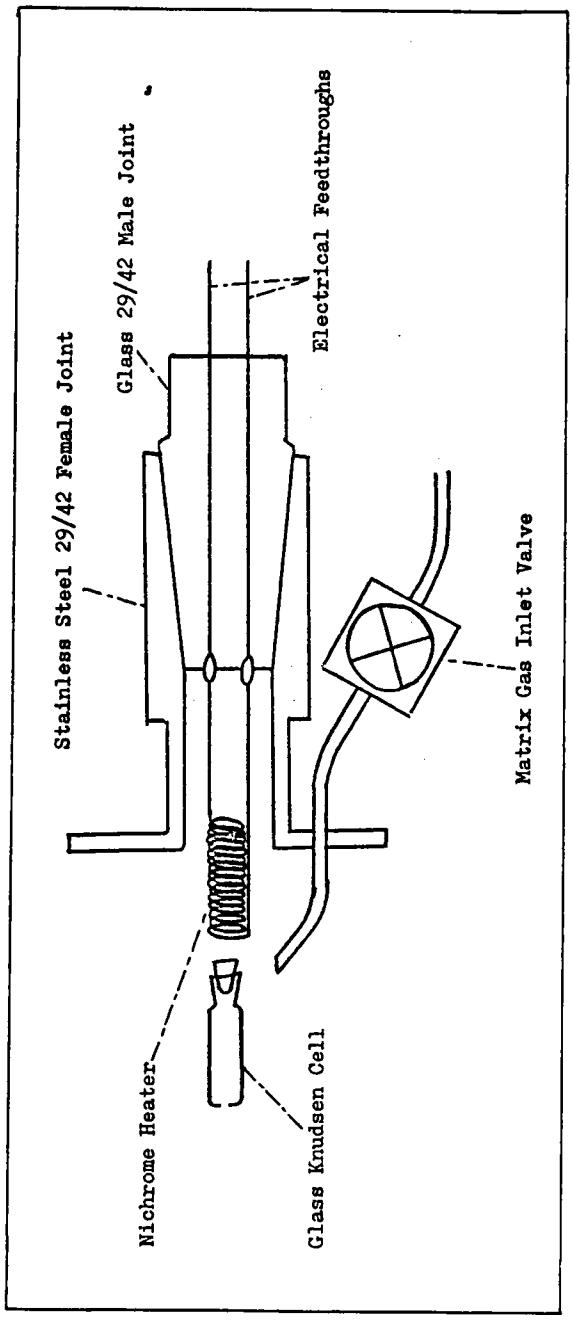

Figure 10. Knudsen oven assembly used with the Spectrim refrigerator.

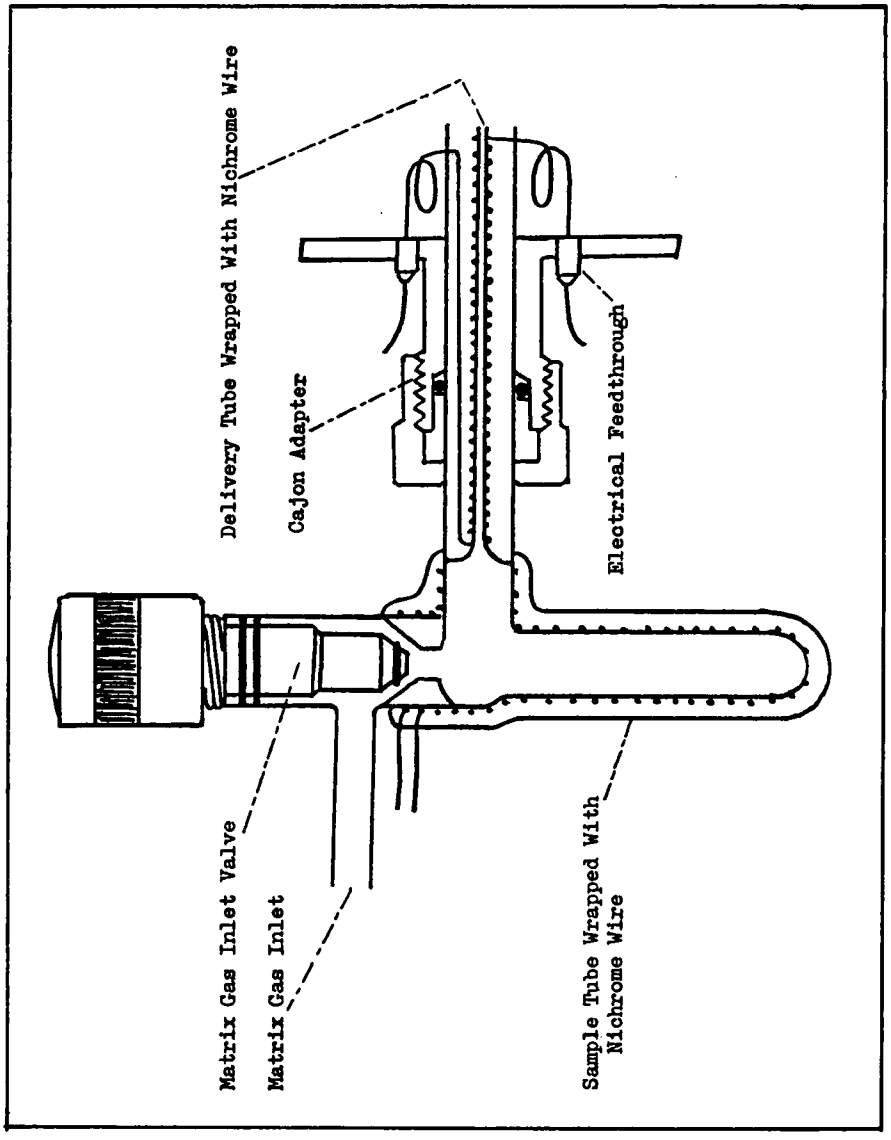

Figure 11. External cell assembly.

sample. The sample tube was also coated with Sauereisen cement to hold the wire in place and to spread the heat more evenly. The matrix gas was admitted through the 1/4" side arm and thus some degree of premixing occurred with the use of this cell. This cell was inserted through a 3/8" Cajon "Ultratorr" adapter (Crawford Fitting Co., Solon, Ohio) soldered onto a brass plate. The plate contained two electrical feedthroughs for connection to the delivery tube wire wrap. This design also allowed the cell to be moved back and forth while the cryostat was instrumented and under vacuum. Placement of the end of the delivery tube to within a few millimeters of the window to concentrate the deposit into a smaller region was possible with this cell. After deposition, the cell could be pulled back to clear the window for spectrometric observation.

3. Vacuum Line

The basic vacuum line has been previously described[52,53]; some changes in the basic design were made in the present work. The line had two sections, shown in Figure 12 (p. 45): a vacuum section and a deposition section. The vacuum section consisted of a CVC diffusion pump (CVC Products, Rochester, New York) backed by a Welch "Duo Seal" mechanical pump. The vacuum section was constructed of 1/2" copper tubing. Circle Seal shutoff valves (Anaheim, California) were connected such that the diffusion pump could be bypassed to enable initial evacuation of the cryostats. Liquid nitrogen cold traps were also used to prevent pump oil from entering the cryostats or the deposition section of the line and to achieve a higher pumping speed. A 1/2" stainless steel flexible tube was used to connect the vacuum line to

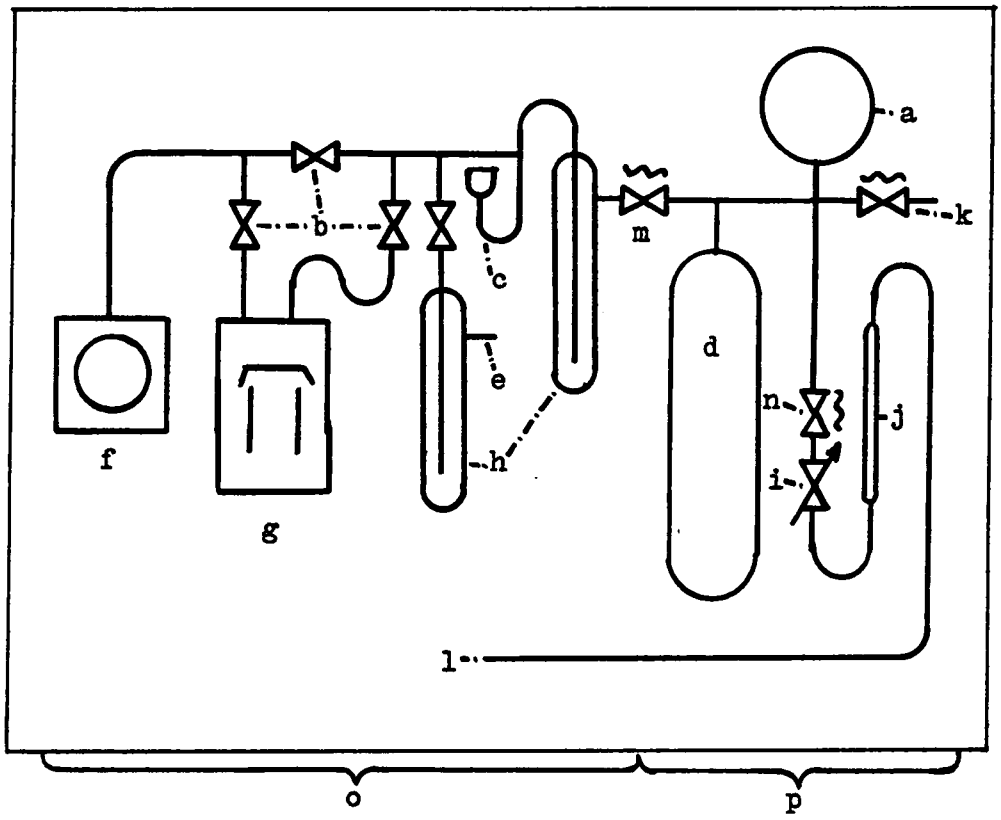

Figure 12. Schematic diagram of vacuum line.

a. Pressure gauge, b. Diffusion pump bypass valves, c. Thermocouple pressure gauge, d. Matrix gas reservoir, e. Outlet to cryostat, f. Mechanical rotary pump, g. Diffusion pump, h. Liquid nitrogen cold traps, i. Metering valve, j. Flowmeter, k. Recharging valve, l. Deposition line to cryostat head, m. Valve separating vacuum section from deposition section, n. Shutoff valve, o. Vacuum section, p. Deposition section.

both cryostats and to the vacuum jacket of the Heli-Tran transfer line.

Bellows seal valves connected the vacuum section to the deposition section via a liquid nitrogen cold trap. This section was fabricated from 1/4" copper tubing and a 1500 mL glass storage bottle connected with a glass-metal transition tube. This bottle contained the matrix gas. A Robertshaw "Accragauge" (Knoxville, Tennessee) was used to monitor the gas pressure. A bellows seal metering valve (B-4-BMG, "Nupro," Crawford Fitting Co., Solon, Ohio) and flowmeter ("Lab Crest," Warminster, Pennsylvania) were used to regulate the gas flow. Connection to the sublimation cells was made by 1/8" copper tubing which contained three loops which were used as a cold trap. A Cajon VCR gland (Crawford Fitting Co., Solon, Ohio) silver-soldered to the end of the 1/8" tube made the connection directly to the internal assembly and to the external cell via an adapter.

The deposition section of the vacuum line was refilled with matrix gas through a bellows seal valve acting as an inlet port. Evacuation of the deposition section to less than 10^{-4} torr for at least one hour always preceeded a refilling.

4. Steady-State Spectrometer

The instrument used for steady-state fluorometry has been described previously.[52] It consists of the following components:

1. A 2500 watt mercury-xenon compact arc lamp (Model 929B, Conrad-Hanovia, Newark, New Jersey) powered by a Schoeffel LPS 400 power supply.

2. A 1/4 meter, high throughput excitation monochromator (GM-250, Schoeffel Instrument Corp., Westwood, New Jersey).

3. Collection optics and a sample chamber.

4. A 3/4 meter emission monochromator (Model 1702, Spex Industries, Metuchen, New Jersey) with a 1200 groove/mm grating "blazed" at 300 nm.

5. Detection electronics consisting of an RCA 8850 photomultiplier and seven ORTEC (Oak Ridge, Tennessee) NIM modules: 9201 photomultiplier base, 456 high voltage power supply, 9301 preamplifier, 9302 amplifier-discriminator, 9315 photon counter, 9320 sampling and control unit, and 9325 D/A converter, all powered by a 401A NIM power bin.

6. A strip chart recorder (Speedomax W, Leeds and Northrup, Philadelphia, Pennsylvania).

A schematic diagram of this spectrometer is shown in Figure 13 (p. 48).

5. Dye Laser Spectrometer

The laser spectrometer was constructed from commercial components. The excitation source was a Molectron (Sunnyvale, California) DL-14P dye laser pumped by a Molectron UV-24 nitrogen laser. A Hewlett-Packard 8013B pulse generator supplied a trigger signal to the nitrogen laser. This external trigger served as a remote control for turning the nitrogen laser on and off and for setting the repetition rate.

When needed, the dye laser output was frequency doubled by one of two potassium dihydrogen phosphate (KDP) crystals also supplied by Molectron. The wavelength being doubled determined the choice of KDP crystals. For reasons stated in Chapter III, a polarizing filter

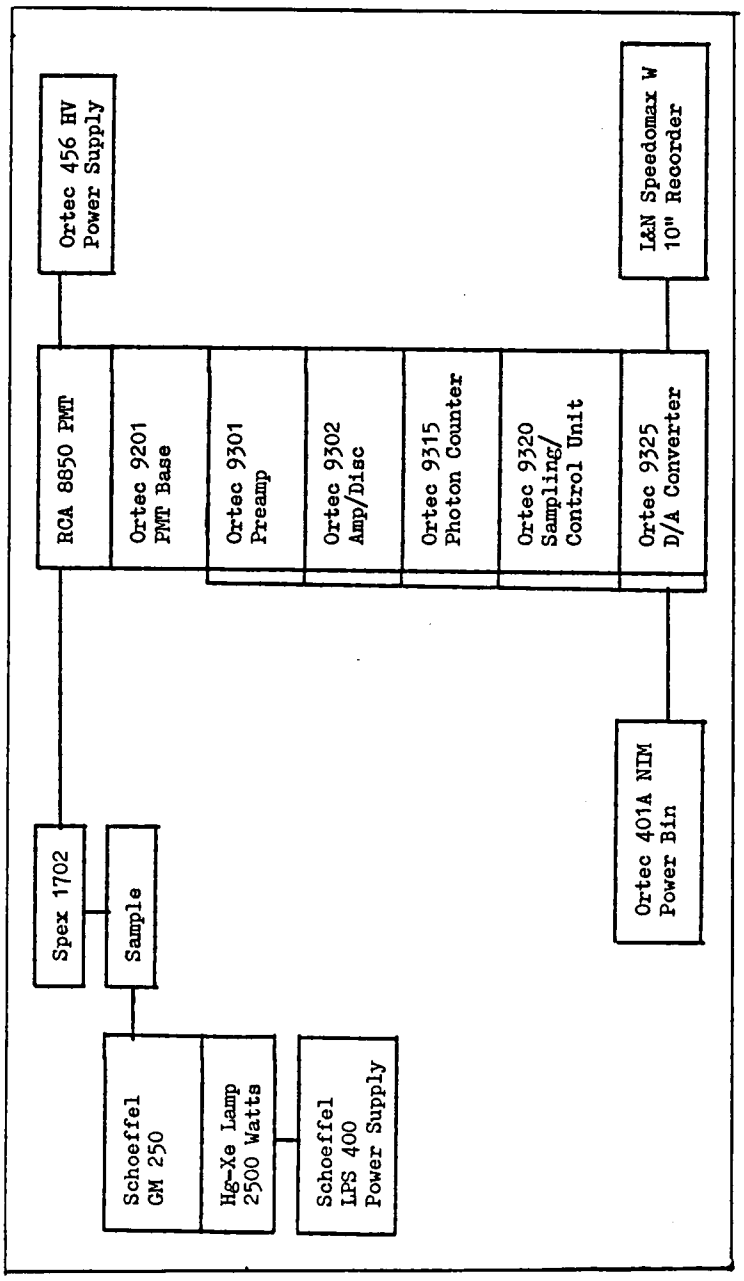

Figure 13. Schematic diagram of the steady state fluorometer.

was sometimes placed along the optical axis of the dye laser between the oscillator output mirror and the amplifier dye cell. The polarizer was placed such that only the horizontal components of the emission were passed.

A 1" diameter convex lens of 50 mm focal length was used to focus the fluorescence emission onto the entrance slit of the monochromator.

The emission monochromator was a Jobin-Yvon HR-1000 (Instruments SA, Metuchen, New Jersey) with an 1800 groove/mm, 120 x 140 mm, holographic grating "blazed" at 300 nm. The focal length was one meter and the aperture ratio was f/6.8. This monochromator exhibited a reciprocal linear dispersion of 8.0 Å/mm.

Photoelectric detection was accomplished by an RCA 8850 photomultiplier powered by an ORTEC (Oak Ridge, Tennessee) 456 high voltage power supply. A Tektronix (Beaverton, Oregon) sampling oscilloscope processed the PMT signal. The timed and amplified signal from the oscilloscope was plotted on an Omnigraphic 2000 XY recorder (Houston Instruments, Austin, Texas). The oscilloscope was a 5440 mainframe with a 5S14N dual trace delayed sweep sampler module. A 5A45 vertical amplifier was also used in conjunction with laser pulse energy measurements. The oscilloscope was triggered by a GTE high speed optical detector (Model 525, GTE Sylvania, Mountain View, California) placed in the dye laser at a point where it was exposed to the remainder of the nitrogen pump beam which had passed through the two beam splitters inside the dye laser.

A diagram of this spectrometer is shown in Figure 14 (p. 50).

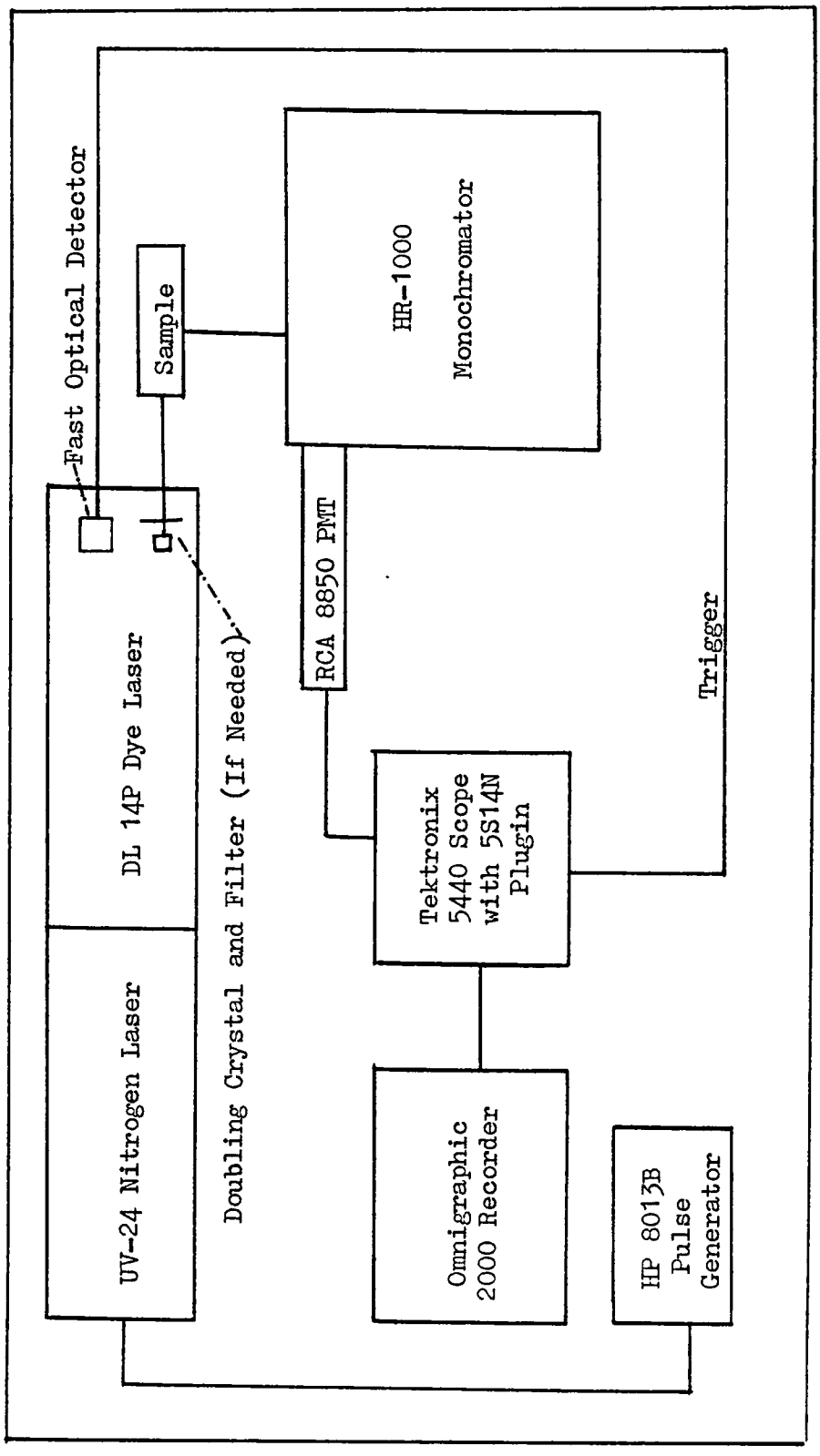

Figure 14. Schematic diagram of the dye laser spectrometer.

C. Procedures

1. Sample Preparation

Prior to preparation of a deposit, the Knudsen cell, sapphire window, and window mount were cleaned twice in boiling hexane and then twice in boiling acetone. The inside of the head and the area of the cryostat around the electrical feedthroughs and the window mount were swabbed with Kimwipes soaked in hot hexane. If the external cell was used, the valve stem was removed and the inside of the cell was rinsed repeatedly with boiling hexane and then with boiling acetone. The window used with the Heli-Tran was cleaned in the same manner as the window for the Spectrim. The vacuum shroud and head of the Heli-Tran (one unit) was swabbed with Kimwipes soaked in hot hexane. Acetone was never used to clean either head as the Viton O-rings in the heads were subject to chemical attack by acetone. This cleaning procedure was used prior to each deposit.

The sample was introduced into the Knudsen cell or the external cell (by removing the valve stem) by pipetting with either a Hamilton 701N syringe or a 10 microliter Oxford pipette. A gentle stream of air was passed over the sample to evaporate the solvent. The cell was then closed and mounted onto the head. After the head was installed onto the cryostat, the head and vacuum shroud were evacuated. The procedure for cooldown of each type of cryostat is described in Section B and in Appendix II.

Deposits made with the Heli-Tran were normally made at 15-20 K, and the sample temperature was lowered to 4.2 K after completion of a deposit. Since the helium flow was slowed slightly to raise the

temperature to 15-20 K, this procedure enabled a slight reduction in liquid helium consumption, compared with that encountered in the preparation of deposits at 4.2 K. Deposits made in this manner were generally clearer than they would have been if made at 4.2 K.

The matrix gas flow rate was generally maintained at about one millimole per hour. Matrix gas was deposited for five minutes prior to deposition of the sample. Deposition of the sample was accomplished by applying a multistep voltage ramp across the heater, which heated the sample cell to a final temperature of 80-100 C. The Knudsen cell was heated for 30-35 minutes, while the external cell was heated for 40-45 minutes. Preliminary experiments indicated that heating of the external cell for less than 40 minutes failed to deposit all of the sample, while 30 minutes generally sufficed for the Knudsen cell. The voltage applied to the delivery tube heater on the external cell was kept constantly high throughout the deposition to make sure that no sample condensed inside the delivery tube. The voltage applied was such that the temperature of the delivery tube remained at about 120 C. Matrix gas flow continued throughout the deposition and for 5-10 minutes after the heating was discontinued. Deposition of just matrix gas both before and after deposition of the sample assured that the solute molecules were "sandwiched" between matrix molecules only and were not adjacent to the window or to empty space. The cryostat was then ready to be disconnected from the deposition line after shutoff of all valves. The sample was then ready for fluorescence analysis.

2. Fluorescence Analysis

Procedures for steady-state fluorescence analysis were quite straightforward. After the cryostat was mounted in the fluorometer, the excitation wavelength, the monochromator slit width, the scan rate, the photon counting time and range, and the initial wavelength were chosen and set. The scan was begun and a fluorescence spectrum was obtained.

Operation of the dye laser spectrometer (DLS) was somewhat more complicated in certain respects. The dye cell translation and rotation controls (used to tune the laser) affected the angle at which the laser beam was emitted. It was necessary to retune the laser each time the dye or the dye cells were changed, and sometimes when the wavelength was changed for a given dye. Thus it was necessary to realign the sample in the DLS each time a new sample was placed in the DLS. This was accomplished by opening the monochromator slits to 500 μm, setting the monochromator wavelength to zero, removing the PMT (which was mounted such that it would simply swing away), looking into the exit slit at the zero order reflection from the grating, and visually aligning the sample with the DLS. This procedure became necessary when the helium-neon laser normally used for this purpose ceased to function. This procedure was followed with the laser on and the laser beam incident upon the sample.

After alignment, the monochromator was set at a wavelength at which it passed a fluorescence signal. At this time, the PMT power supply voltage, the oscilloscope sensitivity (vertical calibration), and the delay were set. The delay was measured from the point of the

fluorescence decay curve at which it began to rise from the baseline to the point on the decay curve set with the SCAN control on the oscilloscope. The choice of delay was often a compromise between discrimination from background and maximization of the fluorescence signal. Some sources of this background are discussed in Chapter III. After establishing the desired delay, the initial wavelength was set and the scan was begun.

Because emission bands which occur in site selection spectroscopy are very narrow, the response of the recorder had to be quite fast to obtain undistorted band shapes. For this reason, scan speeds were decreased whenever narrow bands were expected. Also, a 47 μF filtering capacitor normally placed across the recorder input terminals to filter out higher frequencies (noise) was removed to reduce the time constant of the recorder. This action had the unfortunate effect of increasing the noise level.

Peak heights were used as indicators of concentration. For precision measurements and quantitative measurements, an internal standard was used to negate, as effectively as possible, inconsistencies in the deposition procedure and excitation. The ratio of the analyte peak height to the internal standard peak height was plotted against sample size in all quantitative plots.

CHAPTER III

RESULTS AND DISCUSSION

A. Preliminary Studies of Instrumentation

During the preliminary stages of this work, two studies were undertaken to lessen the confusion which had existed among workers in this laboratory. Neither is directly related to the problem of this dissertation, but are included to clarify and organize some scattered information.

1. Contamination

The first study was designed to define the various sources and levels of contamination which has plagued this laboratory in the past.[52,53] TABLE III (p. 56) summarizes the procedure used in this study. A deposit of 100 ng each of pyrene, chrysene, benz(a)anthracene, and 4 μg of triphenylene was made to purposely induce the memory effect. Five N_2 blank deposits were then made. With the first two blank deposits made under the normal conditions of deposition at that time (superficial cleaning and no cold trap on the deposition line), the pyrene contamination decreased by roughly half. Thus the memory effect is strong with respect to pyrene. Other PAHs also demonstrated this effect; benzo(k)fluoranthene, benzo(b)fluorene, and benzo(a)pyrene are good examples. Generally, those compounds with high volatilities (naphthalene and anthracene for example) do not interfere with subsequent deposits.

When great care is taken to thoroughly cleanse the vacuum

TABLE III

SUMMARY OF PROCEDURE TO ISOLATE CONTAMINATION

No.	Deposit	Conditions	Contamination[1]	Comments
1	100 ng ea. of pyrene, chrysene, benz(a)-anthracene, and 4 ug triphenylene	Normal	——	Made to induce memory effect
2	N_2 blank	Normal	0.50	Memory effect for pyrene is strong
3	N_2 blank	Normal	0.25	
4	N_2 blank	Cleaned shroud	0.02	Memory effect due primarily to condensation of pyrene in vacuum shroud
5	N_2 blank	Deposition line immersed in LN_2	0.01	Pyrene was present in the N_2 matrix gas and was trapped by the cold trap
6	N_2 blank	Normal	0.02	

[1] Amounts are approximate and are relative to the pyrene fluorescence intensity of the initial deposit.

shroud and head with hot hexane, pyrene contamination is reduced significantly. This experiment, along with experience, indicated that the interfering PAHs condensed onto the inside of the vacuum shroud during deposition and/or warmup.

The best solution to this problem is to thoroughly cleanse the inside of the cryostat, especially the vacuum shroud. Although this can easily be done on the Model 21 cryostat used by Bilotta,[53] the Model 20 used in the majority of this work is not amenable to this procedure because the vacuum shroud is closed off from the rest of the cryostat. In this case, gentle heating of the vacuum shroud with a heating tape while evacuating the cryostat overnight produced very nearly the same results. It is recommended that the present Model 20 cryostat be retrofitted to a Model 21 cryostat when possible as cleaning the shroud has proven to be far more reliable than the heating method of reducing the memory effect.

It was thought that the remaining pyrene was present in the deposition section of the vacuum line. The deposition line was coiled into three loops which were immersed in liquid N_2 during a deposition. This procedure also cut the pyrene contamination as demonstrated with the next blank deposit which was made without liquid N_2; removing the liquid N_2 increased the pyrene contamination. At this level of contamination, however, experimental error could possibly yield this difference. A series of N_2 blank deposits were made in which increasing amounts of N_2 were deposited in 30 minutes per deposit. The pyrene fluorescence intensity was roughly linear with the amount of N_2 deposited.

A small amount of pyrene (equivalent to about 1 ng or less) was left in subsequent blanks and was never reduced. This contamination is attributed to the outgassing of the o-rings within the cryostat.[52,53]

A common practice of the members of this laboratory was to keep the roughing vacuum valve on the cryostat open during cooldown until a specified temperature was reached. The specified temperature varied with the particular worker and was usually 50-120 K. At approximately 20 K and below, the cryostat is a more effective cryopump than the mechanical pump. If the roughing valve is left open too long (i. e., the temperature becomes too low), pump oil vapor can diffuse to the cryostat and contaminate the deposit. This method of contamination was verified by leaving the roughing valve open during a blank deposit. The degree of contamination which occurred in this manner depended upon how long the valve remained open. This contamination usually formed a strong, broad background in the range of 330-460 nm. The solution to this problem is obvious. The roughing valve must be closed before the cryostat is cool enough to become an effective cryopump. Experience indicated that the valve should be closed at around 80 K or above.

The crevices formed in the joints between the sapphire window and its mount also formed spots where PAHs clung tenaciously. Boiling these parts in either acetone and/or hexane significantly reduced this source of the memory effect.

PAHs are also apparently strongly adsorbed onto the indium foil used for thermal contact between joints in the window and window mount.

This was verified by examining both new and used pieces of indium foil. Although no spectral contamination was ever attributed to PAHs adsorbed onto the indium, the use of indium foil was reduced to a minimum as a precaution.

In summary, there are a variety of sources of contamination, not all of which have been previously recognized. The memory effect is strong but can be reduced greatly by proper and thorough cleaning. Although this problem is quite obvious, it has not always been recognized. Contamination resulting from leaving the roughing vacuum valve open has been seen even when the valve is closed at temperatures as high as 80 K. A contaminated line and the above sources of contamination usually result in pyrene levels equivalent to 1-100 ng or more in extreme cases. Levels below about 1 ng are attributed to outgassing of o-rings and little can be done about this source except to eliminate as many o-rings as possible.

2. Sublimation Cells

The second study compared three types of sublimation cells or ovens which are used in this laboratory. Two types are described in Chapter II while the third (not otherwise used in this work) was described by Stroupe[52] and Bilotta.[53] Stroupe argued that the Knudsen cell design described in Chapter II was not useful for large volumes (greater than 20 μL) and that the 7/25 ground glass joint acted as a heat sink and condensed part of the PAHs on the joint rather than depositing them on the window. The volume problem was overcome merely by placing only about 10-20 μL of the sample in the cell at a time, evaporating the solvent, and repeating. Alternatively, more

concentrated samples could be used. To determine to what degree the glass joint acted as a heat sink, a chromel/alumel thermocouple was placed in the glass joint and the temperature was monitored during a simulated deposition. The temperature of the joint went to 100 C within 10 minutes of heating. This temperature is high enough to sublime all of the PAHs commonly used in this laboratory under normal deposition conditions. Although PAHs may initially condense partially on the glass joint in the early stages of deposition, they are effectively deposited during the latter stages. This predeposition of PAHs on the glass joint should actually have the effect of spreading the PAHs more evenly through the deposit by delaying the deposition of part of the sample. Deposits of equal amounts of benzo(a)pyrene were made with both the Knudsen cell type used in this work and the coolable type used by both Stroupe[52] and Bilotta[53] and were found to yield the same fluorescence intensities within experimental error.

The third type, an external coolable cell, was also compared to the first two. At first this cell yielded lower intensities, but this problem was solved by increasing the deposition time by about 10 minutes. This cell had a long (about 8 cm) thin tube through which the sample had to pass before entering the cryostat head. Apparently, this tube slowed the passage of the sample so that more time was needed for complete deposition.

Each cell was found to have slightly different operating characteristics and applications, but all yielded the same results for the majority of operations and so none is "better" than another for most applications.

The non-coolable Knudsen type was chosen for this work because of its simplicity, ease of operation, and high degree of reliability. The coolable Knudsen type used by Stroupe and Bilotta is an excellent oven, but was subject to an occasional electrical short and subsequent "burning out." The external, coolable cell was chosen for use on the Heli-Tran system because of the smaller head which prevented the inclusion of a relatively large oven inside the head. This cell also proved highly reliable.

B. Major Instrumental Problems and Solutions

Major problems developed with both the monochromator used for the laser studies and the laser itself. In certain cases, these problems actually prevented the observation of site selection and were very obnoxious.

1. HR-1000 Monochromator

Although the monochromator was specified to have a very low stray light level, two significant sources of stray light and one of scattered light within the monochromator were found and corrected. In all three cases, the cause was poor engineering of the monochromator, or uses of the monochromator not envisioned by the manufacturer.

The stray light manifested itself as a large signal, unaffected by the wavelength setting, which totally obscured the fluorometric signal in the worst cases and added a strong background in the best. Time resolution aided tremendously in discriminating against the stray light but the dynamic range of the photomultiplier (PMT) was not great enough to prevent the saturation of the photocathode and to detect

low levels of analyte (or analytes with short lifetimes) at the same time. Figures 15 (p. 63) and 16 (p. 64) illustrate the sources of the problem and their solutions. The emission monochromator was designed to accept gratings much larger than the 120 x 140 mm grating installed in this instrument. This meant that the collimating mirrors were much larger than were necessary for the intended use of this monochromator. The extra areas of the mirrors reflected the image of the entrance slit directly onto the exit slit output mirror. The reflections of the entrance slit passed the exit slit at a different angle than the light from the grating, but were still detected by the PMT. Placement of baffles in the positions indicated in Figures 15 (p. 63) and 16 (p. 64) blocked the passage of the stray light. These baffles were well out of the way of the light from the grating. To verify the elimination of the stray light, measurements of signal intensities from a deposit with and without the baffles in place were made. With the baffles in, the signal due to the fluorescence plus the background stray light decreased by the amount of the background only. The background of a blank deposit with the baffles in matched the background obtained when the entrance slit was totally blocked.

Much of the time, two strong bands appeared about 5 nm and 7 nm to the red of the laser line and were about 10-20% of the intensity of the laser line. As site selection involves excitation very close to the emission wavelengths, these bands proved extremely bothersome. The problem was traced to two surfaces in the monochromator's exit slit mount which were not properly blackened to prevent the scattering of light. As the monochromator was scanned

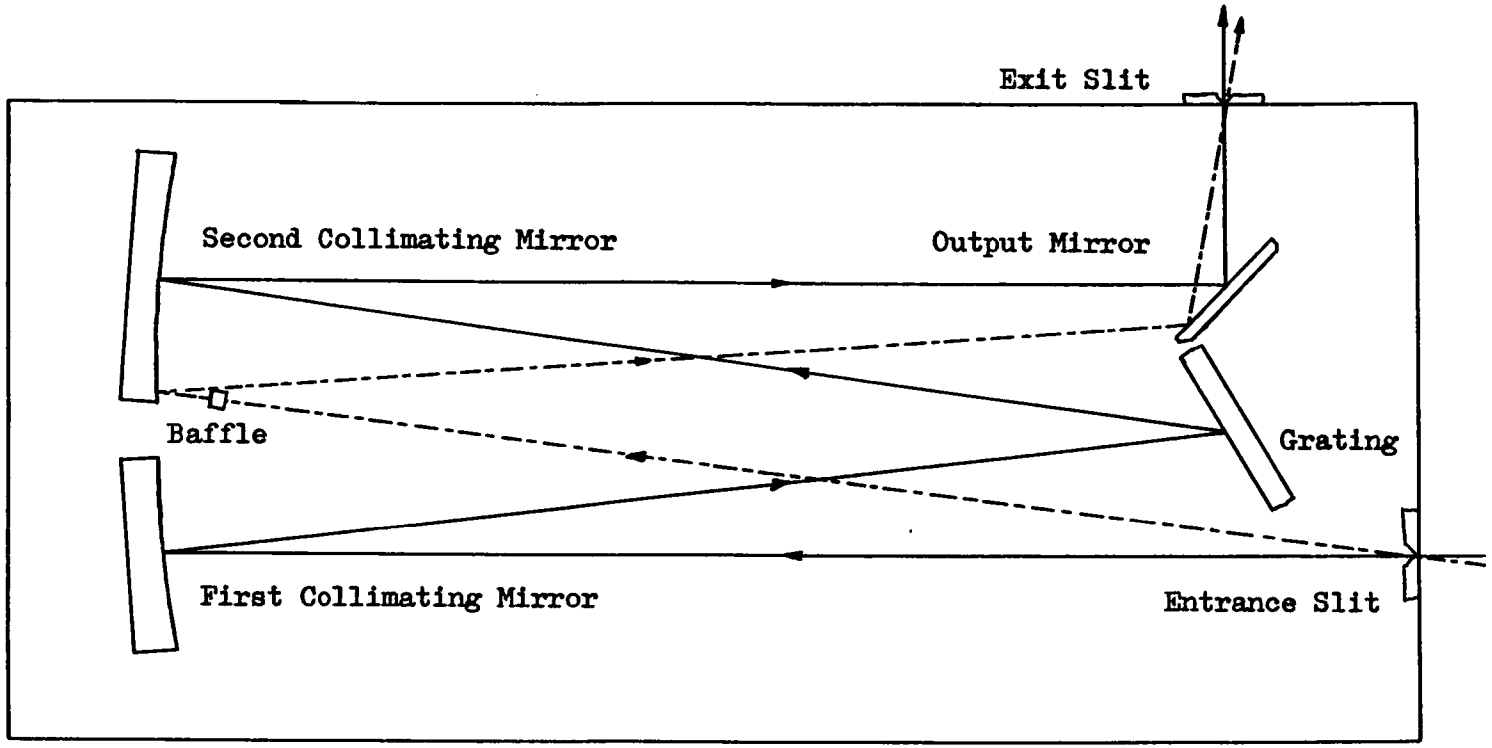

Figure 15. Emission monochromator showing first source of stray light.

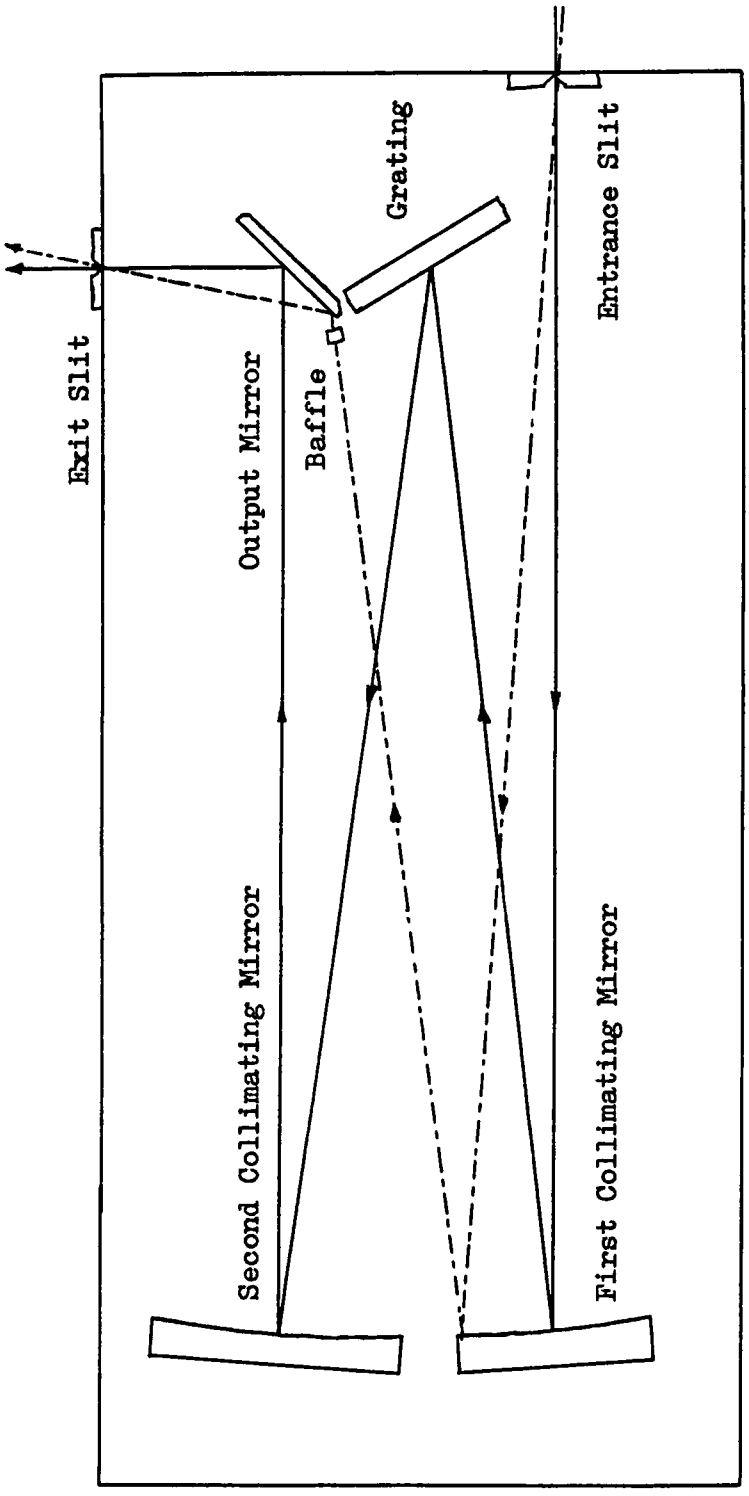

Figure 16. Emission monochromator showing second source of stray light.

to longer wavelengths from the laser line, the laser light would move in the direction indicated by the double arrow in Figure 17 (p. 66). When the laser light struck surfaces "a" (the slit opening mechanism) and "b" (part of the slit mount), it would scatter off of these surfaces with part of the scattered light emerging through the exit slit to the PMT. The lines 5 nm and 7 nm to the red of the laser line were the result of the laser scattering off of surfaces "a" and "b," respectively. Placement of a baffle in the position indicated prevented this scattering from occurring by blocking the laser light from either of these surfaces.

2. Dye Fluorescence

A strong background in the vicinity of the lasing wavelength as shown in Figure 18 (p. 67) also posed serious problems. The spectra in Figure 18 were obtained by scattering the laser emission with a cuvette of dairy milk. The sharp band is the lasing wavelength severely broadened by the use of relatively wide slits. The broad band centered at about 437 nm was found to be stray dye fluorescence from the oscillator cell in the laser which was amplified by the amplifier dye cell. The great intensity of this broad band relative to the lasing wavelength is a manifestation of the wide monochromator bandpass (2 Å) used to obtain these spectra. The laser line has a very narrow bandwidth (0.1 Å or less) and so had relatively low integrated intensity. The broad band has a low absolute intensity but a high integrated intensity as a result of its width. The PMT is an integrating detector over the bandwidth of the monochromator. Thus the intensity of the broad band appeared to be a significant

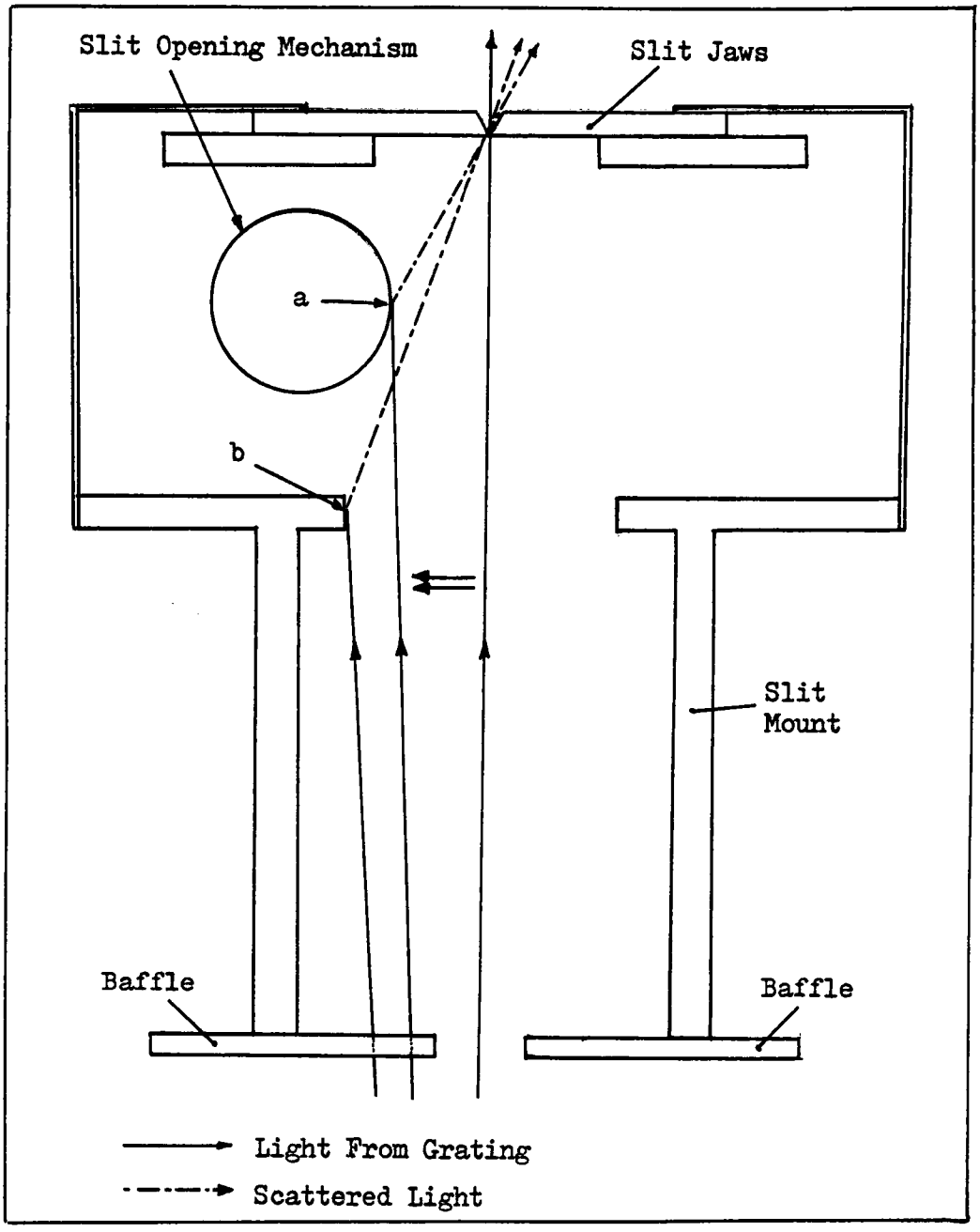

Figure 17. Cutaway of slit mount.

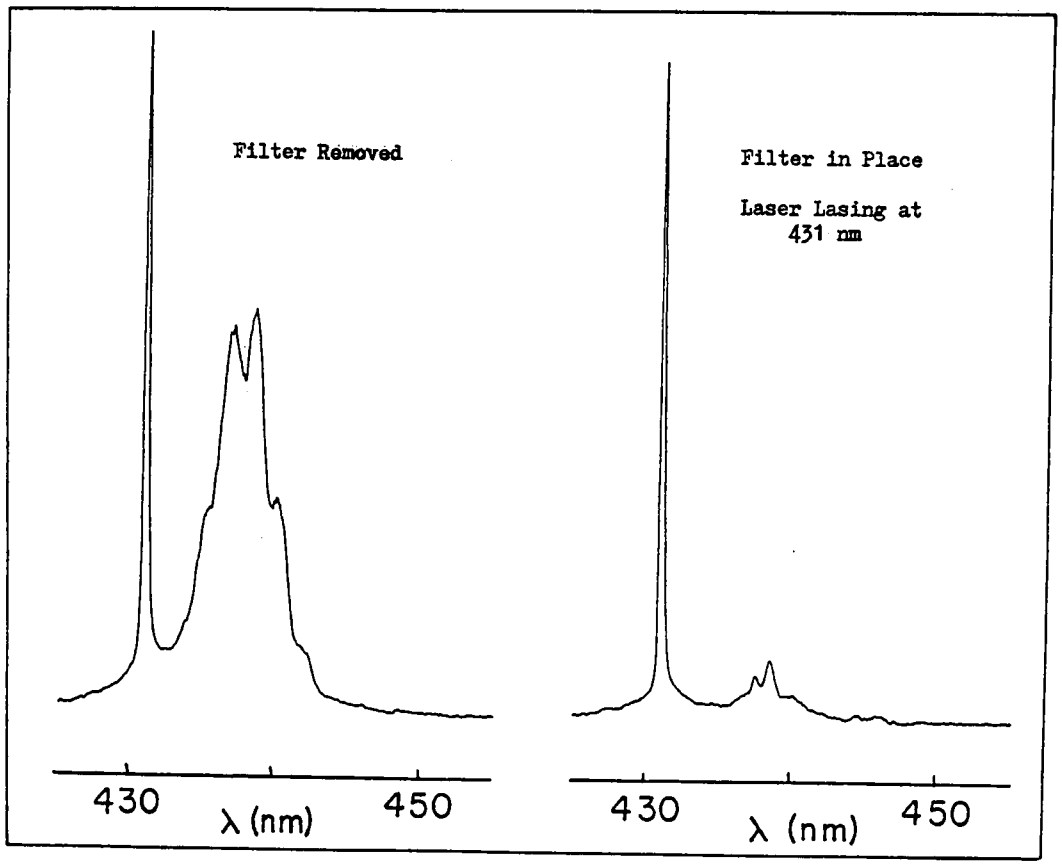

Figure 18. Effect of polarizing filter on stray dye fluorescence.

fraction of the intensity of the lasing line. By narrowing the slits, the broad band intensity dropped to less than 1% of the lasing line intensity. This broad band occurred with all laser dyes used in this study and was always centered at the peak lasing wavelength of each respective laser dye. The shorter wavelength dyes were particularily strong offenders. These bands often interfered with fluorescence spectra as they were commonly much stronger than the sample fluorescence emissions. This problem was severe when small quantities of analyte were being measured or the analyte being measured had a relatively short fluorescence lifetime.

The solution to this problem was the placement of a polarizing filter in the optical axis such that the filter passed only the horizontal component of the emission from the oscillator. This polarizer was placed between the amplifier dye cell and the oscillator output mirror. The laser radiation was passed easily as it was polarized horizontally. The stray dye fluorescence was preferentially polarized vertically and so was discriminated against. The spectrum of the laser resulting from the insertion of the polarizer is also shown in Figure 18 (p. 67). The broad band is greatly reduced but the laser line is virtually unaffected.

For several of the laser dyes, some of the stray dye fluorescence remained when the polarizer was included. This fluorescence could be either fluorescence from the oscillator dye cell which was polarized horizontally and/or fluorescence from the amplifier dye cell. An attempt to reduce this fluorescence further was made by removing the polarizer and using a small (1/3 meter) monochromator to separate

the lasing wavelength from the fluorescence. The monochromator separated the two components but also decreased the intensity of the laser line. A comparison of the effectiveness of the polarizer vs. the monochromator using scattered laser light was made. Although the monochromator was more efficient at separating the two components of the laser emission, the greater intensity (approximately twice as great) offered by the polarizer prompted the decision to use the polarizer for this work. The effect of the use of these two methods on the resolution of an actual deposit of benzo(a)pyrene was also examined; the discussion of this experiment is found on page 92.

3. Detector Electronics

When the DLS was originally set up, the synchronizing signal from the N_2 laser was used to trigger the sampling oscilloscope. This trigger source soon proved unsatisfactory because of severe jitter (about 50 ns) in the time between the synchronizing signal and the actual firing of the N_2 pump beam (about 700 ns). The time jitter is inherent to high voltage thyratrons of the type used in the N_2 laser. To overcome this triggering problem, a fast photodiode was placed in the dye laser such that it was exposed to a small fraction of the N_2 pump beam. The signal from the photodiode was used to trigger the oscilloscope and proved to be absent of detectable time jitter. As fluorescence lifetimes for PAHs are commonly below 100 ns, a minimum of time jitter is important.

Another problem which went unrecognized for an extended period of time was due to exposing the PMT to light levels high enough to place the PMT out of its linear range. This effect is easily recog-

nized by measuring the width of the light pulse causing the effect or by decreasing the PMT voltage and measuring the intensity of the light. When this problem occurs, the pulse width is severely broadened in time and decreasing the PMT voltage will not decrease the measured intensity until the PMT is restored to its linear range.

Although these problems were minor and easily solved, they are included here primarily to aid those following in this work to understand the operation of the DLS.

C. Continuum Source Excitation (CSE) in Matrix Isolation Fluorometry (MIF)

1. Comparison of Matrices

Site selection (SS) is but one way to obtain narrow band emission spectra. Increased resolution can also be accomplished by choosing a matrix in which inhomogeneous broadening is reduced to a minimum. Thus, a comparison of three matrix materials, N_2, Ar, and heptane, was made to ascertain the effect of the matrix on the emission spectra of PAHs, with the effect of the matrix on spectral resolution being of primary interest.

A summary of these comparisons is shown in TABLE IV (p. 71).

PAHs isolated in N_2 generally exhibit relatively large emission bandwidths (20-200 cm^{-1}) and little structure in their fluorescence spectra. PAHs isolated in heptane, on the other hand, exhibit spectra wherein the emission bands consist of a series of multiplets, each with a width on the order of 10-50 cm^{-1}. Perylene is an exception in that it exhibits only one sharp (about 10 cm^{-1} wide) emission band for each transition to a different vibrational state in the

TABLE IV

COMPARISON OF MATRIX SYSTEMS

	N_2	Ar	Heptane
Bandwidth	20–200 cm^{-1}	10–200 cm^{-1}	10–50 cm^{-1}
Intensity[a]	————	Low	High
Wavelength Shift[a]	————	0–4 nm to red	0–20 nm to red
Photodecomposition	No	No[b]	Yes

[a]Relative to N_2 matrices.

[b]The mono- and dihydroxynaphthalenes do undergo photodecomposition in Ar matrices.

ground electronic state, rather than several sharp bands. The origin of the multiplets is presumed to result from the tendency of PAH molecules to imbed themselves preferentially in one of a few orientations within the solvent cage structure. Each single narrow band arises from those molecules of the same type imbedded in the same (or very nearly the same) orientation. More discussion on this subject as well as experimental evidence which gives rise to this conclusion is found in Section G of this Chapter.

The spectra observed in Ar matrices vary considerably. Benz(a)anthracene (BaA) and benzo(a)pyrene (BaP) both exhibit similar spectra (i. e., sharp bands) in Ar and heptane. However, most PAHs exhibit similar bandwidths in Ar and N_2 matrices with the exception of perylene, the bandwidths for which are approximately 130 cm^{-1} and 90 cm^{-1} in Ar and N_2 matrices, respectively. Figure 19 (p. 73) illustrates an example of the effect of the matrix material on the emission spectra.

Fluorescence quantum efficiencies for the PAHs in Ar matrices are generally reduced as compared with those observed in N_2 matrices. This reduction of the quantum efficiency in Ar varies considerably between compounds. For many PAHs, the reduction is virtually total; they simply do not exhibit detectable fluorescence in Ar. BkF, however, exhibits almost the same quantum efficiency in Ar as in N_2. In heptane, most PAHs demonstrate considerable enhancement of the emission intensity as compared to the same PAHs imbedded in either N_2 or Ar. For example, BkF exhibits a two- to threefold increase in fluorescence intensity in heptane matrices as compared with N_2

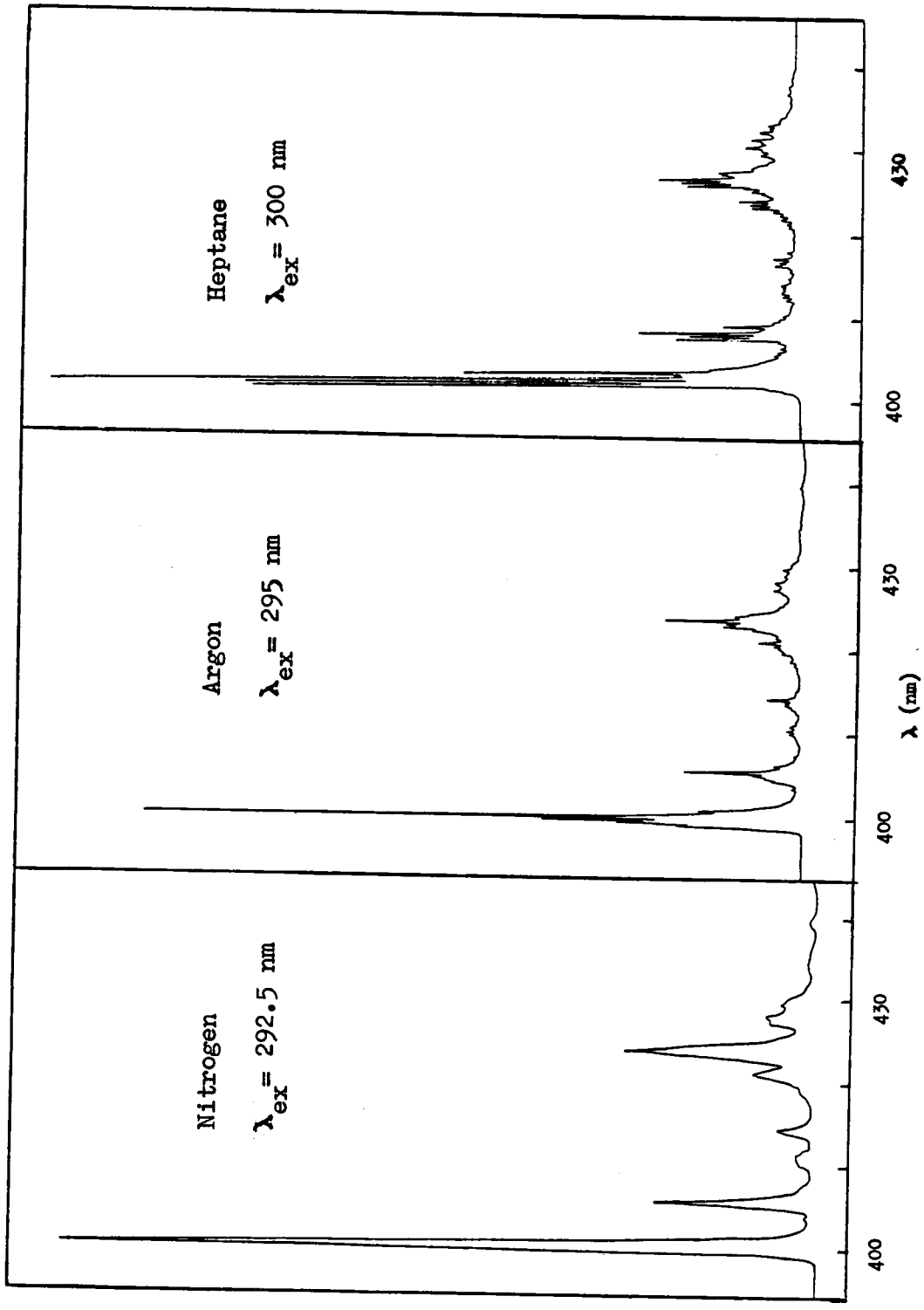

Figure 19. Emission spectra of benzo(a)pyrene in various matrices.

matrices. This increase in emission intensity is attributed to the compression of the intensity into a smaller wavelength region (increased resolution) rather than to an increase in the quantum efficiency.[32]

Emission spectra of PAHs in heptane matrices show a red shift relative to those observed in N_2 matrices which may be as much as 20 nm (for perylene). Not all PAHs exhibit the same degree of shift. For example, BkF and BaP have major emissions at 397 nm and 400 nm, respectively, in N_2 and emissions at 403.7 nm and 403.3 nm, respectively, in heptane. In other words, the principal fluorescence bands of BaP and BkF interchange positions as the matrix is changed from N_2 to heptane. It is therefore essential, in the use of these spectra for "fingerprinting" purposes, to be certain that the reference library spectra were obtained in the same matrix as that employed for the sample in question. The use of Ar as a matrix also led to a red shift in the PAH emission spectra relative to the spectra obtained in N_2 matrices, but the magnitude of the shift in PAH emission wavelengths is much smaller than the shift in heptane matrices (about 4 nm maximum).

Because the fluorescence intensities and the emission wavelengths of PAHs change when changing matrices, identification of components in complex mixtures can be facilitated by proper choice of matrix. For example, a deposit in heptane showing a major emission at about 403.5 nm could contain either BaP, BkF, or both. A deposit in nitrogen of the same sample would probably clarify which component is present or, if both are present, would give a rough

estimate of the relative amounts of each present in the sample. If a particular component of interest fluoresces relatively efficiently in Ar, then the use of Ar as a matrix material would simplify the spectra of a complex mixture by reducing the emission intensities of most of the other components. Thus, the use of several different matrix systems in the characterization of a complex sample can be quite advantageous.

The final comparison of these three matrices is that most PAHs undergo photodecomposition in heptane matrices. Most PAHs do not exhibit this effect in either N_2 or Ar. The one exception to this rule found to this point is the set of mono- and dihydroxynaphthalenes which do undergo photodecomposition in Ar matrices. Thus, when photodecomposition is expected to be a problem, spectra should be obtained relatively quickly.

2. Qualitative Analysis of Real Samples by CSE-MIF

At the time this work was initiated, CSE-MIF had proven itself as a useful method of analysis for PAHs. Resolution of complex mixtures was significantly improved over room temperature fluorometry of the same mixtures.[22] CSE-MIF also avoided some of the disadvantages of Shpol'skii fluorescence, such as aggregation, and demonstrated some advantages of its own, such as greater choice of possible solvent systems and a higher degree of quantitative reproducibility.

To ascertain the ability of CSE-MIF in the characterization of real samples, a qualitative analysis of "Fraction-75" (introduced in Chapter I) was undertaken. This sample was obtained from W. R. Griest of Oak Ridge National Laboratory and is a liquid

chromatographic fraction of a water sample taken from an effluent from a coking plant. A total of twenty PAHs was identified in this sample by GC-MS at Oak Ridge.

Figure 2 (p. 12) is a representative spectrum of Fraction-75 matrix isolated in N_2. As shown, most fluorescence peaks are well resolved from those of the other components and identification is accomplished easily for those components for which library spectra are available. TABLE V (p. 77) lists the compounds identified by CSE-MIF along with those compounds identified by MI-FTIR in a simultaneous study by Hinton.[54] CSE-MIF also yielded an intense unknown band at 424 nm. This band represents a major component of the sample for which identification would presumably be easy if the proper library spectrum was available. A number of possible compounds was examined in an attempt to identify this peak, but to no avail. This example clearly demonstrates one major disadvantage of fluorometric techniques; library spectra must be available for identification. Other compounds which may have been present in the sample did not fluoresce with sufficient intensity, were present at very low concentrations, and/or exhibited spectral overlap with the emissions of other components. For example, the identifications of benzo(e)pyrene (BeP) and anthracene remain tentative, as the peaks which match the main fluorescence peaks of BeP and anthracene are almost completely buried in the spectral features of other components.

Although the spectra obtained from Fraction-75 were excellent (this analysis would have been impossible by RTF), they still

TABLE V

LIST OF COMPOUNDS IDENTIFIED IN FRACTION-75

Compound	SS-MIF	MI-FTIR[a]
Anthracene	T	T
Benz(a)anthracene	D	D
Benzo(k)fluoranthene	D	-
Benzo(b)fluorene	D	-
Benzo(a)pyrene	D	D
Benzo(e)pyrene	T	-
Chrysene	D	D
Fluoranthene	-	D
Perylene	D	-
Phenanthrene	-	T
Pyrene	D	D

D - Definite Identification

T - Tentative Identification

[a]From reference 54.

exhibit a major limitation of CSE-MIF; many cases of incomplete resolution of spectral components still remain. For example, no excitation wavelength and/or matrix material has been found for CSE-MIF which will spectrally resolve the spectrum of BaP from that of BkF.

The emission bandwidths of matrix isolated PAHs vary over a considerable range (20-200 cm^{-1}). The compounds whose emission bands are the broadest present the most difficulty and are the ones for which laser excitation would presumably be the most beneficial. Laser excitation offers three potential methods by which resolution of complex mixtures can be enhanced. The methods are time resolution, selective excitation, and site selection. These are discussed in Sections D, E, and F/G, respectively.

D. Time Resolution in MIF

Figure 20 (p. 79) shows the spectra from a deposit of Fraction-75 isolated in N_2 and using laser excitation. The spectra labeled "B" are delayed by 20 ns with respect to the spectra labeled "A." Spectrum "B" (313 nm excitation) shows a marked increase in the resolution of BaP from BkF. At a sufficient delay from the laser pulse, the BaP is almost totally resolved from the BkF. The advantages of time resolution in MIF have previously been discussed[36], and the present example represents an additional demonstration of the effect.

Time resolution was used extensively throughout this research, but usually for another reason. Scattered and stray light, along with background dye fluorescence, often interfered significantly

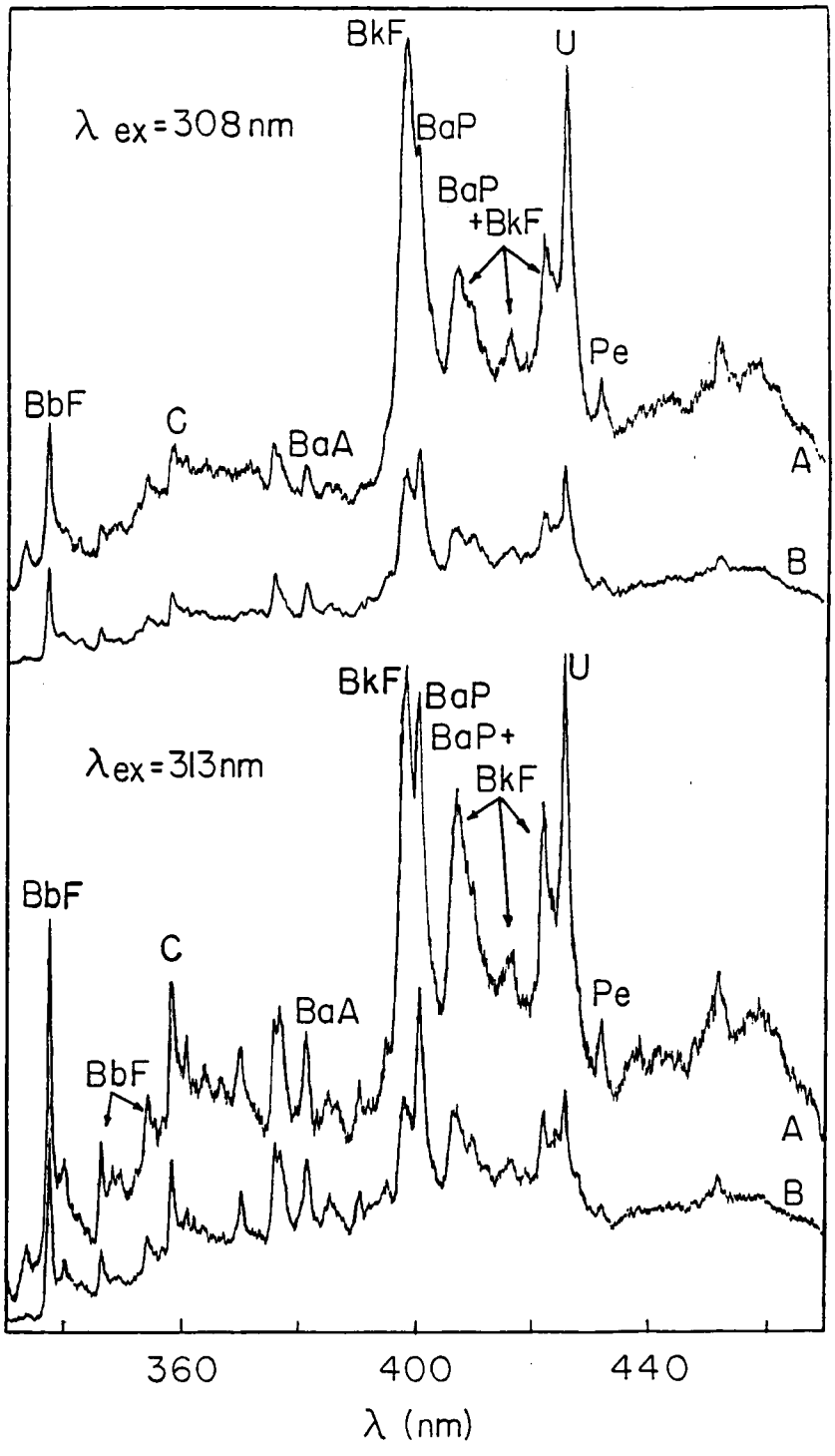

Figure 20. Laser excited fluorescence spectra of Fraction-75 in N_2.

A: 5 ns delay from laser pulse; B: 25 ns delay from laser pulse.

with the acquisition of fluorescence spectra. Each of these sources of interference was virtually coincident with the laser pulse. By setting the delay (point of measurement) at some time after the laser pulse, discrimination against such interferences was accomplished very effectively.

E. Selective Excitation Using Laser Illumination

One advantage of laser excitation which results from the monochromaticity of laser light is the potential for a higher degree of selective excitation as compared with CSE. This possibility is diagrammed in Figure 21 (p. 81) which shows the overlapping absorption profiles of two components, A and B. At any excitation wavelength (whether by laser or by broadband source) between "a" and "b," both A and B will be excited to varying degrees. Laser excitation at wavelengths "a" and "b," however, will selectively excite components A and B, respectively. Broadband excitation (as shown by the dotted lines) at either of these nominal wavelengths will excite both components, as shown by the overlap between the excitation and absorption profiles.

Several mixtures of PAHs were examined to ascertain to what degree, if any, use of the laser would enhance the ability to accomplish selective excitation as compared with the CSE source. This study was done using the same range of excitation wavelengths (about 250-320 nm) as used for the CSE instrument. The mixture of BaP and BkF was of particular interest as their emission spectra severely overlap in N_2 and Ar matrices. Examination by CSE-MIF in these

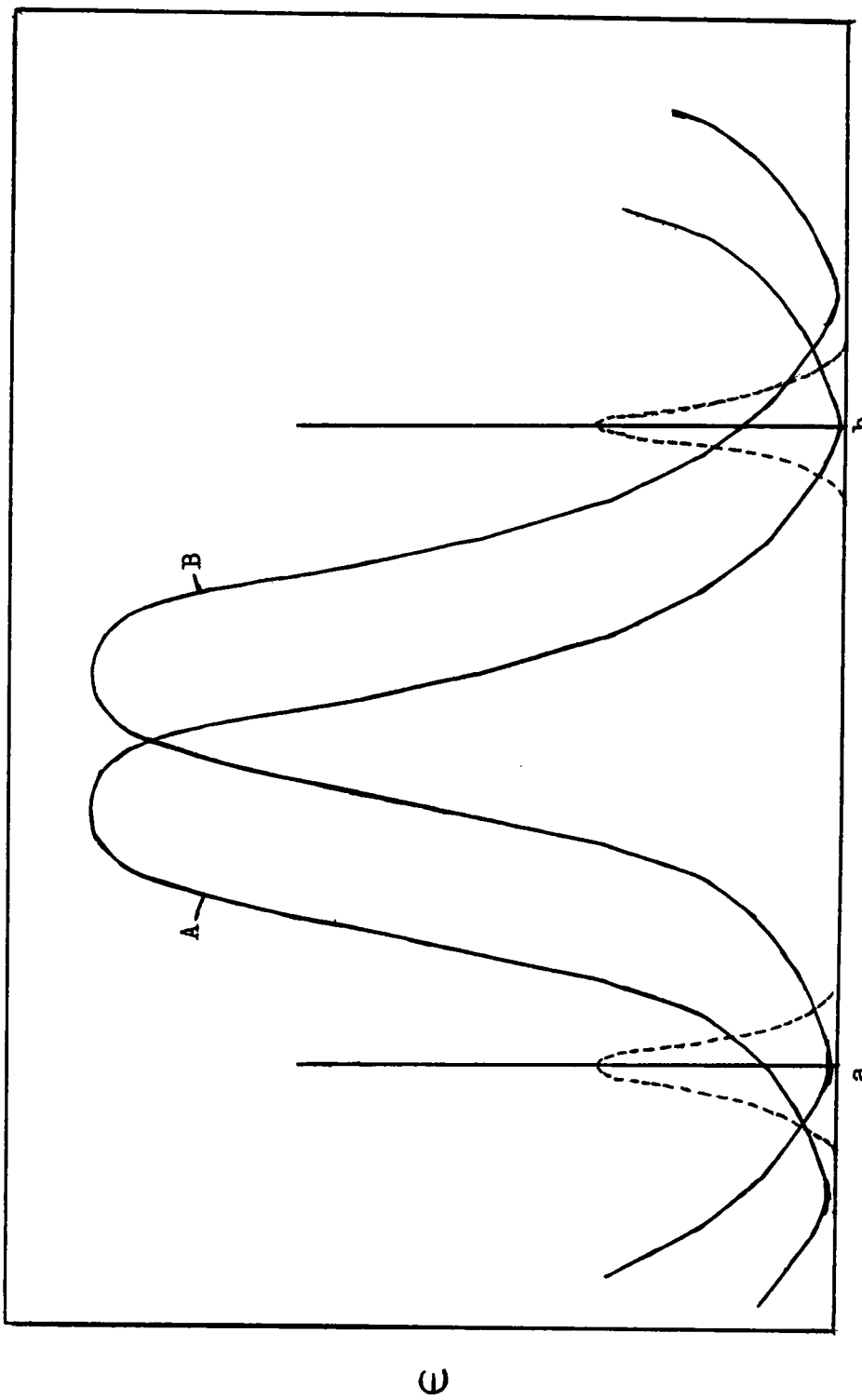

Figure 21. Illustration of selective excitation by laser excitation.

matrices failed to identify any excitation wavelength at which BaP could be excited with no contribution from BkF. Although laser excitation was able to partially reduce the BkF contribution, the reduction was not significant and would be useful only rarely.

Other mixtures exhibited the same effect; no significant increase in selective excitation can be attributed to laser excitation in the 250-320 nm range in N_2 or Ar matrices. As an example, Figure 20 (p. 79) also shows fluorescence spectra of Fraction-75 (in N_2) using the laser for selective excitation. Even though the excitation wavelengths differ by only 5 nm (spectra labeled "A"), the BaP peak at 400 nm is much better resolved from the adjacent BkF peak at 397 nm at the excitation wavelength of 313 nm. The broadband excitation of the CSE source "washed out" this effect.

Thus, the laser offered a slightly increased degree of selectivity as compared with CSE. It is apparent from the inability to effectively use selective excitation in this wavelength region (250-320 nm) that the absorption bands of PAHs in this region exhibit considerable overlap in Ar and N_2 matrices. This overlap occurs both between different compounds and between the different absorption bands of the same compound. Little advantage (in terms of selectivity) is offered by use of laser excitation in fluorescence spectrometry under the conditions of severe inhomogeneous broadening which usually pertains for PAHs in N_2 and Ar matrices.

F. Site Selection of PAHs in Frozen Solutions

Initial attempts to view the effect of site selection were made on known systems. Until the present time, all published work on site selection fluorescence was done on frozen solution systems.

The first system chosen for study was tetracene in 2-methyltetrahydrofuran frozen solution.[45] Upon excitation of the tetracene into its 0-0 absorption band (about 472 nm) at 15 K, no line narrowing was observed. Shifting the excitation wavelength a few nanometers did not result in a similar shift in emission wavelength. Thus, site selection was not being observed. Because of the possibility that the laser bandwidth was too large, the laser emission bandwidth was measured and found to be less than 1 cm^{-1} at all excitation wavelengths. An intracavity etalon was installed which reduced the laser emission bandwidth to less than 0.03 cm^{-1}. No improvement in the sample emission bandwidths was seen with the reduced excitation bandwidth.

The second test case chosen for study was perylene in a frozen ethanol matrix at both 15 K and 4.2 K.[42] When the perylene was excited into its 0-0 absorption band (about 442 nm), a definite reduction of emission bandwidth occurred when laser excitation was used. Small shifts in excitation wavelength resulted in similar shifts in the emission wavelength. These effects are shown in Figure 22 (p. 84) and the pertinent data from these spectra are found in TABLE VI (p. 85). These data were taken from spectra obtained at 4.2 K.

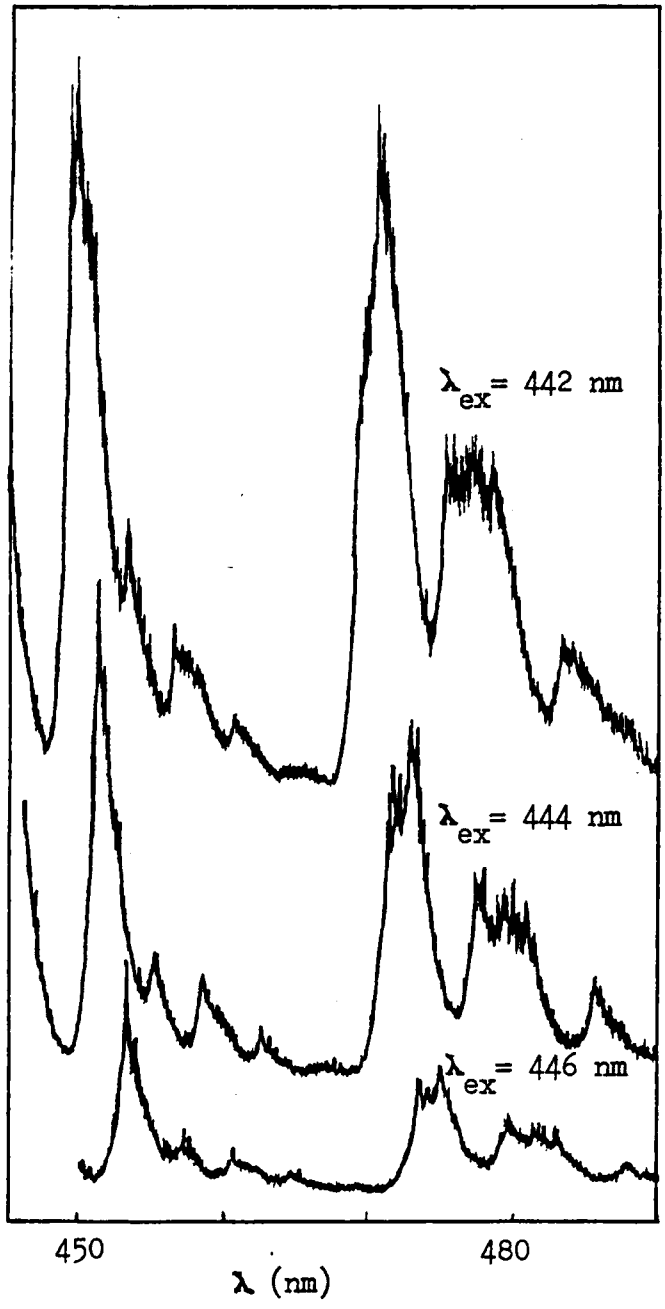

Figure 22. Site selection of perylene in ethanol at 15 K.

TABLE VI

SITE SELECTION OF PERYLENE IN ETHANOL FROZEN SOLUTION

Excitation Mode	Excitation Wavelength	Emission Wavelength	Emission Bandwidth
CSE	248 nm	451 nm	188 cm^{-1}
Laser	442	451	108
Laser	444	452	58
Laser	446	454	38

The data from Figure 22 (p. 84) and TABLE VI (p. 85) demonstrate that site selection is occurring. The peak wavelength shifts with a shift in the excitation wavelength because a different subset of the broad distribution of sites is being selectively excited. As the excitation wavelength is shifted towards shorter wavelengths, two things happen. First, the bandwidth becomes larger because the laser is exciting not only the 0-0 absorption band of the sites whose 0-0 transition energy matches that of the laser but also the absorption phonon wings (PWs) of those sites whose 0-0 transition energy is less than that of the laser. Therefore a larger subset of the distribution of sites is excited when a higher excitation energy is used. Second, the intensity of the emission peak increases because a greater fraction of the solute molecules are excited with an increase in excitation energy.

Although site selection is occurring, the lack of a distinct and intense ZPL was disturbing. Spectra of this type would be expected if the temperature of the solute was too high. As a result, a blank frozen solution was made in which a thermocouple (chromel vs. gold: 0.07% iron) was imbedded in the sample. Upon cooling to 4.2 K, the sample temperature decreased to 142 K and remained at this temperature even when the cold tip temperature had been at 4.2 K for more than 80 minutes. The conclusion was that either the cryostat did not have the cooling capacity to cool the relatively large volume of sample and/or the sample was making poor thermal contact with the cold tip of the cryostat. The relatively high temperature of the sample presumably was the reason for the

lack of a sharp and intense ZPL. As a result of these severe temperature problems, the analysis of frozen solutions was abandoned.

G. Site Selection of Matrix Isolated PAHs

1. Site Selection in N_2 Matrices

Initial attempts at seeing site selection in matrix isolated PAHs were made using N_2 as the matrix material. The results were disappointing. Of the compounds studied (BkF, perylene, BaP, benz(a)anthracene, and tetracene), only BkF and perylene demonstrated any degree of site selection in N_2 matrices. In both cases, the only evidence of site selection was a shift in the peak wavelength of a strong PW with a shift in the excitation wavelength. There was no evidence of a ZPL. Some bandwidth reduction occurred, but only to the limits imposed by the PW (50-100 cm^{-1}). Figure 23 (p. 88) illustrates this effect for perylene.

In view of the temperature problem with the frozen solutions, a similar temperature measurement investigation was carried out with the sapphire window. Three attempts to place a thermocouple in the center of the sapphire window were made to monitor the window temperature and to compare it with the temperature of the window mount to which a second thermocouple was attached. In all three attempts, the thermocouple on the window (which was attached merely by imbedding the thermocouple in a spot of "Cry-Con" grease, Air Products, Allentown, PA) lost thermal contact at around 100 K. No other method was found to satisfactorily secure the thermocouple to the center of the window. However, as long as the thermocouple

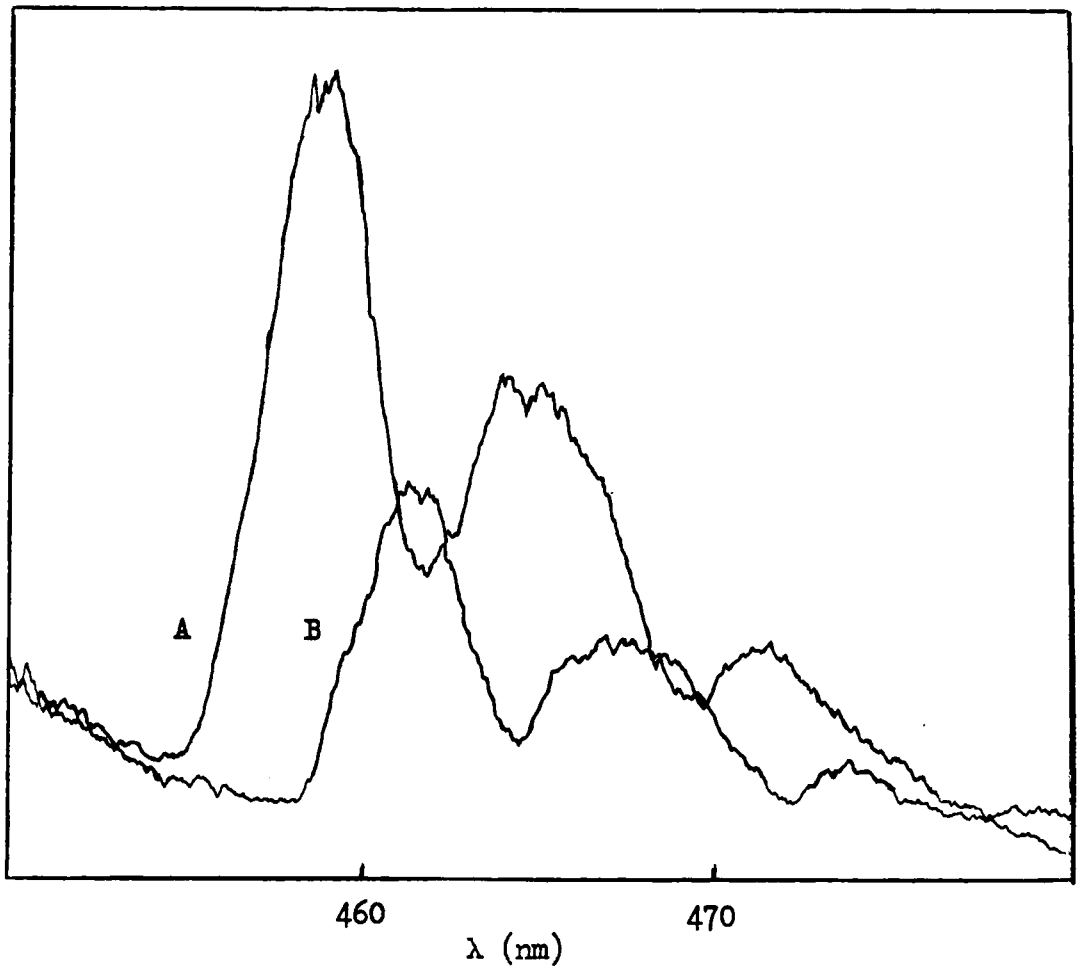

Figure 23. Site selection of perylene in N_2 at 15 K.

A: Excitation wavelength = 430 nm;
B: Excitation wavelength = 433 nm.

retained good thermal contact, the temperature of the window was within three degrees of the temperature of the window mount at all times. Since the thermal conductivity of sapphire between 100 K and 4.2 K does not vary significantly (in fact, the thermal conductivity of sapphire at 4.2 K is three times that at 300 K)[57], it is not expected that excessively high temperatures prevented the observation of site selection in N_2 matrices.

Another possible problem is that the temperature during the deposition process may vary considerably; the gases depositing on the window are relatively hot. Whether such a temperature variation during deposition occurs and how fast the deposit recovers if it does occur had not been investigated. To check this possible problem, a thermocouple was soldered onto a piece of copper which was put in place of the sapphire window and a blank deposit was made directly on the thermocouple. The temperature of the thermocouple (4.2 K) remained constant throughout the deposition. Therefore, variation of temperature during deposition should not be a problem.

Since the temperature problems were ruled out and the excitation bandwidth seemed not to be a problem (the laser bandwidth was rechecked and measurements concurred with previous measurements), it was concluded that a large coupling (large Debye-Waller factor) between the electronic transition and the phonon modes of the N_2 matrix was preventing the observation of distinct and intense ZPLs. In addition, perylene isolated in other matrix systems was subsequently found to exhibit excellent site selection under the same conditions of deposition and excitation. N_2 was therefore ruled out as a matrix system for site selection.

One interesting effect, which was observed in a N_2 matrix, was not duplicated in any other matrix. At an excitation wavelength of 429 nm with the DLS, perylene in N_2 exhibits superradiant emission. The result of this effect is shown in Figure 24 (p. 91). The single sharp band is 10 cm^{-1} wide as compared to 100 cm^{-1} at 15 K for the same band. The intensity of this band was found to be proportional to the square of the excitation pulse energy which is consistent with superradiant emission.[58] This effect was never reproduced in a mixture nor was any other compound found which possessed this ability. Though interesting, it is at present a useless fluke and is included only for completeness.

2. Site Selection in Ar and Heptane Matrices

Ar and heptane matrices are treated together as PAHs exhibit similar site selection properties in these matrices. As previously mentioned, BaP molecules deposit preferentially into one of four (in Ar) or five (in heptane) major orientations, or sites, within the matrix. Each set of sites gives rise to a spectrum consisting of narrow (about 10 cm^{-1}) bands. When all sites are excited, as with a broadband source, all sites fluoresce with nearly equal efficiency, giving rise to a spectrum consisting of a series of multiplets, with each multiplet arising from virtually identical sites within the matrix.

If the above argument is valid, then by using site selection techniques, it should be possible to separately excite each individual multiplet, thus simplifying the spectrum. Maple[32] demonstrated a strong dependence of the BaP spectrum (in heptane) on

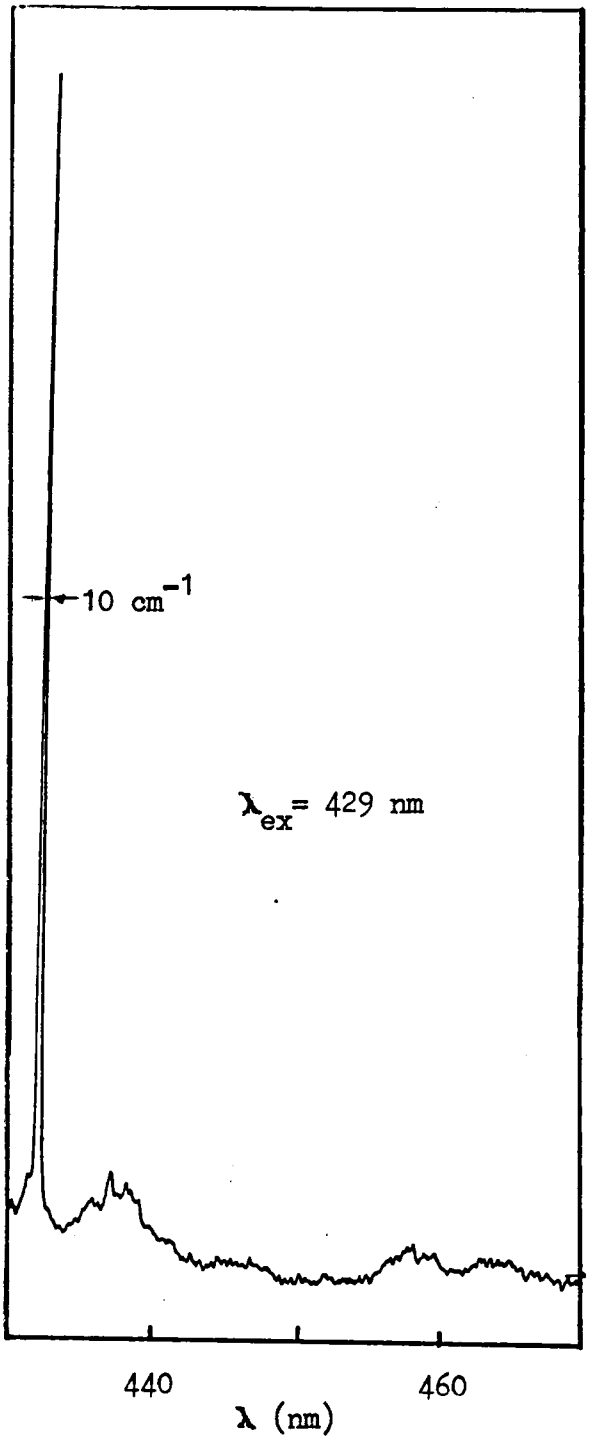

Figure 24. Superradiance of perylene in N_2 at 15 K.

the excitation wavelength, but was unable to selectively excite each multiplet. Subsequent investigation revealed that this inability to selectively excite each multiplet was due to the background dye fluorescence from the laser (see Section B, this Chapter), which excited all sites to some degree. Thus, a strong background continually manifested itself in the spectrum. The polarizer placed in the laser (Section B, this Chapter) reduced the background dye fluorescence from the laser and thus the background in the BaP spectrum. Figure 25 (p. 93) demonstrates the effect the presence or absence of the polarizer has on the spectrum of BaP in heptane. With the polarizer in place, the fluorescence from the sites other than the one being principally excited is reduced over that which is exhibited when the polarizer is removed from the laser. Figure 26 (p. 94) shows the effect of the laser in selectively exciting each multiplet.

Further probing of the wavelength dependence of the spectra of BaP upon the excitation wavelength revealed that each site referred to above was actually composed of a narrow distribution of sites rather than a single site. Figure 27 (p. 95) demonstrates that a single multiplet was also shifted with a shift in the excitation wavelength. Thus, site selection has been accomplished for vapor deposited PAHs. Figure 28 (p. 96) gives a vivid demonstration of what site selection can do to improve spectral resolution of the fluorescence spectra of matrix isolated PAHs. Both spectra are fluorescence spectra of BaP matrix isolated in Ar. The left spectrum was obtained by CSE while the right used site selection techniques.

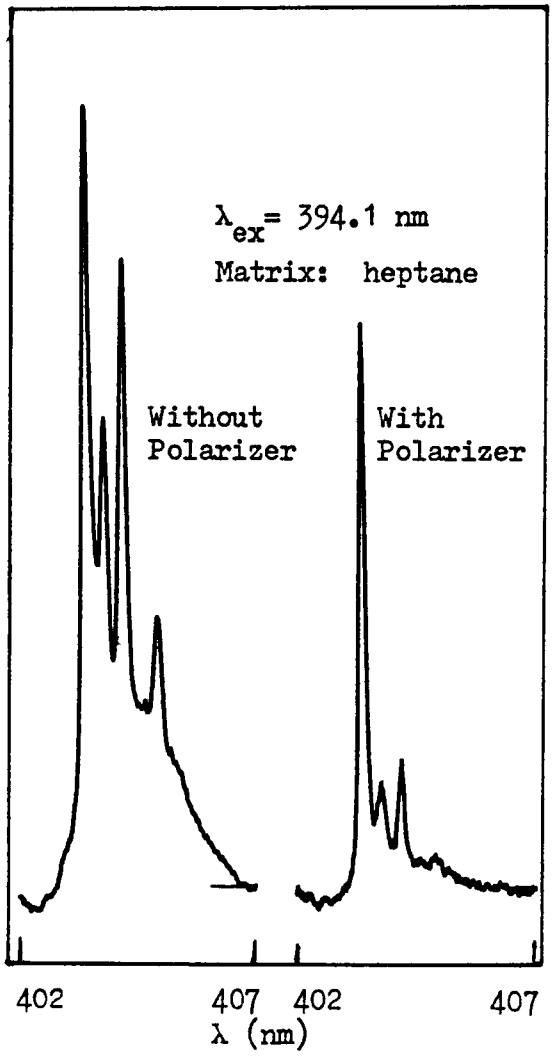

Figure 25. Effect of presence or absence of polarizer on benzo(a)-pyrene emission spectrum.

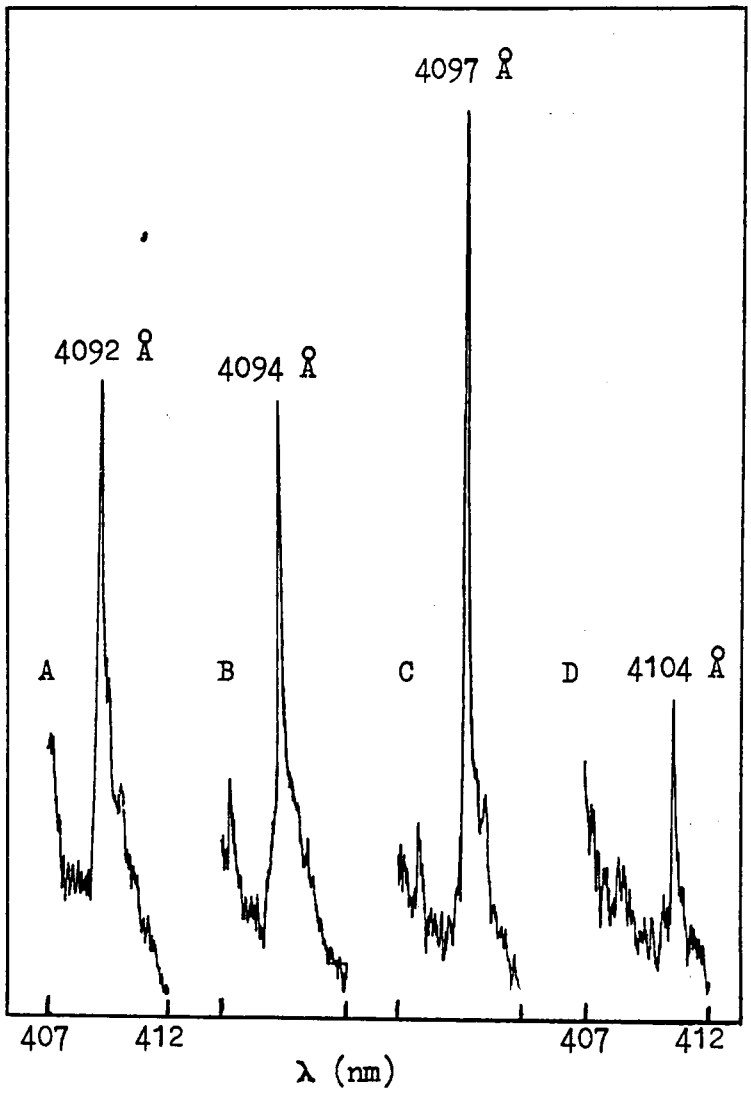

Figure 26. Selective excitation of benzo(a)-pyrene multiplets in heptane at 15 K.

Excitation wavelengths: A= 403.2 nm; B= 403.4 nm; C= 403.7 nm; D= 404.4 nm.

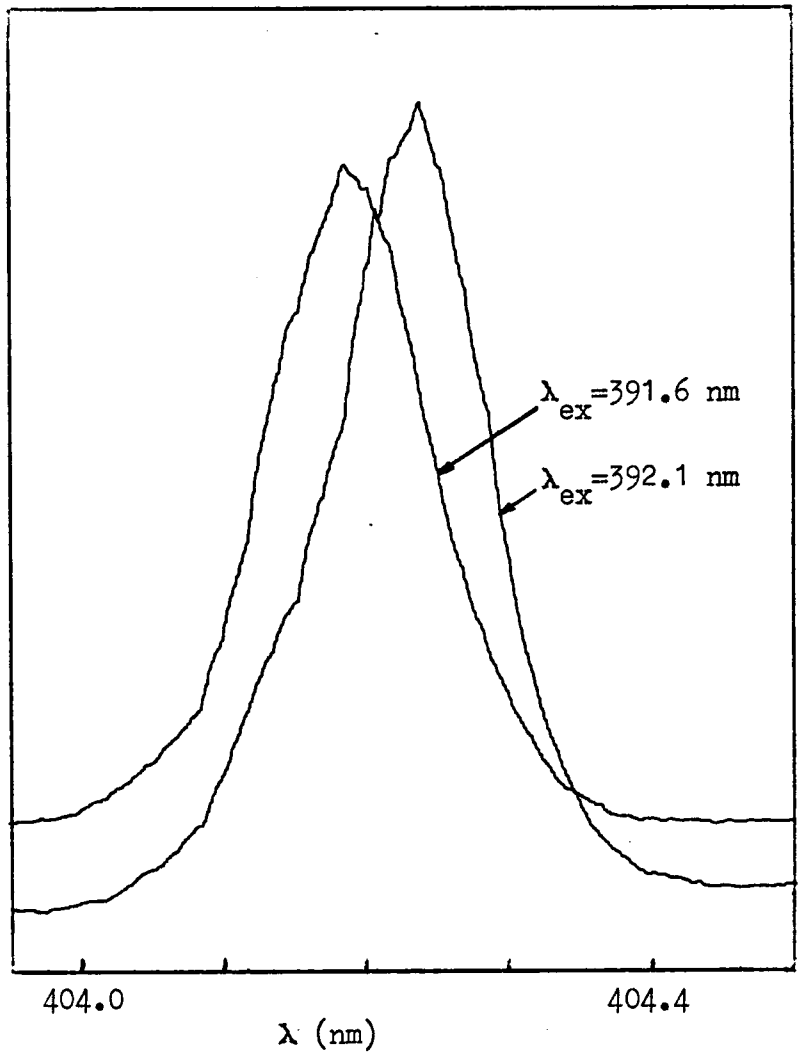

Figure 27. Demonstration of a distribution of sites within a single multiplet of benzo(a)pyrene in heptane at 15 K.

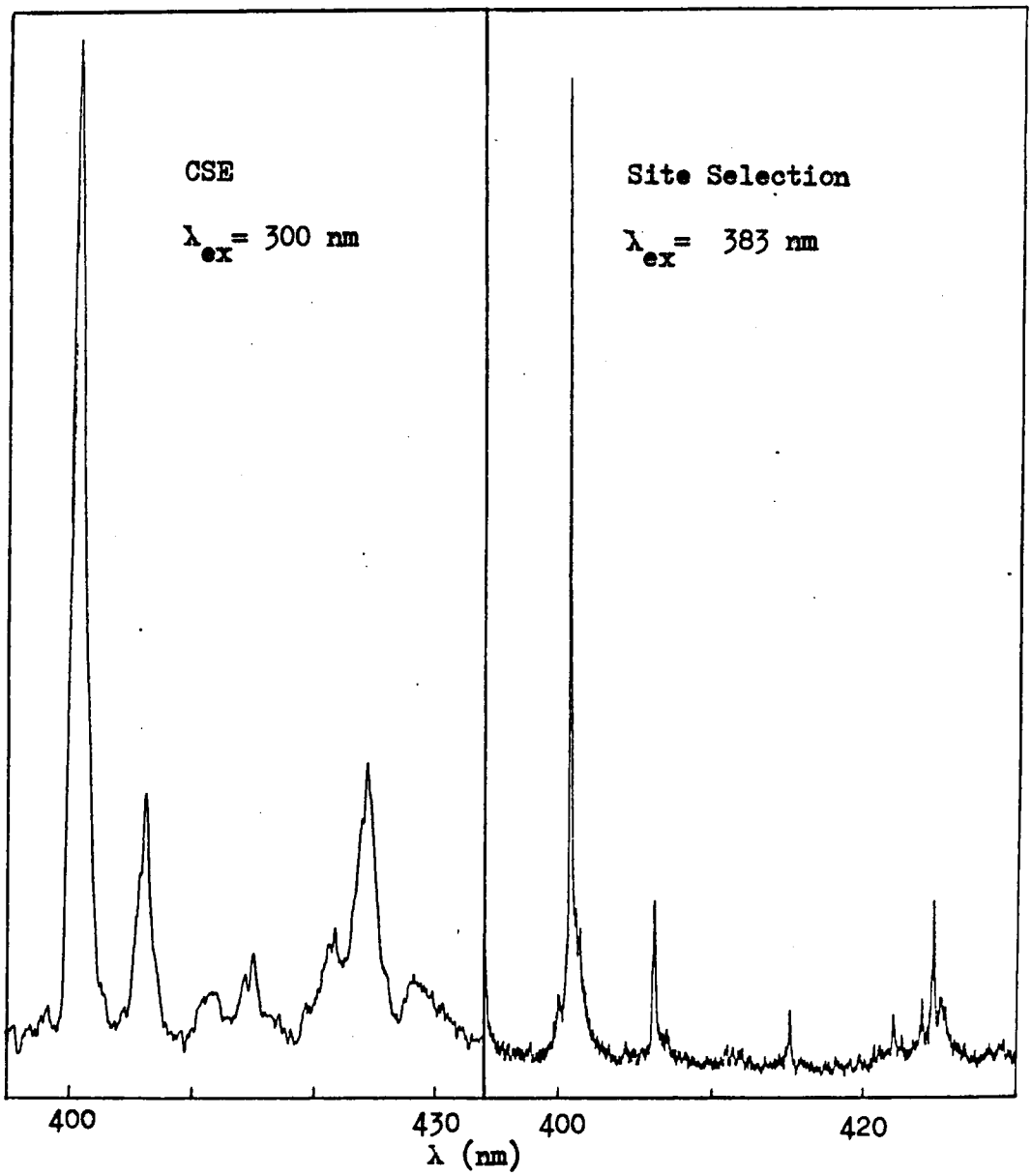

Figure 28. Fluorescence spectra of benzo(a)pyrene in argon at 15 K using CSE and site selection.

Similar behavior has been demonstrated for all compounds listed in TABLE VII (p. 98) under the conditions listed. Figures 29-31 (pp. 99-101) show further examples of the ability of site selection techniques to reduce the inhomogeneously broadened emission bandwidths of matrix isolated PAHs. The hydroxynaphthalenes exhibit quite large bandwidths relative to the parent PAHs, but these bandwidths represent an eight- to ten-fold reduction as compared with those of CSE spectra of the same compounds in the same matrices. Thus, it appears that, for the hydroxynaphthalenes in argon or perfluoro-n-hexane, about 20 cm^{-1} is the limit to which inhomogeneous broadening can be reduced by this technique.

An extensive survey was conducted to ascertain the general applicability of site selection. This survey was conducted using argon as the matrix. Out of a total of twenty-six PAHs studied, only those ten compounds listed in TABLE VII (p. 98) demonstrated site selection capabilities. Attempts at obtaining site selection from the other sixteen PAHs, listed in TABLE VIII (p. 102), failed to produce spectra exhibiting significant improvement over those obtained by the usual CSE technique. Attempts to observe site selection were made for all compounds by exciting into the first vibronic levels. Experience had indicated that this type of excitation was more sensitive than excitation into the 0-0 absorption band. For this purpose, excitation was attempted first at a wavelength within about 5 nm of the 0-0 transition of the PAH under scrutiny. The 0-0 transition was taken as the lowest wavelength emission band of the particular PAH. The excitation wavelength was then

TABLE VII

COMPOUNDS WHICH EXHIBIT SITE SELECTION

Compound[a]	Matrix[b]	Temperature (K)	Minimum Bandwidth (cm^{-1})
BbF	A	15	5
BkF	N,A,H	4.2-15	5
BaP	A,H	4.2-15	3
1,5-DHN	A,P	4.2-15	20
1,7-DHN	A,P	4.2-15	25
2,3-DHN	A	15	25
2,7-DHN	A	15	25
1-Naphthol	A	15	25
2-Naphthol	A	15	25
Perylene	N,A,H	4.2-15	1

[a]BbF: Benzo(b)fluorene; BkF: Benzo(k)fluoranthene; BaP: Benzo-(a)pyrene; DHN: Dihydroxynaphthalene.

[b]A: Argon; N: Nitrogen; H: n-Heptane; P: Perfluoro-n-hexane.

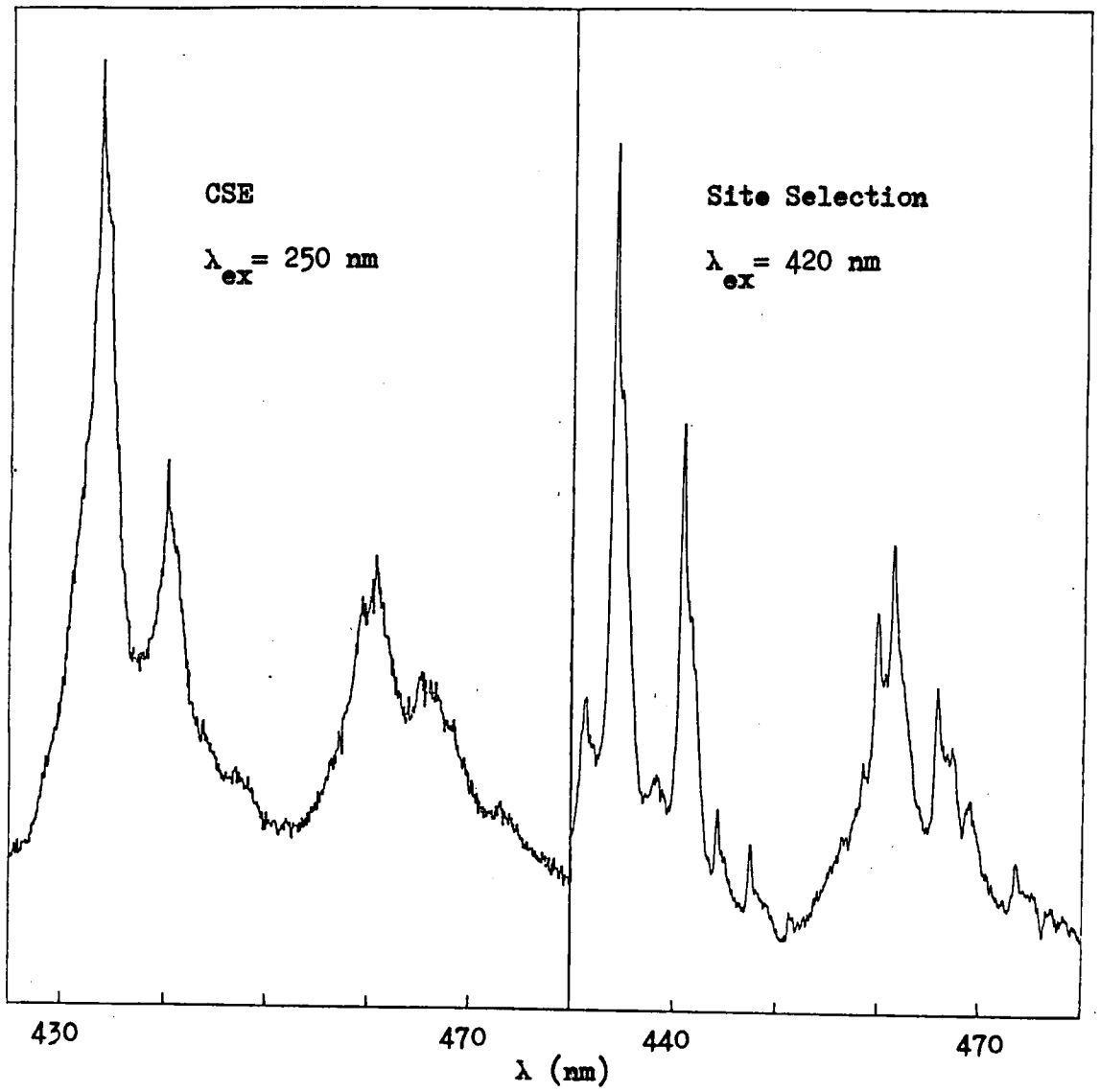

Figure 29. Fluorescence spectra of perylene in argon at 15 K using CSE and site selection.

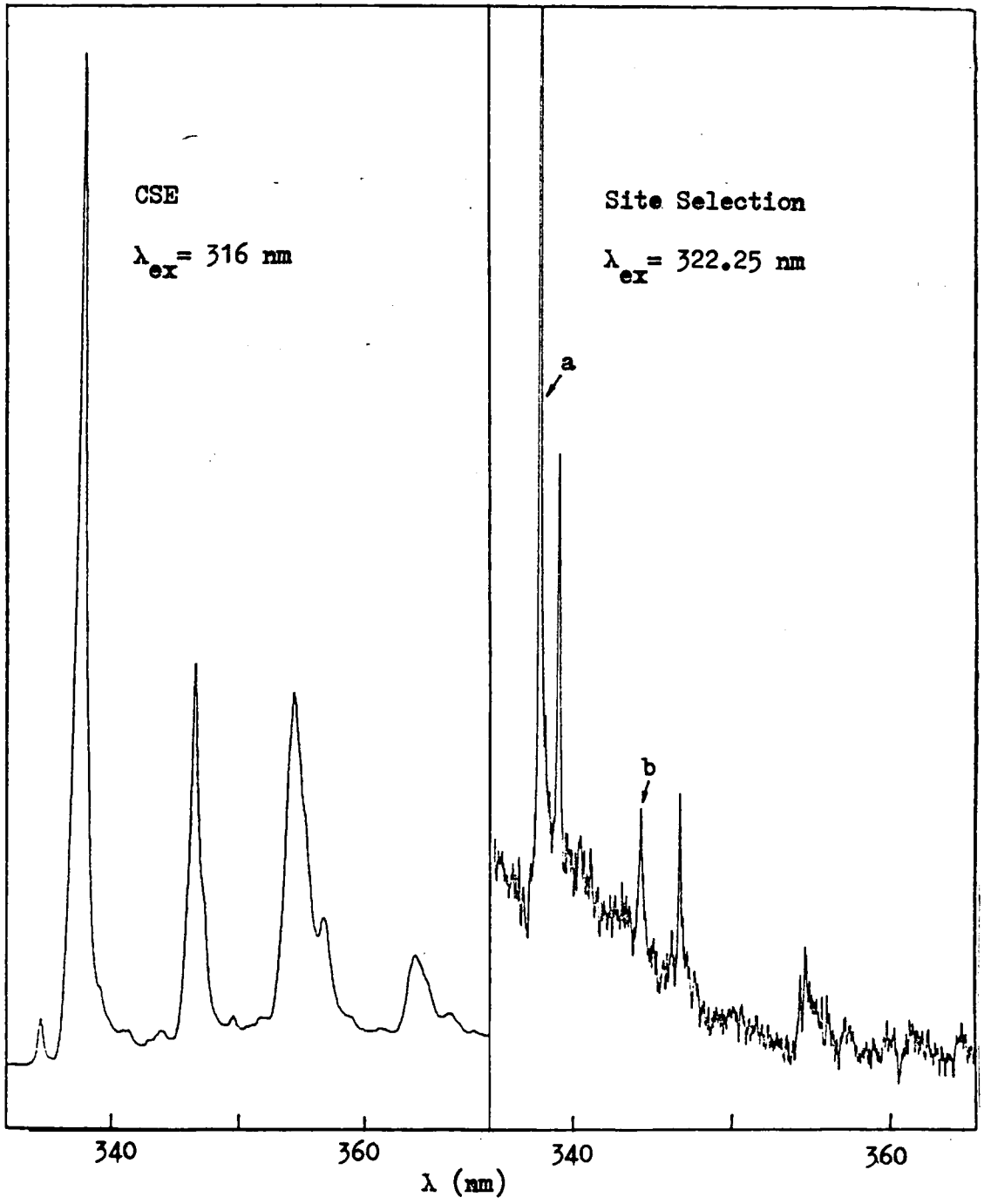

Figure 30. Fluorescence spectra of benzo(b)fluorene in argon at 15 K using CSE and site selection.

[a]Scattered N_2 laser emission.

[b]Stray N_2 laser emission from monochromator. See page 62.

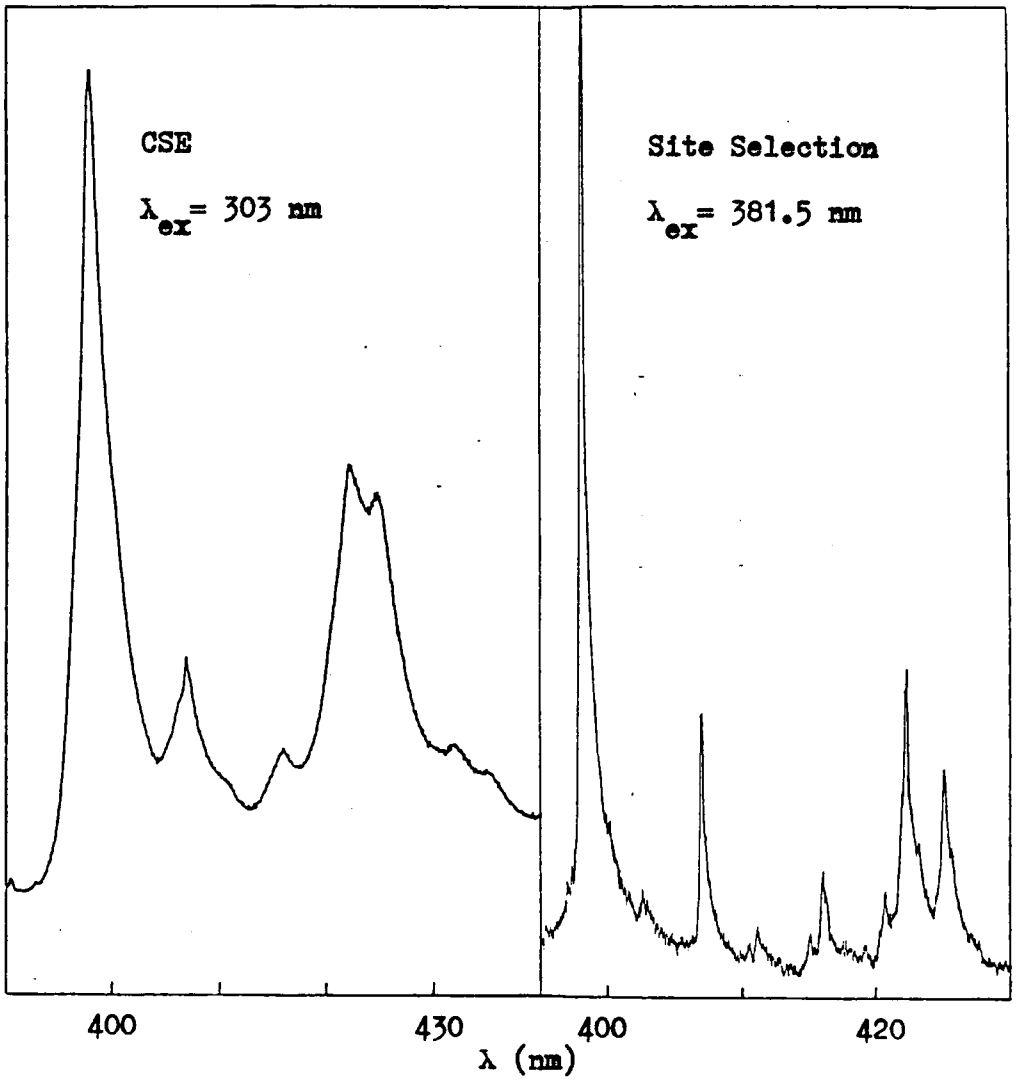

Figure 31. Fluorescence spectra of benzo(k)fluoranthene in in argon at 15 K using CSE and site selection.

TABLE VIII

COMPOUNDS NOT EXHIBITING SITE SELECTION

Compound[a]	Matrix[b]	Temperature (K)
BaF	A	15
BaFla	A	15
BbFla	A	15
Chrysene	A	15
BbC	A	15
Coronene	A	4.2-15
Pentacene	A	15
B(g,h,i)Per	A	15
Pyrene	A	4.2-15
BeP	A,N	15
PP	A	15
BaA	A,N	15
1,2,3,4-DBA	A	15
Fluoranthene	A	15
Tetracene	A,N	4.2-15
Rubrene	A	15

[a] BaF: Benzo(a)fluorene; BaFla: Benzo(a)fluoranthene; BbFla: Benzo(b)fluoranthene; BbC: Benzo(b)chrysene; B(g,h,i)Per: Benzo(g,h,i)perylene; BeP: Benzo(e)pyrene; PP: Pyrenopyrene; BaA: Benzo(a)anthracene; DBA: Dibenzanthracene.

[b] See TABLE VII (p. 98).

decreased in 3-5 nm steps until a spectrum was obtained or until a wavelength difference (between the excitation and 0-0 transition wavelengths) of 50 nm was reached. The 50 nm difference had been previously determined based upon work by Maple[32] which indicated that the region within about 40 nm to the blue side of the 0-0 transition wavelength was the region in which first vibronic excitation would occur for the PAHs. Excitation outside of this range will tend to excite all sites due to the overlap of upper vibronic absorption bands from molecules in different sites.

The inability to obtain spectra of many PAHs when exciting in the wavelength range mentioned above is explained by the relatively low molar absorptivities of many PAHs in that wavelength range. TABLE IX (p. 104) lists the molar absorptivities for several PAHs at several excitation wavelengths. Although these data pertain to PAHs in room temperature isooctane solutions, the trend to very low molar absorptivity when approaching the 0-0 transition (first wavelength listed in each case) will also pertain to PAHs in vapor-deposited matrices at low temperature. This trend proves to be a disadvantage in site selection spectroscopy of PAHs. To accomplish site selection, the excitation wavelength must be at or close to (within about 40 nm) the 0-0 transition wavelength, at which the molar absorptivity is very small. Thus, the limit of detection for site selection is much higher than if lower excitation wavelengths were used.

The above data pertain almost exclusively to excitation of the PAHs into the first vibronic level of the first excited state.

TABLE IX

MOLAR ABSORPTIVITIES FOR SEVERAL PAHS IN ISOOCTANE AT ROOM TEMPERATURE[58]

Compound	Excitation Wavelength (nm)	Molar Absorptivity (M^{-1} cm^{-1})
Triphenylene	341.5	113
	290.1	9,305
	257.6	174,646
Benz(a)anthracene	383.4	850
	358.6	5,075
	299.1	9.978
	287.6	95,000
Tetracene	473.7	9,160
	295.1	24,399
	276.8	292,019
Benzo(e)pyrene	372.3	200
	326.6	4,900
	294.6	12,900
	281.1	97,900
Pyrene	371.1	125
	334.7	59,800
	272.6	57,200
	240.6	91,700
Chrysene	360.8	700
	319.8	13,700
	267.7	163,700

While the sensitivity is lower due to low molar absorptivity, each of the compounds in TABLE VII (p. 98) can be excited with reasonable efficiency into the 0-0 absorption bands. When 0-0 excitation is used, the resulting spectra are normally simpler than when first vibronic excitation is used. The simplification is due to a smaller probability of exciting adjacent sites. Excitation into the first vibronic band in site selection is satisfactory only when a definite energy gap exists between the 0-0 transition energy level of those sites at higher energies and the first vibronic energy levels of those sites at lower energies. Figure 32 (p. 106) illustrates the idea presented here. In case A, a definite energy separation exists between the v=0 and the v=1 levels in S_1. The probability of exciting a site directly into its v=0 level when using a wavelength with energy E_a is small. In case B, however, excitation with energy E_a will populate the v=0 levels of some sites and the v=1 levels of other sites. When more sites are excited, a broader emission band results.

In general, the PAHs which were shown in this work to exhibit site selection can be excited into either the v=0 or the v=1 level of S_1. Excitation into v=1 allows the measurement of the 0-0 emission band. When excitation into the v=0 level is used, emission bands other than the 0-0 band must be used for measurement; otherwise laser scatter would saturate the PMT. Since the 0-0 emission band is generally the most intense band for the PAHs, the use of first vibronic excitation offers a lower limit of detectability over that which would be observed if 0-0 excitation is used. The difference

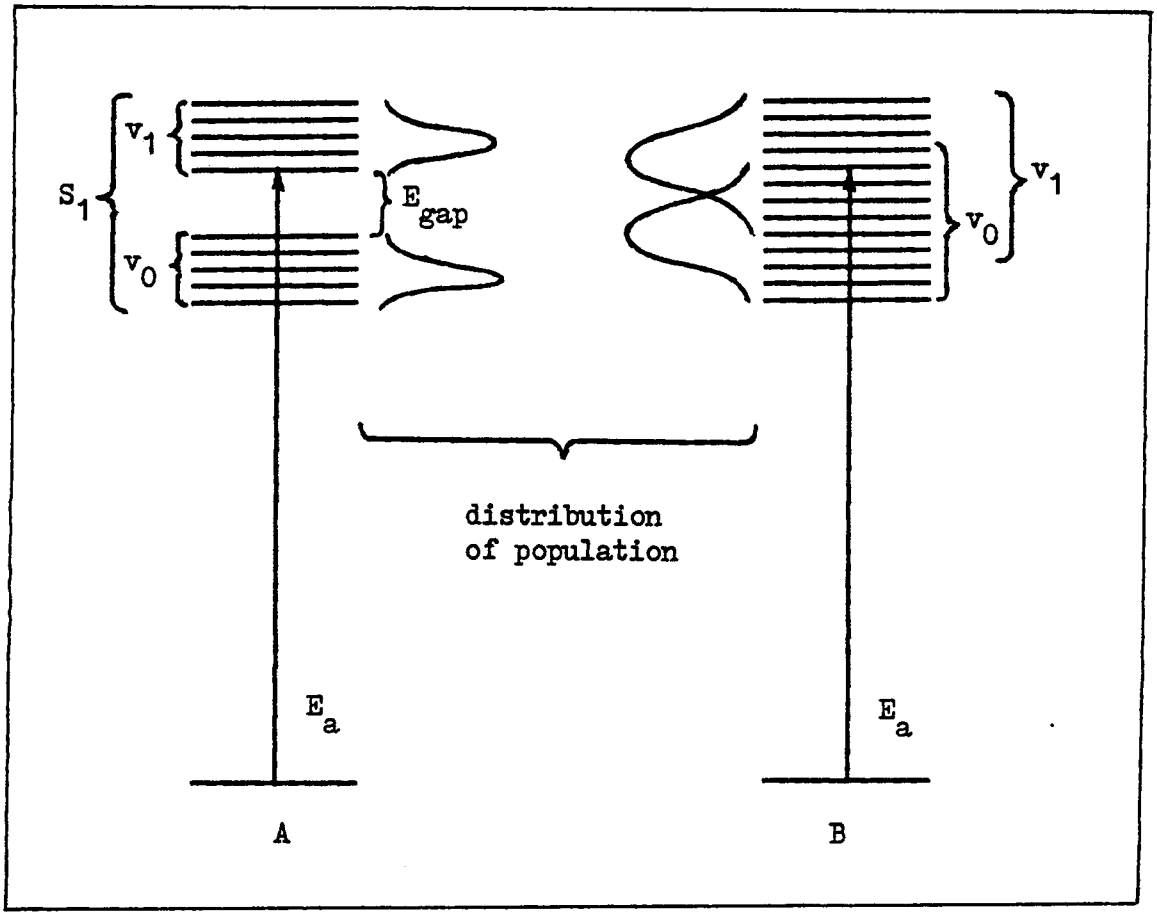

Figure 32. Energy level diagram illustrating the distribution of vibronic energy levels in the first electronic excited state.

A: First vibronic excitation with site selection possible, B: First vibronic excitation with site selection not possible, E_{gap}: Energy difference between v=0 of higher energy sites and v=1 of lower energy sites, E_a: Absorption transition energy.

in the detection limit observed using the two methods of excitation is dependent upon the intensity differences between the 0-0 emission band and the other emission bands and the molar absorptivities of the particular compound at the two excitation wavelengths. For BaP, this difference is a factor of approximately 7-10.

3. Temperature Dependence of Site Selection Fluorescence

Figures 33-35 (pp. 108-110) show examples of the dependence of site selection fluorescence spectra upon the temperature of the sample. As expected, both the bandwidth and the intensities of the PWs are reduced at lower temperatures. TABLE X (p. 111) also demonstrates the effect of temperature on the emission bandwidth. Although the lower temperatures increase resolution and decrease the background (that part which is due to the presence of PWs), the advantages of lower temperatures do not generally appear to outweigh the added cost, complexity, and need for extra precautions. Since site selection spectra could be obtained at 15 K, the great majority of the studies included in this work was performed at 15 K.

4. Qualitative Analysis of a Hydroxynaphthalene Mixture

Analytical site selection spectroscopy is of little use if the technique cannot be applied to mixtures. A synthetic mixture of 200 ng each of 1-naphthol (1-N), 2-naphthol (2-N), 1,5-DHN, 2,3-DHN, 2,7-DHN (DHN: dihydroxynaphthalene) was prepared in an argon matrix at 15 K. Figure 36 (p. 112) is the CSE fluorescence spectrum of the mixture. No peak in this spectrum can be definitely assigned to any one component of the mixture. One especially noteworthy point is that the excitation wavelength for this spectrum

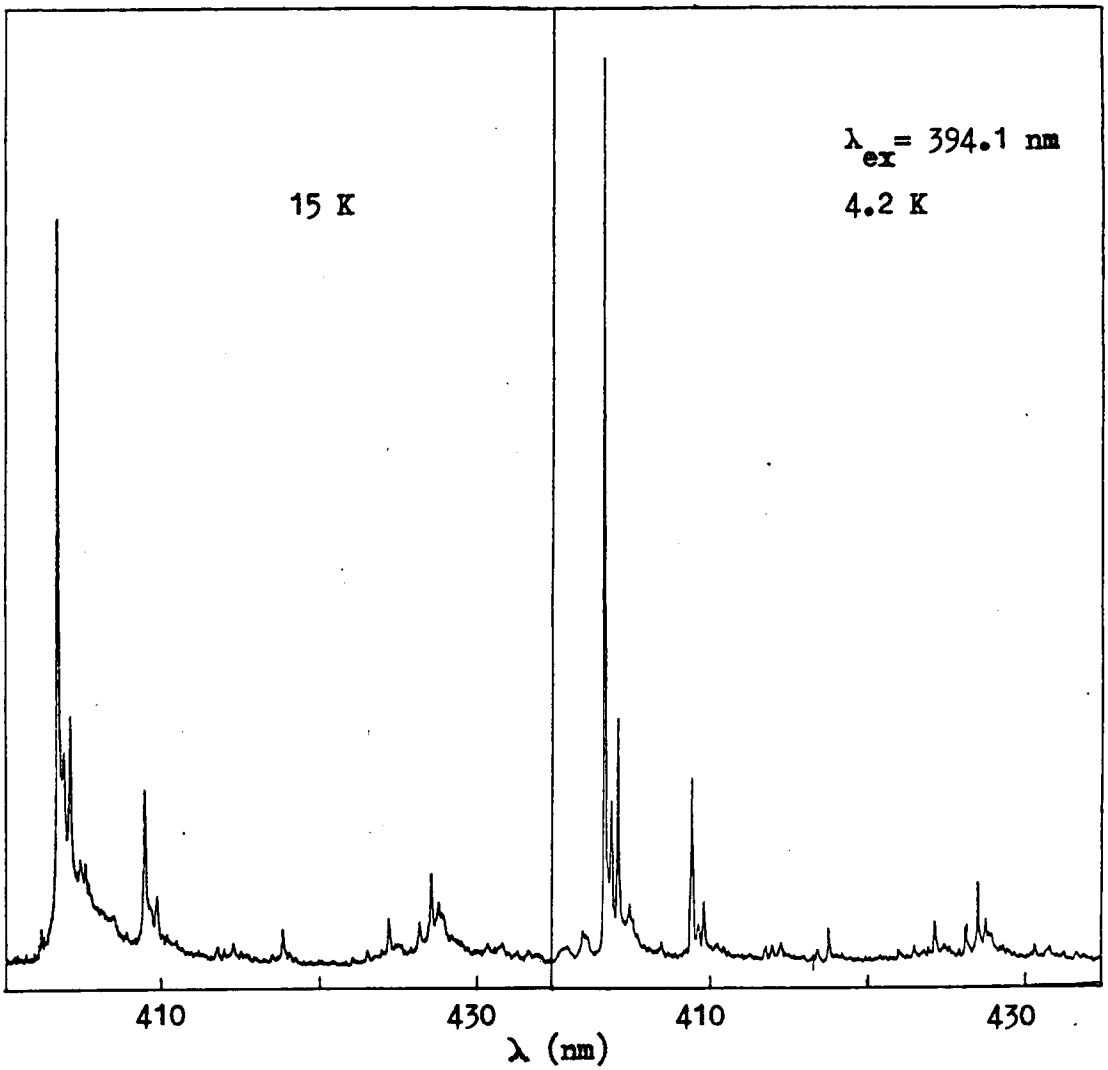

Figure 33. Temperature dependence of site selection of benzo(a)-pyrene in heptane.

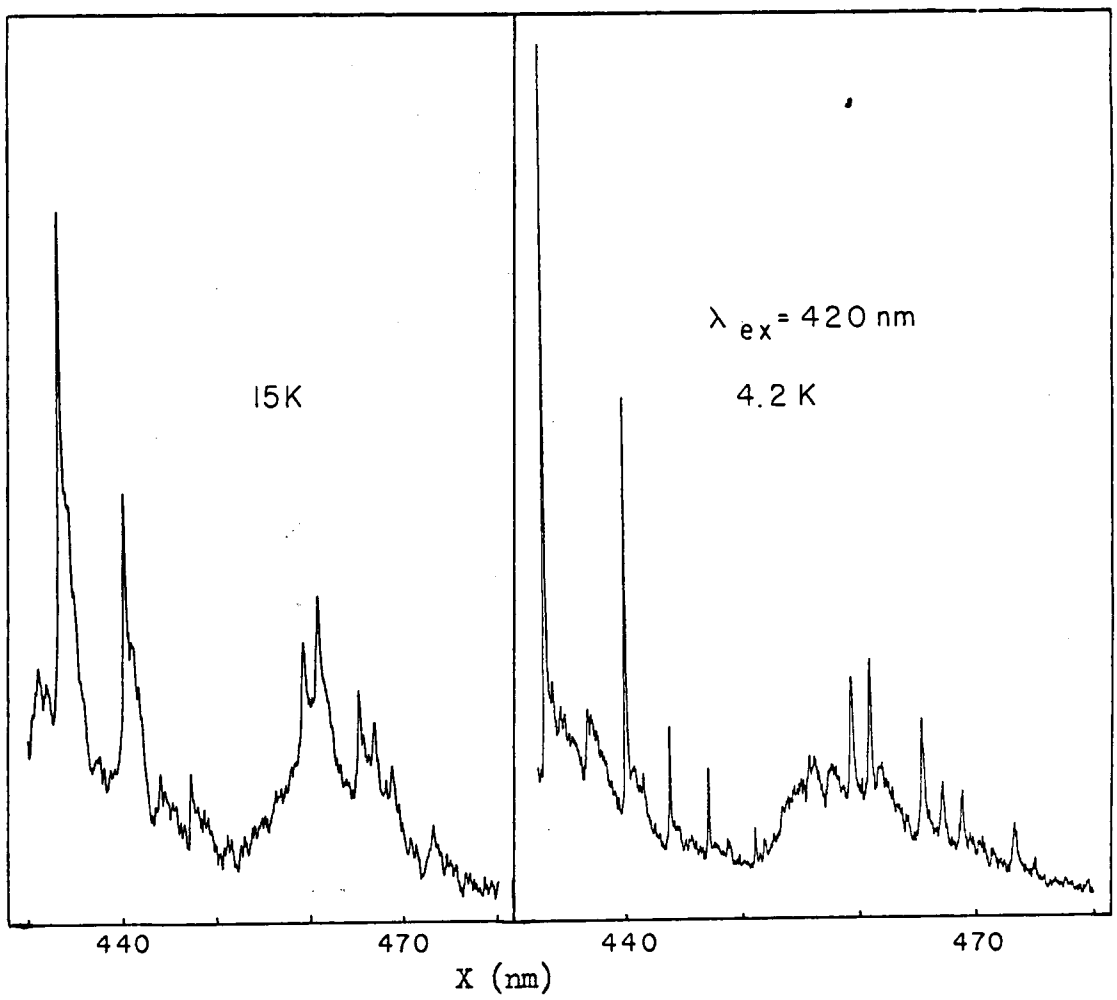

Figure 34. Temperature dependence of site selection of perylene in argon.

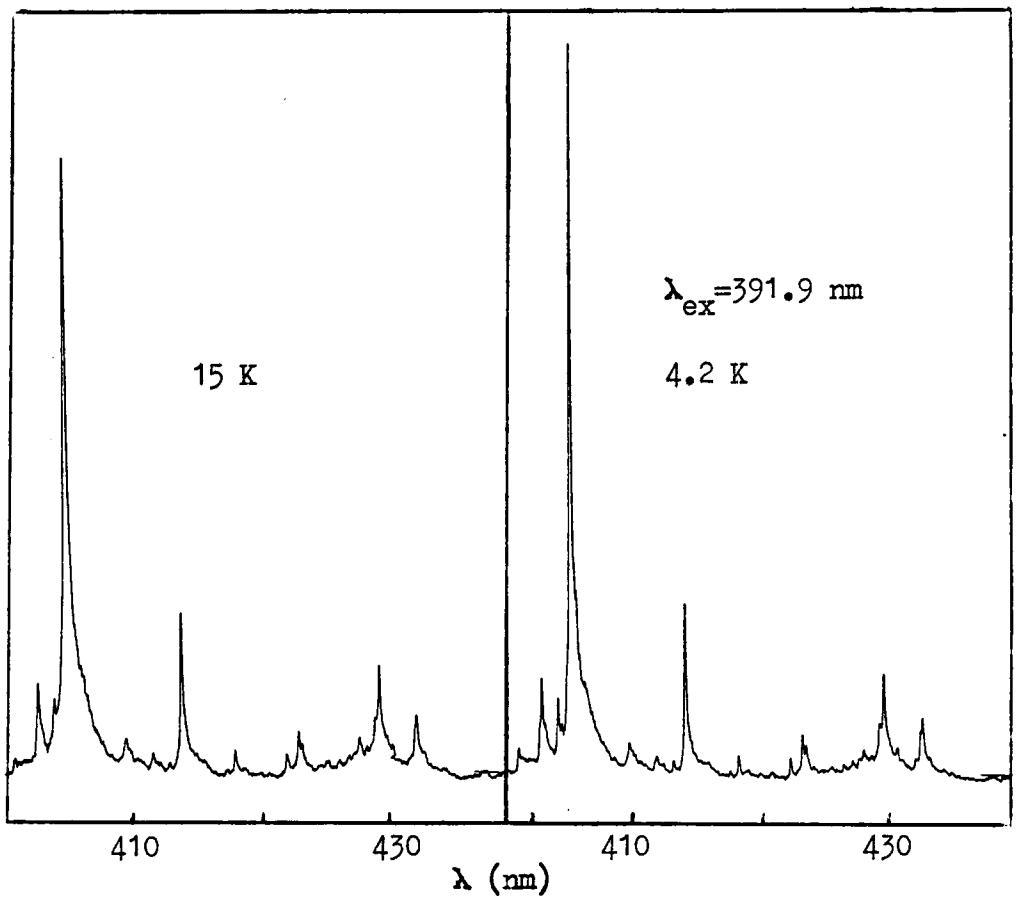

Figure 35. Temperature dependence of benzo(k)fluoranthene in heptane.

TABLE X

TEMPERATURE DEPENDENCE OF EMISSION BANDWIDTHS

Compound[a]	Matrix	Emission Wavelength	Temperature	Bandwidth
1,5-DHN	Ar	328 nm	15 K	87 cm^{-1}
			4.2	41
Perylene	Ar	433	15	5.7
			4.2	1.4
BaP	Ar	400	15	3.5
			4.2	3.4
BkF	Heptane	404	23	8.3
			14	7.1
			4.2	5.4

[a] 1,5-DHN: 1,5-dihydroxynaphthalene; BaP: Benzo(a)pyrene; BkF: Benzo(k)fluoranthene.

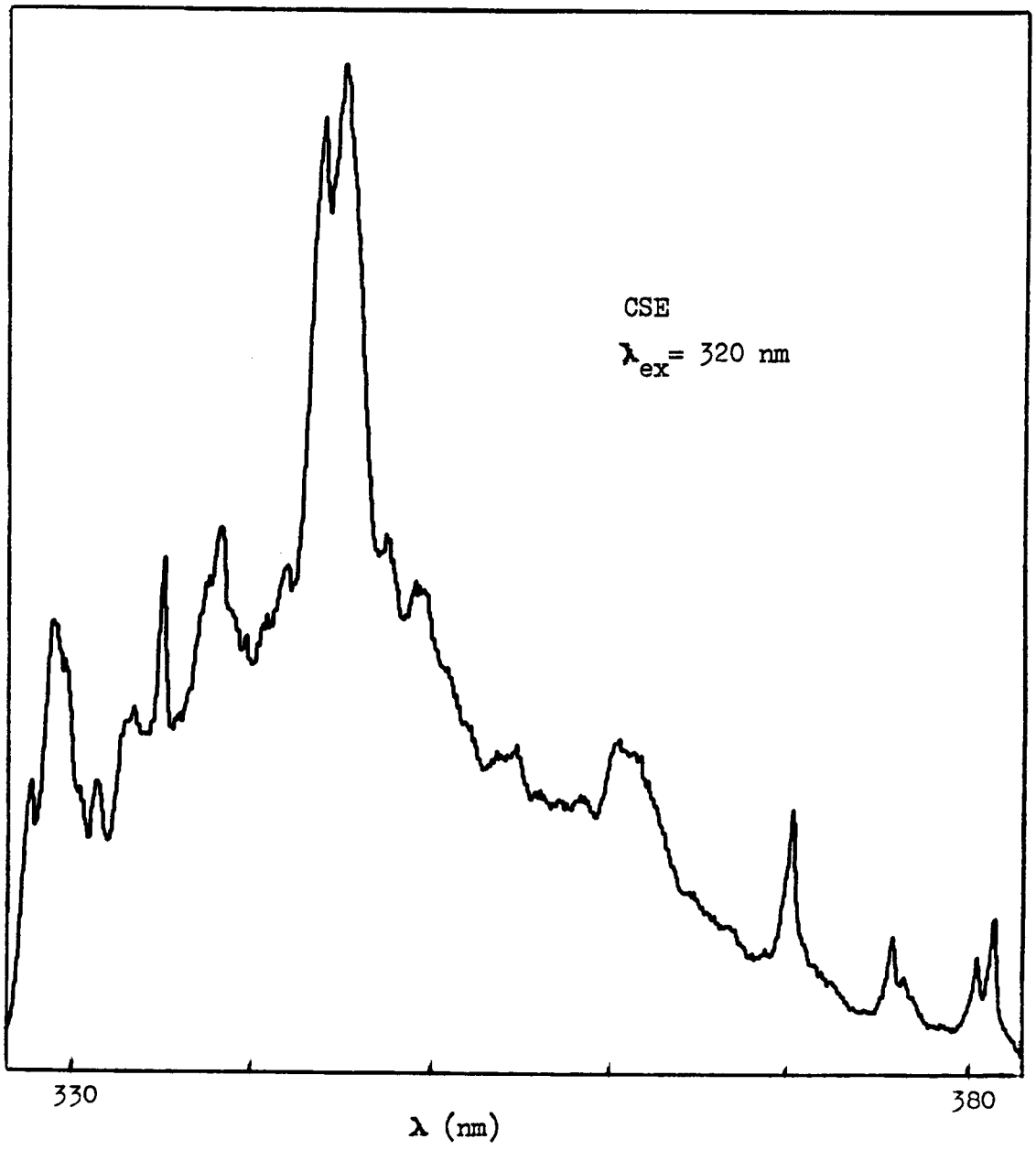

Figure 36. CSE fluorescence spectrum of hydroxynaphthalene mixture in argon at 15 K.

Overlap of component emission is too great to adequately label emission bands.

is within 10 nm of the first emission band. Even when the CSE source is used for excitation within the range of first vibronic excitation, its large bandwidth prevents any line narrowing. This example clearly demonstrates the need for narrow band excitation in site selection.

The laser excited spectra were obtained by separately exciting the sample into the 0-0 absorption bands of the different components. These spectra are shown in Figures 37-40 (pp. 114-117). Figure 37 shows selective excitation of 1,5-DHN in the mixture. A comparison of Figure 37 with a spectrum of 1,5-DHN alone, as shown in Figure 41 (p. 118), gives an excellent match. The other components of the mixture are seen one by one as the excitation wavelength is decreased. Previous experimentation had shown that the distributions of the v=0 and v=1 levels for S_1 of the hydroxynaphthalenes overlap. Thus, use of the shorter excitation wavelengths tends to excite all of the components which emit at longer wavelengths rather than just the one component which is experiencing 0-0 excitation. However, the resulting spectra are still much easier to interpret than the CSE spectrum of the mixture. In fact, the CSE spectrum of this mixture is impossible to interpret.

5. Site Selection of Fraction-75

Section C of this Chapter describes the work on Fraction-75 which was accomplished by CSE. Site selection techniques were applied to this sample to ascertain the applicability of site selection to real samples. Unfortunately, the CSE work and the site selection work on Fraction-75 were separated by approximately two years. A comparison of Figure 42 (p. 119) with Figure 3 (p. 13)

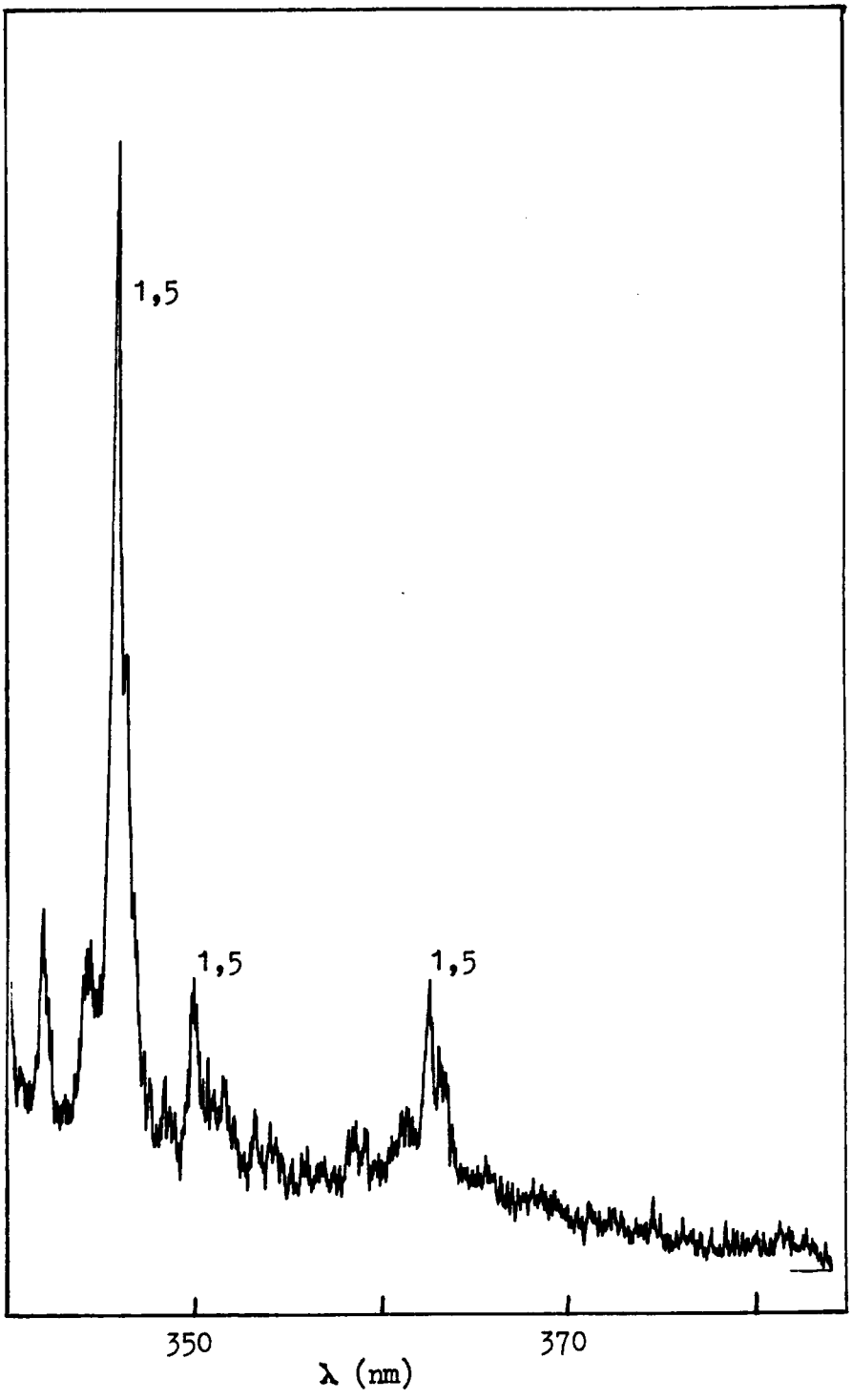

Figure 37. Fluorescence spectrum of hydroxynaphthalene mixture at an excitation wavelength of 329 nm.

1,5: 1,5-Dihydroxynaphthalene.

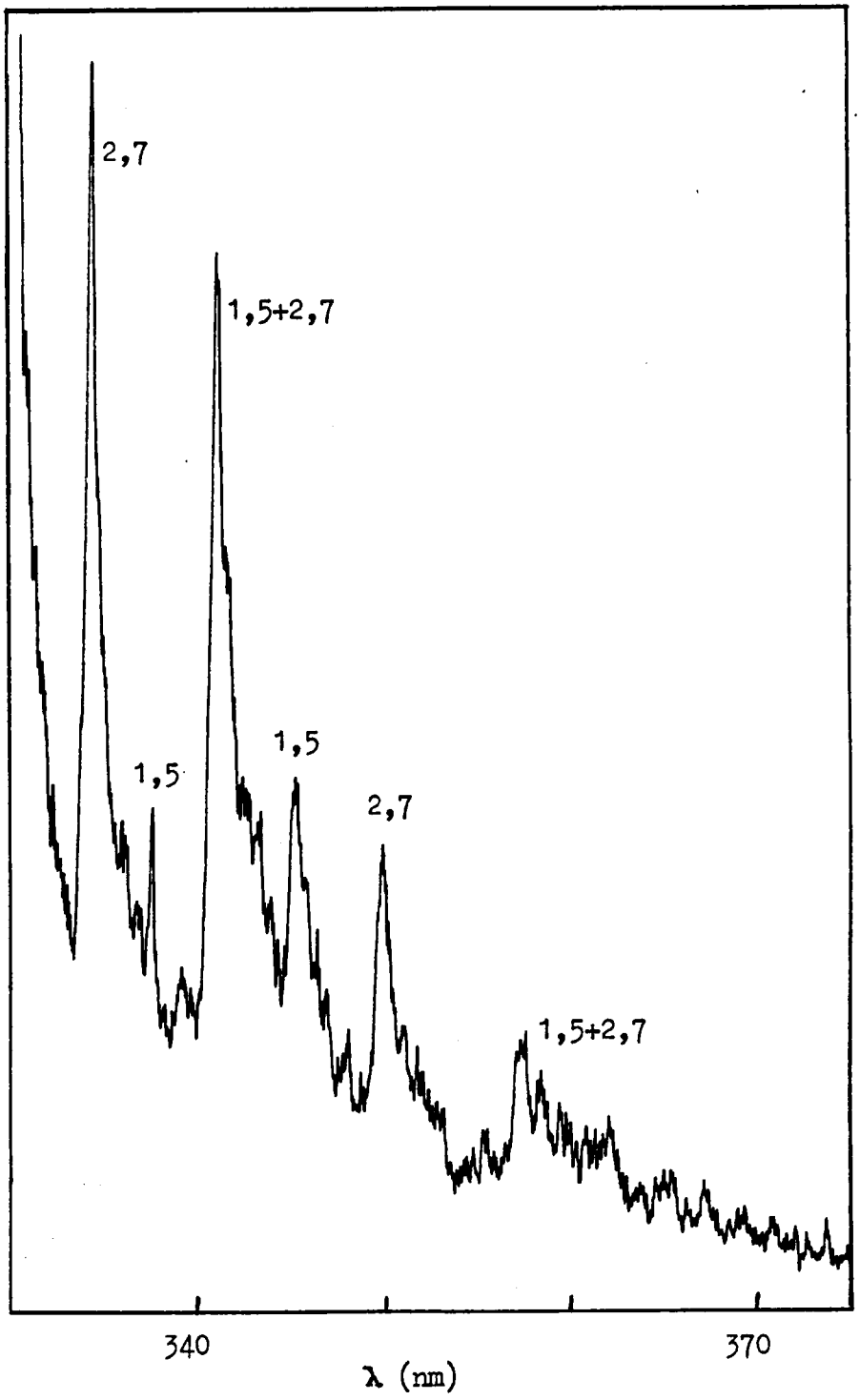

Figure 38. Fluorescence spectrum of hydroxynaphthalene mixture at an excitation wavelength of 325.5 nm.

1,5: 1,5-Dihydroxynaphthalene; 2,7: 2,7-Dihydroxy-naphthalene.

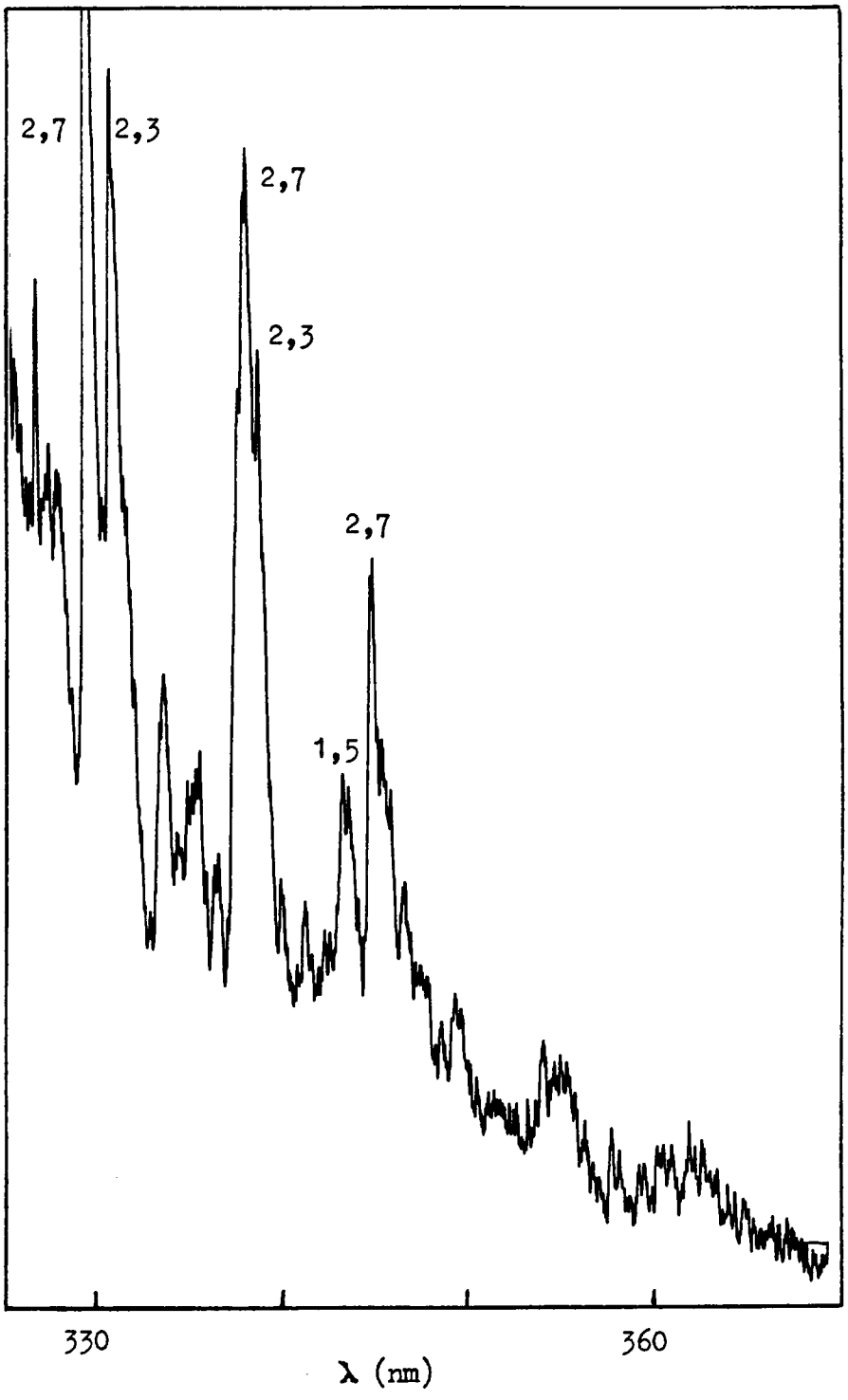

Figure 39. Fluorescence spectrum of hydroxynaphthalene mixture at an excitation wavelength of 322 nm.

1,5: 1,5-Dihydroxynaphthalene; 2,7: 2,7-Dihydroxynaphthalene; 2,3: 2,3-Dihydroxynaphthalene.

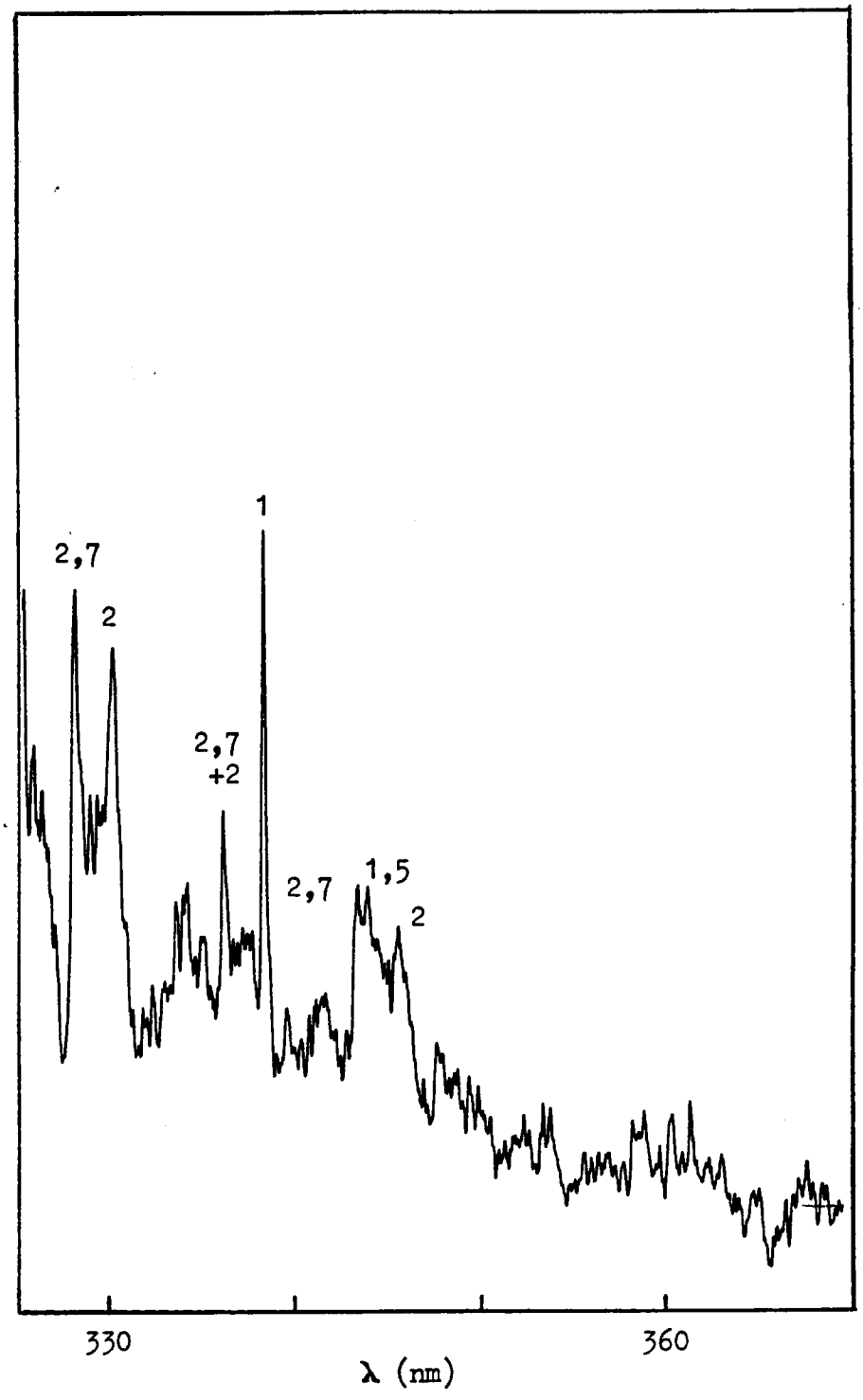

Figure 40. Fluorescence spectrum of hydroxynaphthalene mixture at an excitation wavelength of 320.5 nm.

1,5: 1,5-Dihydroxynaphthalene; 2,7: 2,7-Dihydroxynaphthalene; 2,3: 2,3-Dihydroxynaphthalene;
1: 1-Naphthol; 2: 2-Naphthol.

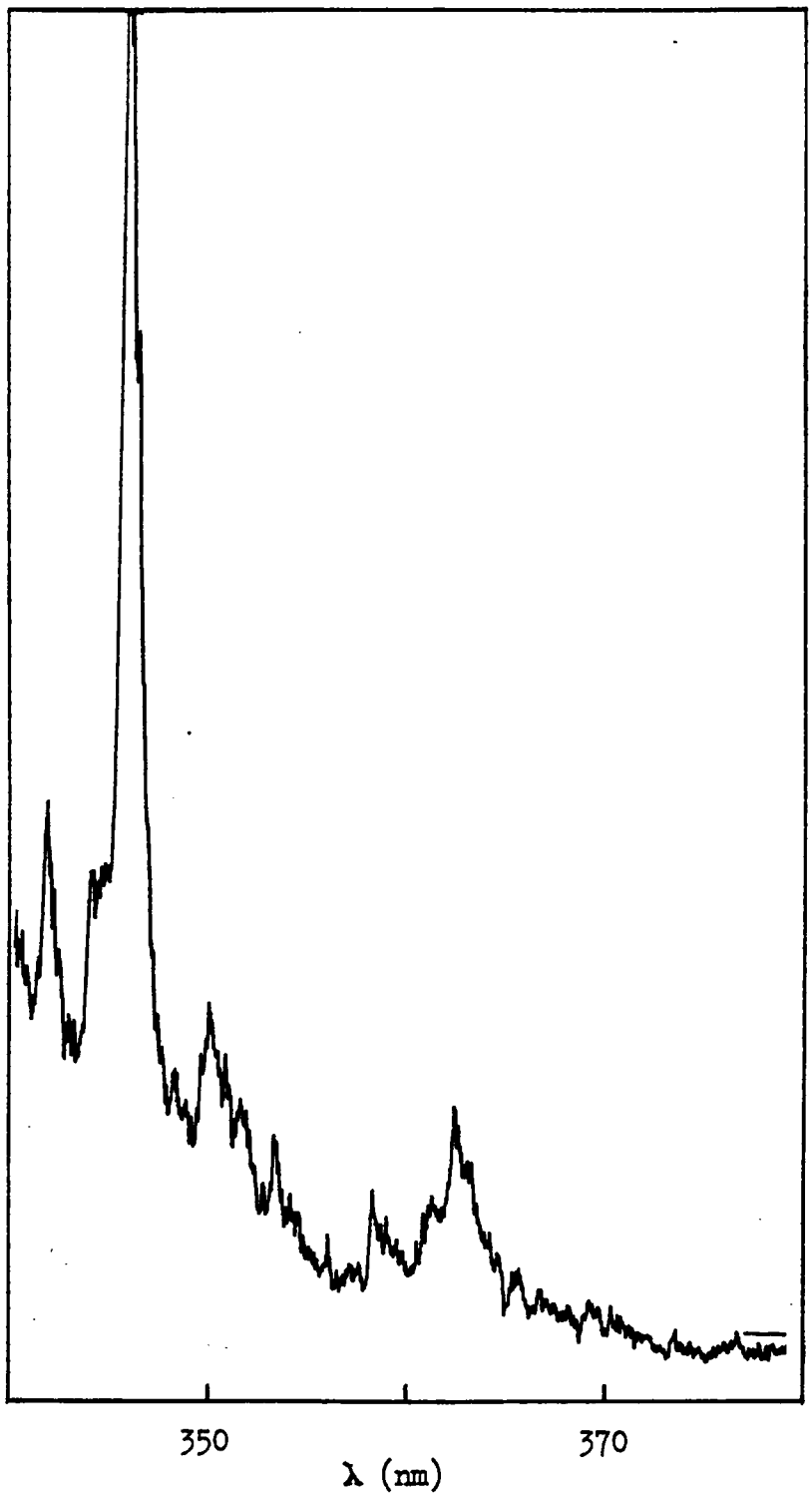

Figure 41. Fluorescence spectrum of 1,5-Dihydroxy-naphthalene in argon.

Excitation wavelength = 329 nm.

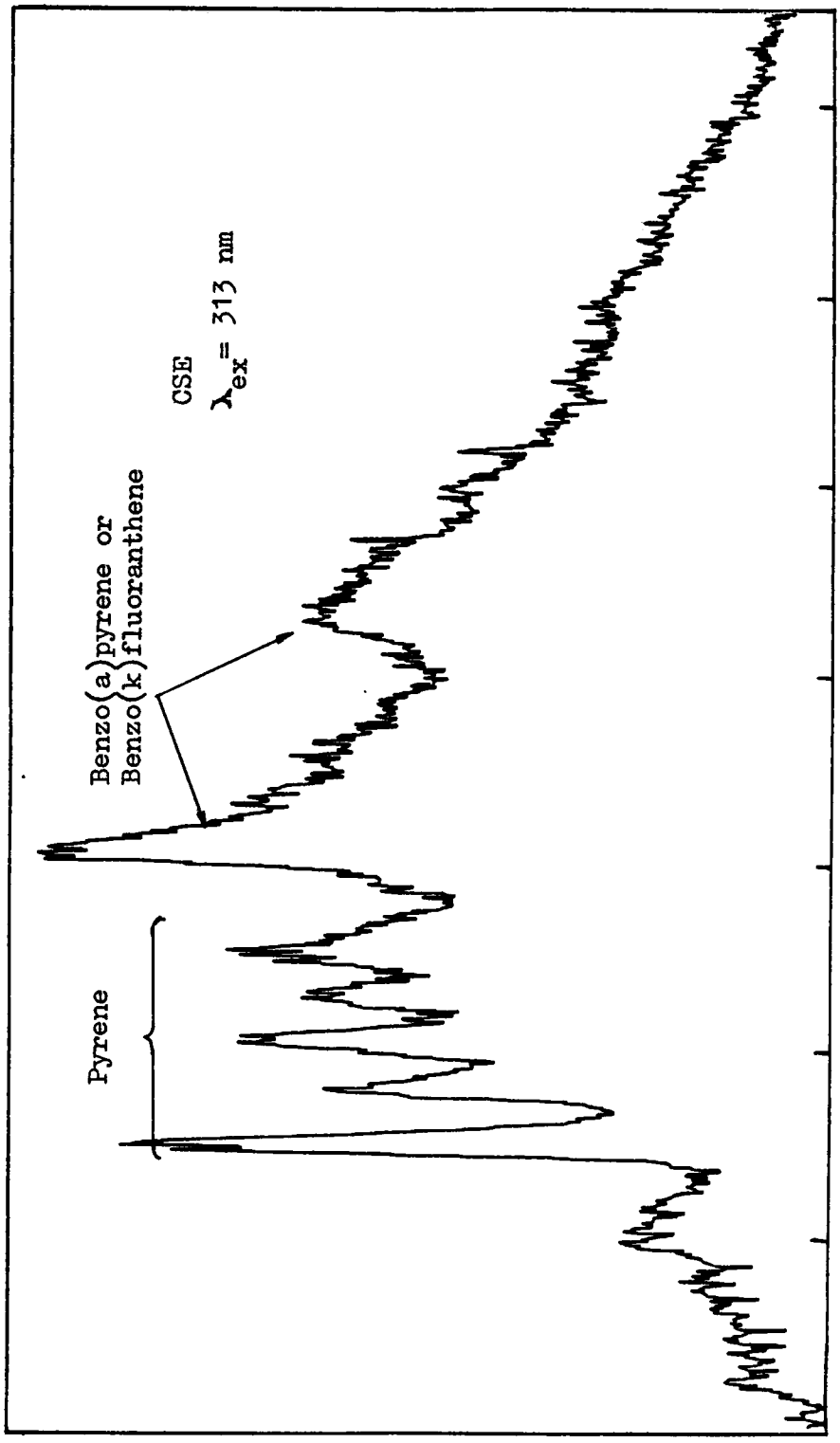

Figure 42. Fluorescence spectrum of two-year-old Fraction-75 in heptane.

demonstrates that the sample was severely degraded with time. Only pyrene and BkF (BaP?) could be identified, and the resolution of both was significantly reduced. However, a site selection spectrum of BaP was obtained easily from this degraded sample, thus proving that the sample still contained BaP even when the CSE spectrum was unable to identify the presence of BaP. Attempts to observe site selection of other components of this degraded Fraction-75 failed.

A synthetic mixture of the compounds listed in TABLE XI (p. 121) was prepared to serve in place of the degraded Fraction-75. This mixture, termed "Syn F-75," contained all PAHs identified in the original Fraction-75 plus some of all PAHs in stock at the time. A CSE spectrum of Syn F-75 is shown in Figure 43 (p. 122). This particular spectrum shows the presence of benzo(b)fluorene, chrysene, pyrene, BkF, and perylene. Emissions from these five components obscure all other components. Figures 44-45 (pp. 123-124) demonstrate that BkF and perylene could be site selected from this mixture. Unlike for the degraded Fraction-75, BaP could not be site selected from Syn F-75. This observation is attributed to large differences between the ratio of BaP to BkF in the two samples.

Thus, site selection techniques are applicable to some complex mixtures and real samples in a qualitative manner.

6. Quantitation of PAHs Using Site Selection

A series of experiments was performed to determine the quantitative capabilities and precision of site selection fluorometry. In all cases, each separate experiment was organized such that the entire experiment could be accomplished in one day with

TABLE XI

CONSTITUENTS OF SYN F-75

Compound	Concentration[a] (µg/ml)
Anthracene	170
Benz(a)anthracene	215
Benzo(b)fluorene	124
Benzo(k)fluoranthene	> 120
Benzo(a)pyrene	261
Benzo(e)pyrene	281
Chrysene	280
Fluoranthene	> 200
Perylene	231
Phenanthrene	241
Pyrene	104
Tetracene	267
Triphenylene	259

[a]Solvent: Dichloromethane

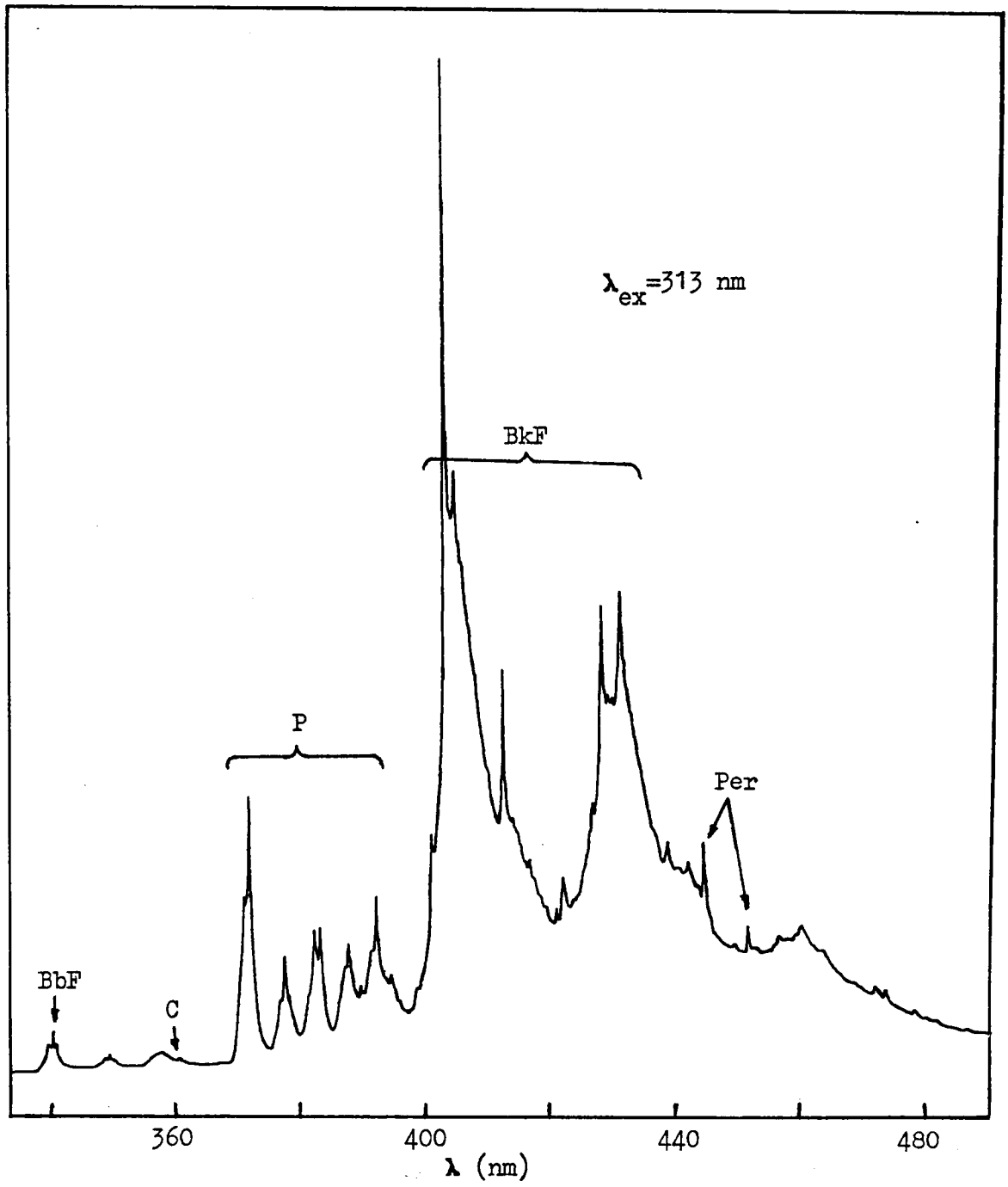

Figure 43. CSE emission spectrum of Syn F-75 in heptane at 15 K.

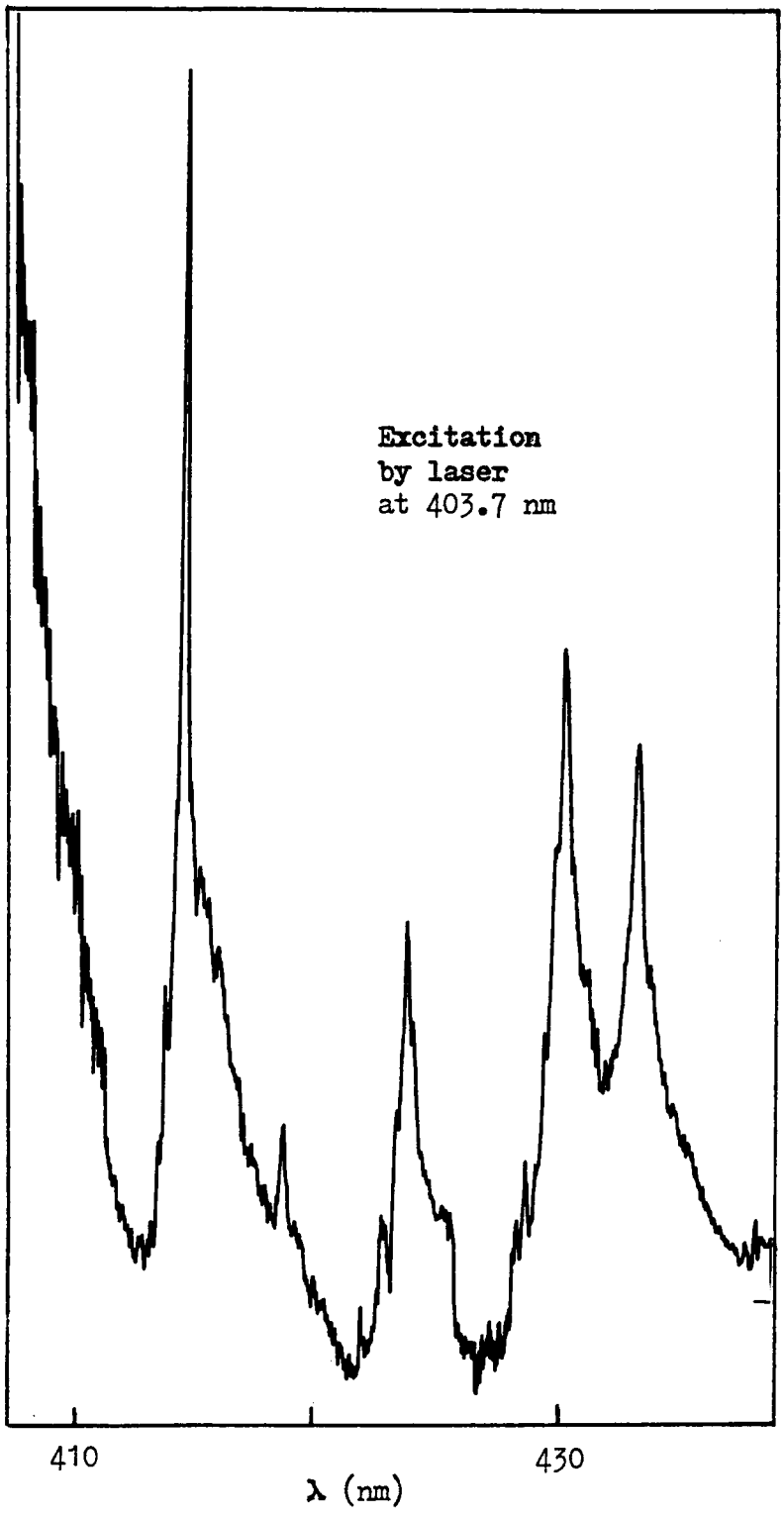

Figure 44. Site selection of benzo(k)fluoranthene from Syn F-75 in heptane at 15 K.

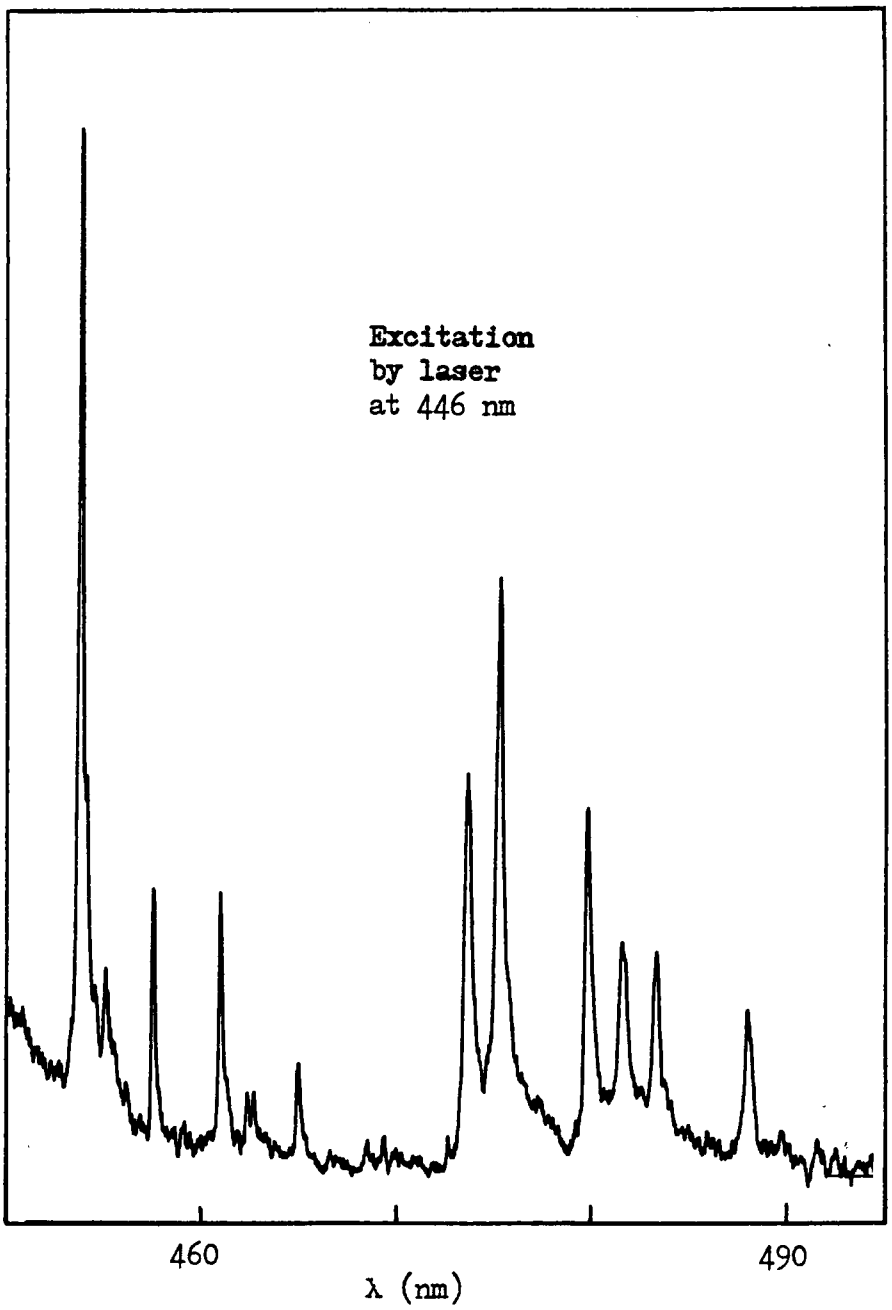

Figure 45. Site selection of perylene from Syn F-75 in heptane at 15 K.

a minimum of laser tuning. Experience had strongly indicated that laser tuning from day to day was somewhat irreproducible. Occasionally, the laser pulse energy observed at a particular wavelength would vary as much as 30-50% from day to day with 10-20% being a common variance. The experiments were limited to single long stretches rather than shorter periods in several different days to reduce the importance of this variable.

Seven deposits of 1,5-DHN ranging from 56 ng to 5.6 μg containing 100 ng of BaP (as the internal standard) were made and used as the first test system. Three of the deposits contained 560 ng of 1,5-DHN and were used in a measurement of quantitative precision. The peak height of the 1,5-DHN fluorescence band (346.3 nm) was ratioed to the peak height of the BaP emission band (400 nm) and the resulting ratio was plotted against the concentration of the 1,5-DHN. The resulting calibration curve is shown in Figure 46 (p. 126) as the upper curve. The nonlinearity of this graph was totally unexpected and first thought to represent bad data resulting from some unknown variable. However, when the absolute intensity of the 1,5-DHN fluorescence was plotted against the amount of 1,5-DHN, as shown in the lower curve of Figure 46, a straight line resulted. The correlation coefficient of this second line is 0.9999.

The hypothesis formulated to explain these results is that the BaP (internal standard) was excited not only by the laser, but also by energy transfer from the 1,5-DHN. At higher concentrations of 1,5-DHN, the BaP fluorescence intensity was greater than at lower levels of 1,5-DHN even though the amount of BaP was the same for

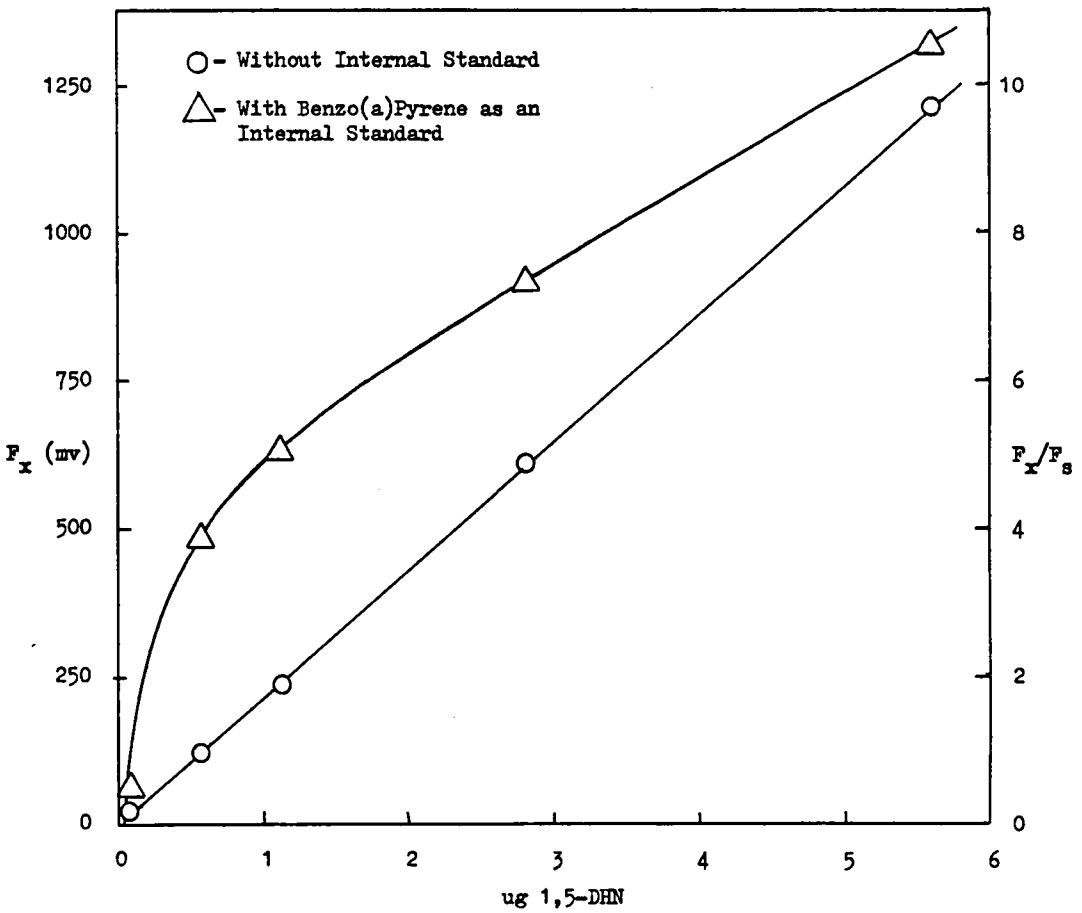

Figure 46. Calibration curve for 1,5-dihydroxynaphthalene using site selection.

all deposits and the laser excitation intensity was approximately the same. Thus, the ratio of analyte to internal standard fell short of the ratio which would be expected at higher concentrations of analyte. This revelation is unfortunate as the absence of this effect has previously been cited as an advantage of MIF over RTF.[22]

Either radiative and/or Förster energy transfer explain these data. Both cases necessitate an overlap of the donor (analyte in this case) emission and the acceptor (internal standard) absorption bands. Thus, this effect occurs when the donor emission is at shorter wavelengths than that of the acceptor. This energy transfer has gone unnoticed until this time as the internal standard used in previous work generally emitted at a shorter wavelength than the analyte. Since the amount of internal standard remains the same (except at very low concentrations) in each deposit, the effect of the internal standard on the analyte is constant. At low concentrations, the amount of internal standard used in previous work was generally the same as the analyte. However, at low concentrations, energy transfer is expected to be greatly reduced.

To have used an internal standard in the present work for which the emission was at shorter wavelengths than that of the analyte would have necessitated using different excitation wavelengths for each compound. Because of the limited range of the laser dyes, different dyes would have been needed and the laser would have to be retuned for each dye and wavelength. As discussed previously, retuning had to be avoided, when possible, to avoid large intensity variations. Thus, in the present work, the fluorescence of the

internal standard was necessarily found at longer wavelengths than that of the analyte. Because the analyte concentration is variable, the effect of the analyte emission on the emission of the internal standard is also variable.

Several tests and observations support the hypothesis of energy transfer to the internal standard from the analyte. First, the plot of absolute intensity of fluorescence as a function of the amount of analyte is a straight line, which would be expected. The high correlation coefficient of this calibration curve indicated that the experiment was within the range of linearity. Second, the nonlinear calibration curve was not obtained until the analyte intensity was ratioed to that of the internal standard. Third, an experiment was performed in which a series of deposits contained equal but varying absolute amounts of BaP and perylene. The BaP fluorescence intensity was divided by that of the perylene and the resulting ratio was plotted against the quantity of BaP. As expected, the ratio increased at lower concentrations and started to level off when the detection limit was reached. The results of this experiment are plotted in Figure 47 (p. 129). The conclusion is that energy transfer in MIF can be much more efficient than previously supposed and, in view of this finding, should be investigated thoroughly to ascertain the extent of this effect.

Which type of energy transfer, Forster or radiative, is taking place is not known, but could be determined experimentally. Radiative energy transfer is dependent upon the pathlength of the sample. Also, the lifetime of the donor is not affected in the presence of

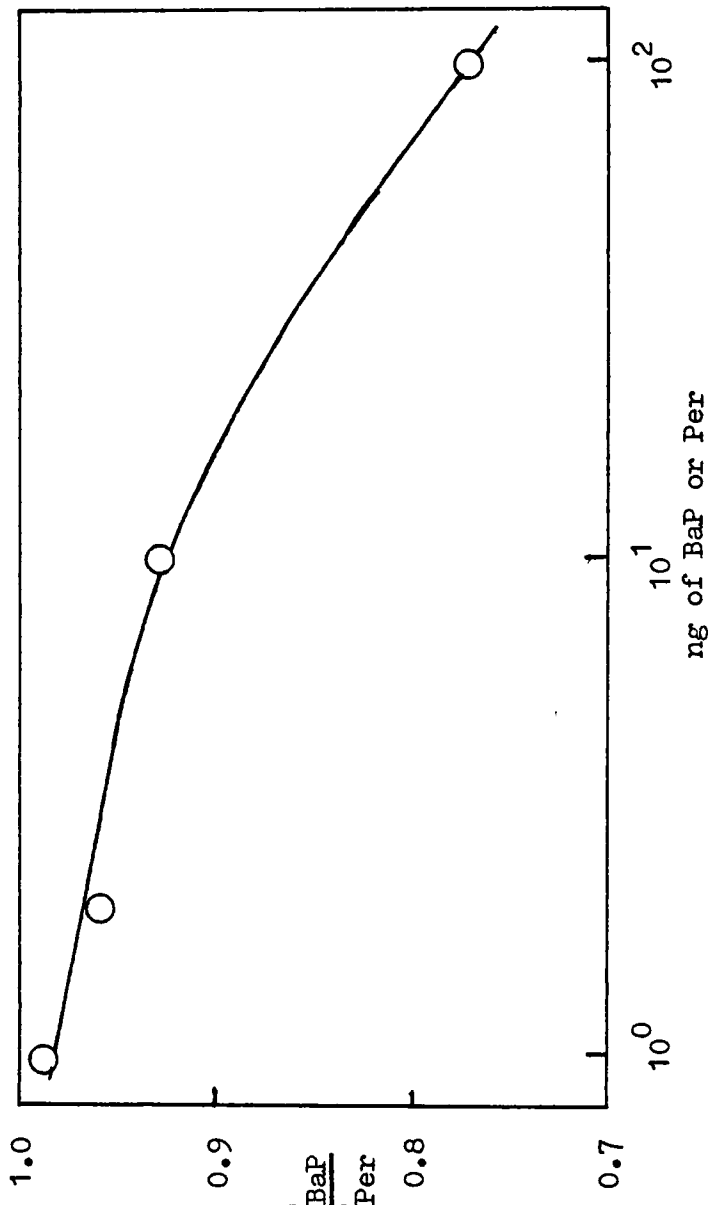

Figure 47. Graph of ratio of fluorescence intensities for constant, one-to-one ratio of benzo(a)pyrene to perylene.

radiative transfer. Förster transfer is not dependent upon the pathlength of the sample and is a quenching mechanism for the donor excited state, thus reducing the donor's fluorescence lifetime. By measuring the donor's lifetime and/or varying the thickness (pathlength) of the deposit while monitoring the ratio of the fluorescence of the two compounds, the type of transfer can be determined.

If Förster transfer is indicated, then increasing the matrix-to-sample ratio should reduce the nonlinearity of the calibration curves by increasing the average distance between solute molecules. Radiative transfer can be reduced by producing a thinner sample, thus reducing the pathlength.

Quantitative calibration curves were also obtained for BaP using perylene as the internal standard. Figure 48 (p. 131) shows the results obtained when site selection was used. The ratioed curve exhibited negative deviations from linearity, as in the experiments with 1,5-DHN, while the plot of absolute intensity of the BaP was linear with a correlation coefficient of 0.9999. Figure 49 (p. 132) shows the calibration curve when CSE was used. The same effect is observed as when laser excitation was used. Thus, the nonlinearity of the ratioed curves is not related to the use of the laser.

These experiments demonstrate that quantitative analysis using site selection is possible, although great care needs to be taken when choosing the internal standard.

Figures 46, 48, and 49 (pp. 126, 131, and 132) each show a rather limited range, although the curves are linear over the entire range for the unratioed curves. The lower limit of PAH

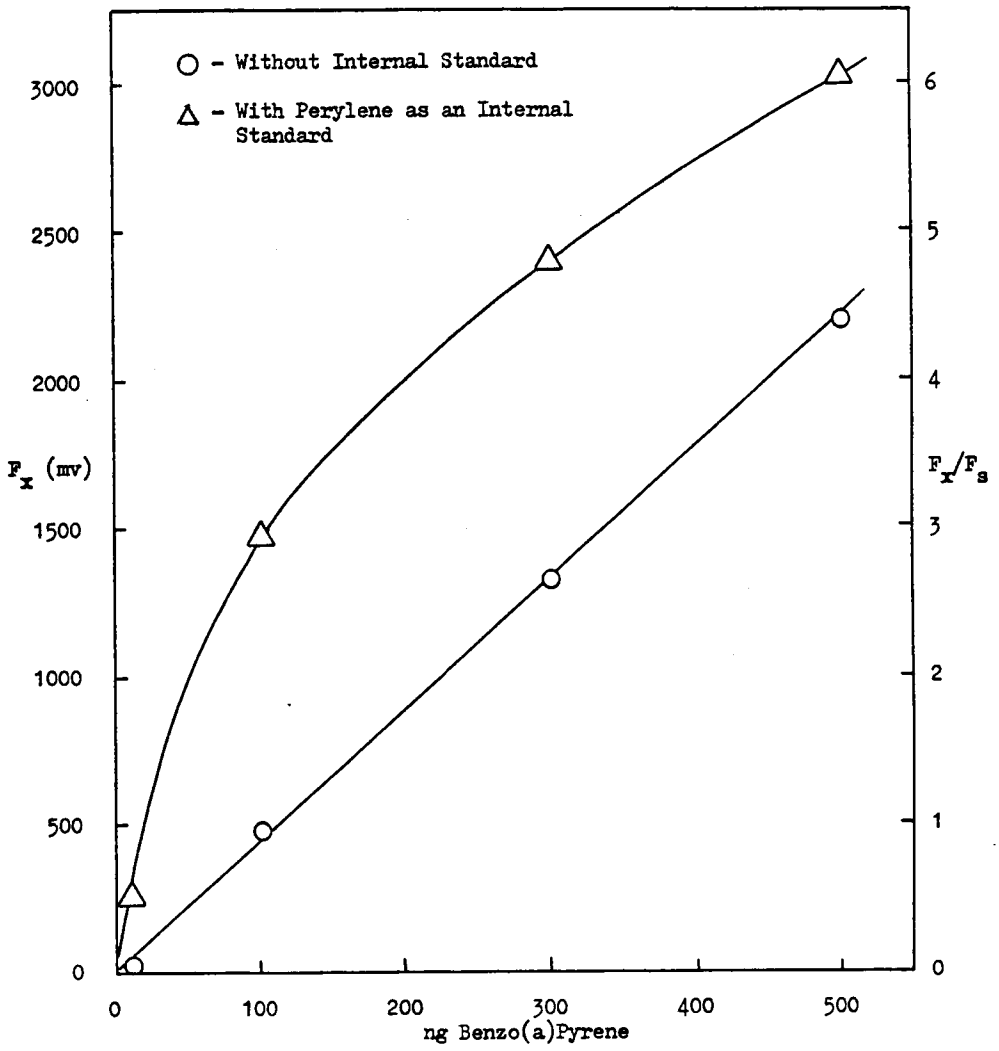

Figure 48. Calibration curve for benzo(a)pyrene in heptane at 15 K using site selection.

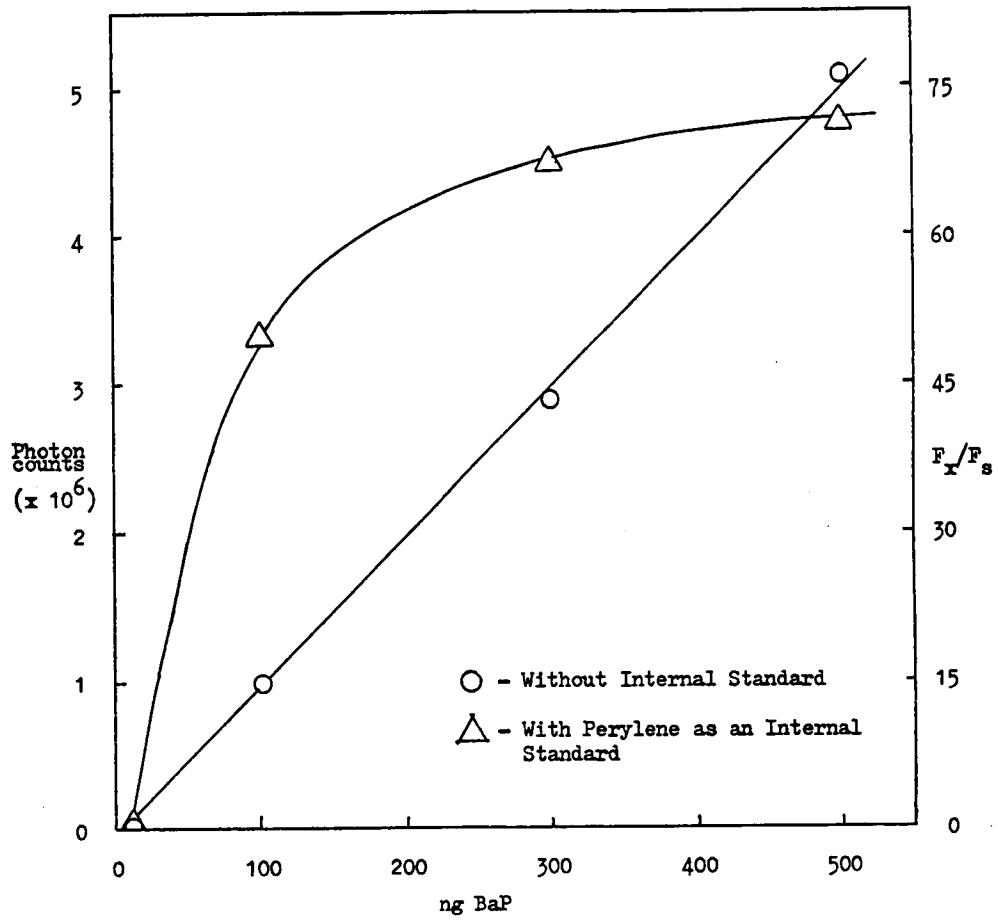

Figure 49. Calibration curve for benzo(a)pyrene in heptane at 15 K using CSE.

concentration for the laser experiments was determined by the noise level of the instrument. The primary noise source was pulse-to-pulse variation in the intensity of the laser. The detection limits for 1,5-DHN in argon and BaP in heptane are 50 ng and 1 ng, respectively, and are limited by the background noise from the laser. The detection limit was defined in this work as that quantity of analyte which yielded a signal equal to three times the noise level. The detection limit can be extended slightly by increasing the time constant of the recorder so as to smooth the noise and increasing the scan time. The result is a large tradeoff of time.

The upper limits of the working curves in this work were determined by the upper limit of voltage measurement of the sampling oscilloscope. That is, the largest quantities of analyte measured resulted in PMT output voltages which approached the upper limit of the oscilloscope. The upper limit of the experiment can be extended by lowering the PMT voltage. The reduced PMT voltage results in a decrease of the signal voltage due to the fluorescence. Thus, a higher level of analyte can be measured by reducing the PMT voltage. Spectra have been obtained with PMT voltages as low as 900 volts (the range was 0-2000 volts).

7. Quantitative Precision of Site Selection Fluorescence

When a deposit is made, the sample molecules distribute themselves in a large variety of different sites. If the distribution of sites were irreproducible, then the fluorescence intensity observed in a site selection experiment would be affected. Thus, a fundamental reason might exist which would cause the analytical

site selection method to be less precise than those methods in which the whole distribution is capable of being excited.

Therefore, the precision of quantitative site selection was also investigated. Although the use of internal standards resulted in nonlinear working curves, three deposits of 560 ng of 1,5-DHN and 100 ng of BaP indicated a slight increase in precision when the internal standard was used. For these deposits, the relative standard deviation was 8.0% when the internal standard was used and 8.3% without the standard. Thus, the precision of analytical site selection with MI approaches the precision of CSE-MIF (on the order of 4-7%[52]).

Twelve deposits of 100 ng each of BaP and perylene were made to ascertain whether the site selection technique is less precise than other fluorometric methods. Six of the deposits were excited at 403.7 nm, a wavelength at which site selection of the BaP occurs. The second set of six was excited at 265 nm, a wavelength at which the entire distribution of sites is excited. Laser excitation was used in both cases so as to eliminate any possible variables between instruments. The second set of deposits was also subjected to CSE analysis so that a comparison could be made between the instruments. An F-test was applied to make a statistical comparison of the variances which were calculated for each method. These results are found in TABLE XII (p. 135). As shown, this experiment indicated that there is no evidence that site selection is less precise than other excitation methods.

TABLE XII

COMPARISON OF PRECISION OF FLUOROMETRIC METHODS

Method	Variance	F-Value[a]	Result at 95% Level[b]
CSE	0.167		
		6.63	Positive
Laser - without Site Selection	0.025		
		1.90	Negative
Laser - with Site Selection	0.048		

[a] F is equal to the ratio of the variances being compared.

[b] Confidence level. A positive result indicates a significant difference between variances.

One very surprising result from this experiment is that the CSE method of excitation appears to be much less precise than the laser methods. The origin of this apparently anomalous result is not apparent. Many more data points would need to be obtained in order to be able to make a definitive statement regarding the relative precision of site selection and non-site selection methods. The present results do not provide any indication that quantitative site selection fluorometric analysis is intrinsically infeasible.

CHAPTER IV

CONCLUSIONS

Site selection fluorescence in matrix-isolated deposits of several PAHs has been observed. Nitrogen appears to exhibit a strong phonon-electron interaction with the guest PAH molecules which results in a general inability to accomplish site selection at nanogram levels. However, argon, heptane, and perfluoro-n-hexane exhibit properties which lend themselves to site selection. Argon is of less utility due to reduced fluorescence quantum yields of the imbedded PAHs as compared with those of the same PAHs imbedded in the other matrices.

Site selection fluorescence is less sensitive than the methods in which the entire distribution is excited. Two reasons account for this fact. First, site selection is fundamentally less sensitive because only a fraction of the sample molecules is excited. Second, the molar absorptivities for the PAHs are generally much lower for the 0-0 absorption band than for the higher energy absorption bands.

Site selection fluorescence can be performed quantitatively, with detection limits presently being limited primarily by pulse-to-pulse laser intensity variations. Improvement of the detection limits should be possible by the use of a signal handling system which normalizes for this factor. The present detection limits for 1,5-DHN in argon and BaP in heptane are 50 ng and 1 ng, respectively. The upper limit of detection observed in this work is defined by

the upper measurement limit of the oscilloscope. The upper limit can be easily extended by manipulation of the detection instrumentation parameters.

Site selection also exhibits quantitative precision which is of the order of 8% relative standard deviation. Results surprisingly indicated that the laser-based methods are more precise than the CSE method. No fundamental reason can be offered for this result and so it should be examined further in terms of its validity and generality.

Some quantitative calibration curves were found to exhibit severe nonlinearity. This effect has been attributed to energy transfer, which has been previously thought to play an insignificant role in MIF. This effect represents a potentially severe impediment to applications of matrix isolation fluorescence to quantitative analysis, and it should therefore be thoroughly investigated.

LIST OF REFERENCES

LIST OF REFERENCES

1. M. R. Guerin, in "Polycyclic Hydrocarbons and Cancer," Vol. I, H. V. Gelboin and P. O. P. Ts'o, Eds., Academic Press, New York, N. Y., 1978.

2. National Academy of Sciences, "Particulate Polycyclic Organic Matter," Washington, D. C., 1972.

3. M. E. Snook, J. Nat. Cancer Inst., 57, 191 (1976).

4. W. Gräf and H. Diehl, Arch. Hyg., 150, 49 (1966).

5. L. Mallet, J. Zanghi, and J. Brisou, C. R. Hebd. Seances Acad. Sci. Ser. D., 264, 1534 (1967).

6. N. H. Ketcham and R. W. Norton, Arch. Environ. Health, 1, 194 (1960).

7. L. E. Stromberg and G. Widmark, J. Chromatogr., 47, 27 (1970).

8. "Project H-Coal: Report on Process Development," R and D Research Report 26, Office of Coal Research, U. S. Dept. of Interior, 1968.

9. C. Heidelberger in "Carcinogenesis - A Comprehensive Survey," Vol. I, R. I. Freudenthal and P. Jones, Eds., Raven Press, New York, N. Y., 1976.

10. J. W. Cook, C. L. Hewett, and I. Hieger, J. Chem. Soc., 395 (1933).

11. C. R. Sawicki and E. Sawicki, Prog. Thin-Layer Chromatogr. Relat. Methods, 3, 233 (1972).

12. L. Toth, J. Chromatogr., 50, 72 (1970).

13. E. Sawicki, Crit. Rev. Anal. Chem., 1, 275 (1970).

14. P. W. Jones, R. D. Giammar, P. E. Strup, and T. B. Stanford, Environ. Sci. Technol., 10, 806 (1976).

15. M. L. Lee, M. Novotny, and K. D. Bartle, Anal. Chem., 48, 1566 (1976).

16. T. Doran and N. G. McTaggart, J. Chromatogr. Sci., 12, 715 (1974).

17. E. J. Baum, in "Polycyclic Hydrocarbons and Cancer," Vol. I, H. V. Gelboin and P. O. P. T'so, Eds., Academic Press, New York, N. Y., 1978.

18. M. Novotny, Anal. Chem., 50, 16A (1978).

19. M. A. Fox and S. W. Staley, Anal. Chem., 48, 992 (1976).

20. H. J. Klimisch, Anal. Chem., 45, 1961 (1973).

21. C. Golden and E. Sawicki, Int. J. Environ. Anal. Chem., 4, 9 (1975).

22. E. L. Wehry and G. Mamantov, Anal. Chem., 51, 643A (1979).

23. G. T. Reedy, S. Bourne, and P. T. Cunningham, presented at the 29th Pittsburgh Conference on Analytical Chemistry and Applied Spectroscopy, Abstract No. 50, Cleveland, Ohio, February, 1978.

24. T. Vo-Dinh, Anal. Chem., 50, 396 (1978).

25. J. H. Rho and J. L. Stuart, Anal. Chem., 50, 620 (1978).

26. E. L. Wehry, R. R. Gore, and R. B. Dickinson, in "Lasers and Chemical Analysis," G. M. Hieftje, F. E. Lytle, and J. C. Travis, Eds., Humana Press, New York, N. Y., 1981 (in press).

27. A. A. Lamola and N. J. Turro, "Energy Transfer and Organic Photochemistry," John Wiley, New York, N. Y., pp. 33-54, 1969.

28. C. A. Parker, "Photoluminescence of Solutions," American Elsevier, New York, N. Y., 1968.

29. E. V. Shpol'skii, A. A. Il'ind, and L. A. Klimova, Dokl. Akad. Nauk. SSSR., 87, 935 (1952).

30. R. J. Lukasiewicz and J. D. Windfordner, Talanta, 19, 381 (1972).

31. E. Whittle, D. A. Dows, and G. C. Pimentel, J. Chem. Phys., 22, 1943 (1954).

32. J. R. Maple, E. L. Wehry, and G. Mamantov, Anal. Chem., 52, 920 (1980).

33. G. J. Diebold, N. Karny, and R. N. Zare, Anal. Chem., 51, 67 (1979).

34. J. H. Richardson, S. M. George, and M. E. Ando, Nat. Bur. Stand. (U. S.) Spec. Pub., 519, 691 (1979); Chem. Abstr., 91, 128804 (1979).

35. N. Ishibashi, T. Ogawa, T. Imasaka, and M. Kunitake, Anal. Chem., 51, 2096 (1979).

36. R. B. Dickinson and E. L. Wehry, Anal. Chem., 51, 778 (1979).

37. I. Abram, R. A. Auerbach, R. R. Birge, B. E. Kohler, and J. M. Stevenson, J. Chem. Phys., 61, 3857 (1974).

38. P. Tokousbalides, E. R. Hinton, R. B. Dickinson, P. V. Bilotta, E. L. Wehry, and G. Mamantov, Anal. Chem., 50, 1189 (1978).

39. R. I. Personov, E. I. Al'shits, L. A. Bykovskaya, and B. M. Kharlamov, Soviet Phys. JETP, 38, 912 (1974).

40. B. E. Kohler, in "Chemical and Biochemical Applications of Lasers," C. B. Moore, Ed., Academic Press, New York, N. Y., Vol. 4, 1979.

41. J. C. Brown, J. M. Hayes, and G. J. Small, in "Lasers and Chemical Analysis," G. M. Hieftje, F. E. Lytle, and J. C. Travis, Eds., Humana Press, New York, N. Y., 1981 (in press).

42. I. I. Abram, R. A. Auerbach, R. R. Birge, B. E. Kohler, and J. M. Stevenson, J. Chem. Phys., 63, 2473 (1975).

43. G. Flatscher, K. Fritz, and J. Friedrich, Z. Naturforsch., A, 31, 1220 (1976).

44. G. Flatscher and J. Friedrich, Chem. Phys. Lett., 50, 32 (1977).

45. W. C. McColgin, A. P. Marchetti, and J. H. Eberly, J. Amer. Chem. Soc., 100, 5622 (1978).

46. E. I. Al'shits, R. I. Personov, and B. M. Kharlamov, Opt. Spec., 41, 474 (1976).

47. V. E. Bondybey and J. H. English, J. Amer. Chem. Soc., 101, 3446 (1979).

48. J. Fünfschilling and D. F. Williams, Photochem. Photobiol., 26, 109 (1977).

49. B. Dellinger, D. S. King, R. M. Hochstrasser, and A. B. Smith, J. Amer. Chem. Soc., 99, 7138 (1977).

50. J. C. Brown, M. C. Edelson, and G. J. Small, Anal. Chem., 50, 1934 (1978).

51. J. C. Brown, J. A. Duncanson, and G. J. Small, submitted to Anal. Chem. (1980).

52. R. C. Stroupe, "Matrix Isolation Fluorescence Spectroscopy of Polycyclic Aromatic Hydrocarbons," Ph.D. Dissertation, University of Tennessee, 1977.

53. P. V. Bilotta, "Matrix Isolation Fluorescence Spectroscopy of Polycyclic Organic Matter," M.S. Thesis, University of Tennessee, 1978.

54. E. R. Hinton, "Quantitative Matrix Isolation Fourier Transform Infrared Spectroscopy of Polycyclic Aromatic Hydrocarbons," Ph.D. Dissertation, University of Tennessee, 1979.

55. V. L. Biddle, "Part I: Fluorometric Determination of Manganese (II) via Catalyzed Enzymatic Oxidation of 2,3-Diketogulonate. Part II: Low Temperature Fluorescence Spectroscopy of Tetrachlorobiphenyls and Dihydroxynaphthalenes," Ph.D. Dissertation, University of Tennessee, 1978.

56. R. S. Becker, I. S. Singh, and E. A. Jackson, J. Chem. Phys., 38, 2144 (1963).

57. B. Meyer, "Low Temperature Spectroscopy," American Elsevier, New York, N. Y., 1971.

58. R. H. Dicke, Phys. Rev., 93, 99 (1954).

APPENDIXES

APPENDIX I

OPERATION OF SAMPLING OSCILLOSCOPE

The Tektronix 5S14N dual-trace delayed-sweep sampler for the 5000 series oscilloscope mainframe is a highly versatile instrument for the measurement of signals with picosecond risetimes. A signal this fast is too fast for real-time oscilloscopes to measure without distortion. An understanding of the theory of sampling and the operation of the 5S14N will save considerable time.

The sampling method of measurement of electrical signals has two primary requirements. Most important, the signal has to be repetitive. A single voltage measurement is made on each pulse during a very narrow time "window." On the 5S14N, the time window is 350 picoseconds. Many measurements are made on at least as many pulses and the accumulation of all the measurements is displayed on the oscilloscope screen (CRT). The time window can be moved to any point on the analytical signal or can be scanned across the width of the analytical signal.

For accurate measurements of short pulses, the position of the time window must be precise. Thus, a precise trigger signal must be available. It is not necessary that the time between repetitions be precise, but the time between the trigger and its analytical signal must be precise. If the latter time period is inconsistent, then the analytical signal will be inaccurately displayed. If this time "jitter" is excessively large, then the displayed signal will be severely distorted.

The 5S14N has two operational delay modes, a delaying sweep and a delayed sweep mode. The delaying mode produces the usual oscilloscope display with the addition of two intensified dots which are controlled by the DELAY ZERO (first dot) and DELAY TIME (second dot) controls. These two dots can be moved anywhere horizontally on the CRT by their respective controls and are useful for measuring time differences such as pulse widths. This is accomplished by setting the first dot at the beginning of the event to be measured and the second dot at the end. The setting of the DELAY TIME control times the sweep calibration gives the time period between the two dots.

In the delayed sweep mode, the oscilloscope trace starts at the position indicated by the second dot. The dots are not visible on the CRT. The sweep rate in the delayed mode can be set separately from the sweep rate in the delaying mode. This allows great versatility in the placement of narrow pulses on the CRT as illustrated in the following example. Figure 50a (p 147) illustrates a short signal which is delayed considerably from the trigger signal. In the delaying sweep mode with the sweep rate set at 100 ns/div, the display would appear as illustrated in Figure 50b (p 147). The signal is easily displayed but is quite narrow. Measuring a decay time or a FWHM for this signal would be difficult. By setting the second dot at 480 ns and switching to the delayed sweep mode, the oscilloscope starts its trace at 480 ns. The delaying sweep rate should be left at 100 ns/div. By placing the delayed sweep rate at 10 ns/div, the display illustrated in Figure 50c (p 147) is obtained. The pulse is now well placed and fills a greater portion of the CRT. Measure-

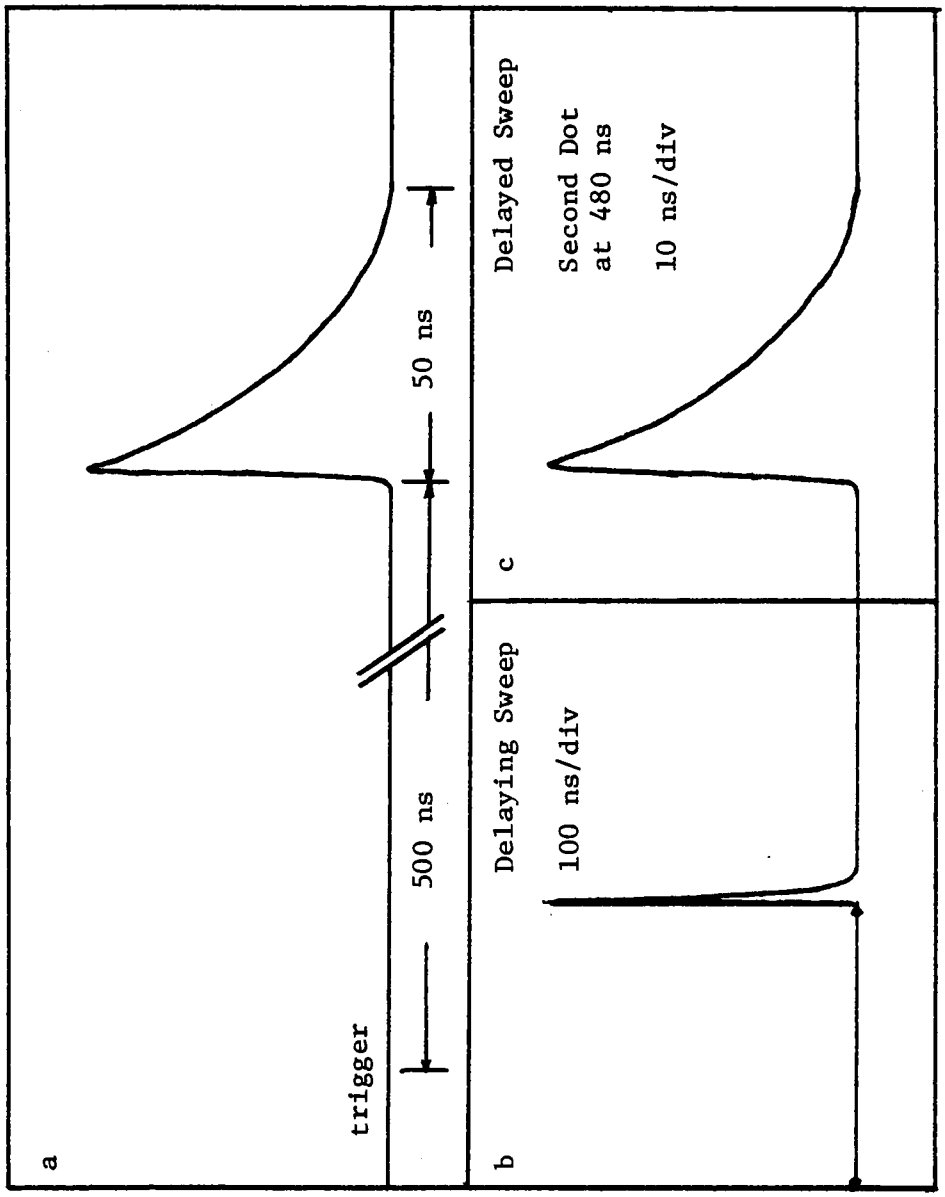

Figure 50. Illustration of delay modes of sampling oscilloscope.

ments are now easier.

The 5S14N can be scanned manually using the SCAN control when the MAN button is depressed. With this and the previous information in mind, a better understanding of the use of the 5S14N with the dye laser spectrometer (DLS) is obtained.

The trigger signal from the photodiode in the dye laser preceeded the fluorescence signal by approximately 40 ns (set by the delay characteristics of the coaxial cables used). Most fluorescence signals required a sweep rate of 10 ns/div. The delayed mode was chosen to place the fluorescence signal in a better position on the CRT. To do this, the DELAY TIME was set at 2.0. The horizontal and vertical outputs were connected to the X-Y recorder for hard copy display. To obtain a fluorescence decay curve, the SINGL SCAN button was depressed (causing the 5S14N to sweep once), the START button was depressed and held, and the recorder pen was lowered. The scan started when the START button was released. This procedure recorded the fluorescence decay curve.

To obtain a spectrum of the fluorophore emission, a strong emission was first displayed on the CRT by setting the monochromator to one of the emission wavelengths. The MAN (manual) button was depressed, which activated the SCAN control. The SCAN was then used to place the electron beam of the CRT on the peak of the fluorescence decay curve for maximum sensitivity or to any known point of the curve for time resolution. The SCAN control was left in this position while the monochromator was scanned over the wavelength region of interest. During the wavelength scan, the recorder time base was

used to scan the recorder, because there was no connection between the monochromator wavelength drive and the recorder X-axis. This procedure allowed a spectrum to be obtained at the delay time set by the SCAN control. The wavelength axis was subsequently established by knowing the starting and stopping points of the scan. This method was needed as the timing electronics in the scan control of the monochromator were found to be faulty.

Two other controls should be mentioned. When the NOISE button is depressed, the oscilloscope averages 3-5 consecutive samples before displaying them as one sample. This has the effect of decreasing the noise in the spectrum. The HOLD OFF control varies the time between samples over a 10 microsecond range. The holdoff time allows the electronics to "settle" before taking another sample. Since the repetition rate of the DLS was normally 8-10 Hz, this control had no effect on this work. The holdoff time was the minimum time between samples and the DLS limited the number of samples per second.

All other controls of the 5S14N are direct analogues to their counterparts on a real-time oscilloscope and operate in the same manner.

APPENDIX II

OPERATION OF LIQUID HELIUM CRYOSTAT

The following is a list of detailed instructions for operation of the Air Products LT-3-110 Heli-Tran liquid helium transfer line and cryostat. Refer to Figures 51-53 (pp. 151-153) for the location of all parts named in the instructions.

A. Initial Insertion

1. Insert cold end dip tube into the cold end and turn the needle valve control 3-4 turns onto the cold end. This fully opens the needle valve.
2. Connect the tip flow outlet to the inlet of the tip flow valve.
3. Purge the Heli-Tran with helium. This is done in the following manner.
    a. Connect the outlet of the regulator on the helium gas bottle to the end of the Dewar dip tube with plastic or rubber tubing and clamps.
    b. Pressurize the Heli-Tran to 30 psi and open the shield and tip flow valves.
    c. Purge in this manner for at least 5 minutes.
    d. Shut the shield and tip flow valves and helium gas bottle to stop purge.
    e. It is best to leave the tubing connected to the helium gas bottle and the Dewar dip tube until the Heli-Tran and/or the helium gas bottle is needed for a subsequent step.
4. Replace the 3/8" withdrawal cap on the top of the liquid helium

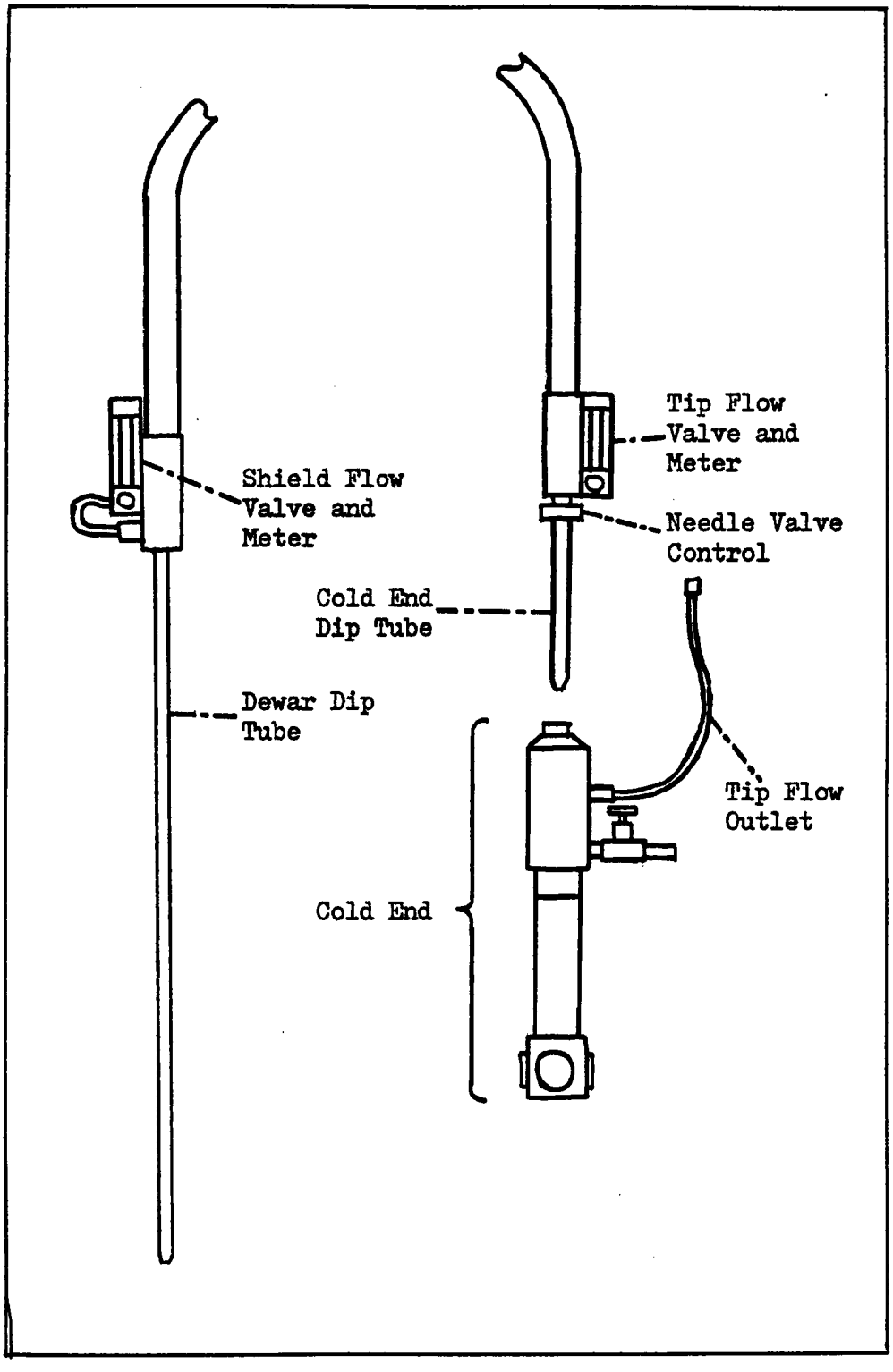

Figure 51. Diagram of Heli-Tran System.

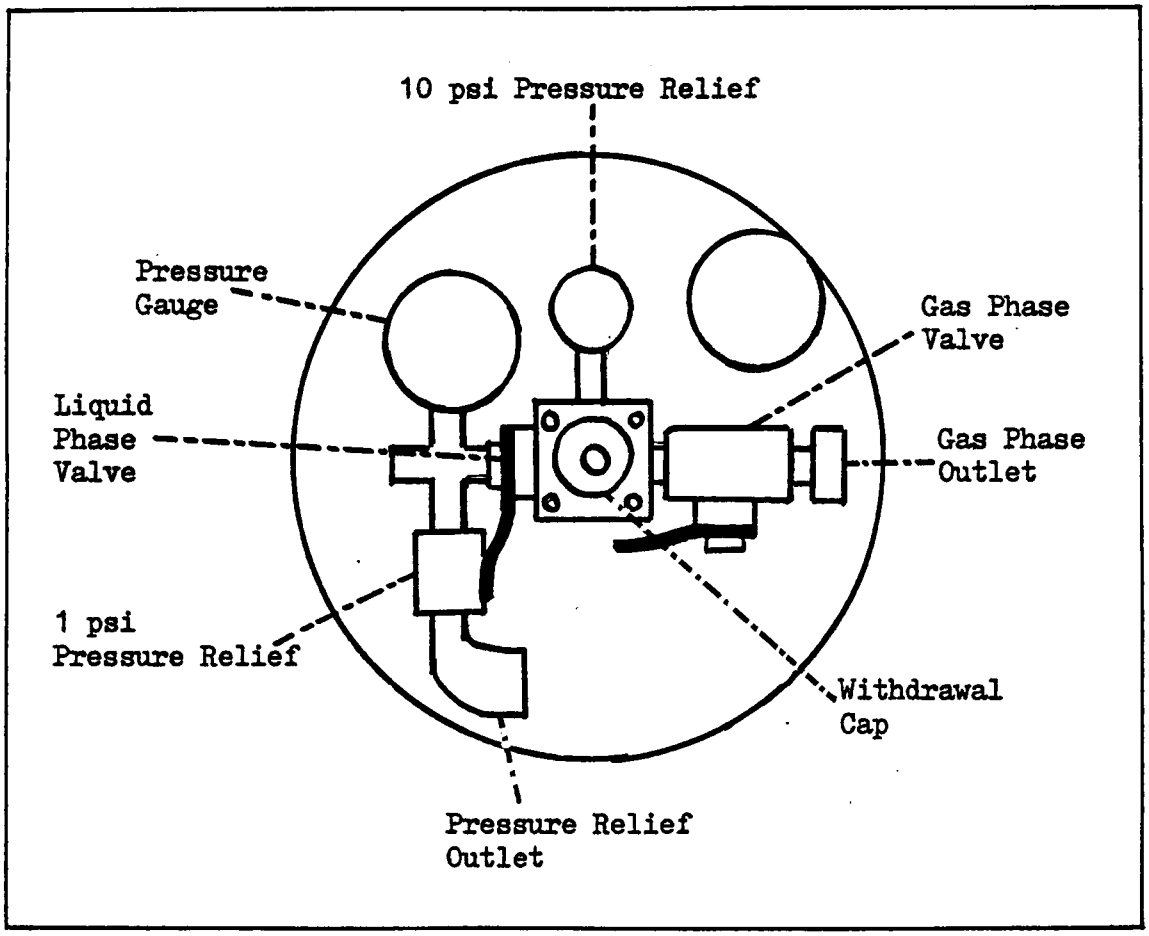

Figure 52. Diagram of top of liquid helium Dewar.

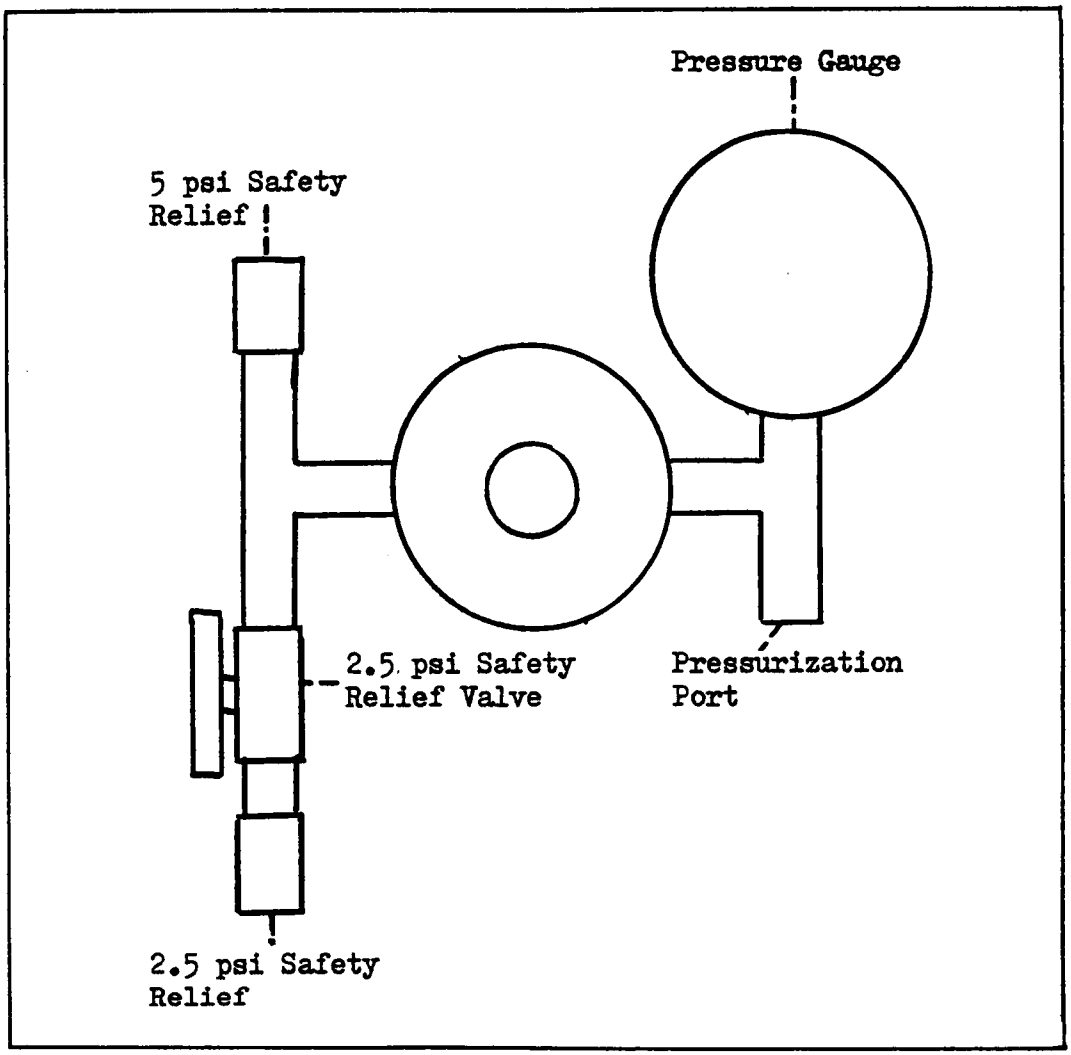

Figure 53. Diagram of top view of Dewar adapter.

Dewar with a 1/2" withdrawal cap. Be sure to replace the 3/8" cap after use.

5. Connect the helium gas bottle to the Dewar adapter pressurization port.
6. Install an end cap onto the pressure relief outlet or close the valve on the pressure relief outlet if the Dewar is so equipped.
7. With the liquid phase valve closed, insert the Dewar adapter through the withdrawal cap until it butts against the liquid phase valve.
8. In a similar manner, insert the Dewar dip tube into the Dewar adapter until it butts against the liquid phase valve.
9. Close the 2.5 psi safety valve on the Dewar adapter.
10. Open the liquid phase valve and insert the Dewar adapter-Dewar dip tube combination until the Dewar adapter is fully inserted. Do not insert the Dewar dip tube any further at this time.
11. Pressurize the Dewar to 5 psi with bottled helium gas.
12. Open the shield and tip flow valves.
13. Purge the Heli-Tran again in this configuration for 5-10 minutes.
14. Fully insert the Dewar dip tube into the Dewar.
15. Shut the tip and shield flow valves.
16. Shut the helium gas bottle valve.

B. Cooldown

1. Assemble the head and oven and install onto the cold end.
2. Evacuate the head and vacuum shroud to 10^{-4} torr.
3. Pressurize the Dewar to 5 psi.
4. Plug in the vent gas heater.

5. Open the shield and tip flow valves.
6. The temperature should decrease to operating temperature in 30-60 minutes. As the temperature approaches 15 K, set the temperature controller to 15 K at a power level of 5 watts, and decrease the tip flow enough to hold the temperature at 15 K.

Note: If, at any time during operation, the shield flow outlet ices up, decrease the shield flow slightly to prevent this condition.

7. Make the deposit in the usual manner while maintaining the temperature at about 15 K.
8. Shut off the heater on the temperature controller and open the tip flow valve fully to lower the temperature of the window to 4.2 K. Once the window temperature reaches 4.2 K, the shield and tip flows can be decreased slightly. They must be left sufficiently open to keep the temperature at the desired level.
9. Obtained the needed spectra.

C. Shut Down

1. Shut the tip and shield flow valves and the helium gas bottle valve. This shuts off all helium flow.
2. Warm the window with the temperature controller at a power level of 20 watts or less.
3. Unplug the vent gas heater.

Note: The primary rule in using the Heli-Tran system is to keep the helium Dewar under positive pressure at all times and to completely purge the entire system with helium gas before allowing liquid helium to enter the Heli-Tran. Failure to do so may result in plugging of

one or more lines within the system by solid air or other undesired substances, with the resulting possibility of violent explosion.

VITA

Randall Robert Gore was born in Loris, South Carolina, on July 15, 1953. After graduation from Albemarle Senior High School of Albemarle, North Carolina in May 1971, he entered Pfeiffer College of Misenheimer, North Carolina. He graduated from Pfeiffer College in 1975 with a B.A. in Chemistry. In the Fall of 1975, he entered the Graduate School of the University of Tennessee in Knoxville, Tennessee where he held a teaching assistantship until 1978. In 1978, he accepted a research assistantship sponsored by the National Science Foundation which he held until the awarding of his Ph.D. degree in Chemistry. Upon graduation, he entered employment with the International Business Machines Corporation in Poughkeepsie, New York.

The author is a certified instructor in Cardiopulmonary Resuscitation for the American Red Cross and the Heart Association. He is also a member of the American Chemical Society.